2006

# Linkages between environmental conditions and recreational king mackerel catch off west-central FLorida

Carrie C. Wall
*University of South Florida*

# Linkages Between Environmental Conditions and Recreational King Mackerel Catch Off West-Central Florida

by

Carrie C. Wall

A thesis submitted in partial fulfillment
of the requirements for the degree of
Master of Science
College of Marine Science
University of South Florida

Major Professor: Frank E. Muller-Karger, Ph.D.
Mitchell A. Roffer, Ph.D.
Mark E. Luther, Ph.D.

Date of Approval:
October 30, 2006

Keywords: *Scomberomorus*, remote sensing, front detection, west Florida shelf, oceanic fronts

**Dedication**

"The best way to observe a fish is to become a fish" *Jacques Cousteau*

I dedicate this work to my parents and my brother J for their relentless encouragement throughout the past 26 years.

**Acknowledgements**

This research was funded by NASA grant number NNG04GF13G; the Old Salt Marine Biology Scholarship courtesy of Florida Sea Grant, the Old Salt Fishing Foundation, and the Alyesworth Foundation for the Advancement of Marine Sciences, Inc.; the Paul L. Getting Memorial Fellowship courtesy of the University of South Florida, College of Marine Science. This research has also received immeasurable support during the kingfish data collection from the Southern Kingfish Association (namely, Jack and Deona Holmes), the Old Salt Fishing Foundation (Tom Verdensky and Jill Foraker), the Alyesworth Foundation (Bob and Dawn Alyesworth), Treasure Island Charities (Doyce Mathis), and Billy's Stone Crab Restaurant (Billy Moore and Steve Fennell). In addition to the support of the local fishing organizations, I am grateful for the help, patience, and cooperation of the dozens of friends and colleagues who assisted in the kingfish data collection, the hundreds of anglers who disclosed the intimate details of their fishing activity, and the thousands of kingfish who unknowingly bit the "wrong" bait.

I would also like to acknowledge Luis Garcia-Rubio for his statistical advice and undying patience; Dave Ullman and Wensheng Yao for their assistance and advice with the frontal detection algorithms; Randy Edwards, Ernst Peebles, Behzad Mahmoudi, and Randy Keys for their fisheries insight and guidance; Robert Weisberg, Vembu Subramanian, Jyotika Virmani, and Jeff Donovan for the use of and assistance with the COMPS and PORTS data; Chuanmin Hu and Ken Carder for their remote sensing expertise; Paul Zandbergen and Jesse Lewis for their help with ArcGIS; Gary Mitchum for his statistical advice, and the IMaRS lab for their assistance, advice, and support throughout this endeavor. I would also like to acknowledge Ryan, my love, for his support, strength and understanding.

Note to the reader: The original document contains color which is necessary to fully understand some figures. The original manuscript is on file with the USF library in Tampa, FL.

## Table of Contents

## List of Tables

## List of Figures

**Linkages Between Environmental Conditions and Recreational King Mackerel Catch off West-Central Florida**

Carrie C. Wall

ABSTRACT

The objective of this study was to determine if fronts sustained up to three days will result in an aggregation of kingfish due to the anticipated accumulation of forage, increasing fishing success at these locations. Automated algorithms to detect frontal features in satellite-derived sea surface temperature, chlorophyll concentration, water clarity, and fluorescence images were successfully adapted for the coastal waters off west-central Florida. The surface ocean fronts were used to study the linkages between environmental conditions and recreational catch statistics of king mackerel (*Scomberomorus cavalla*) during 19 seasonal tournaments held in April to May and October to November of 2004 and 2005. The local winds estimated from a USF Coastal Ocean Monitoring and Prediction System observing station were analyzed with the frontal data to examine factors that influence oceanic frontal formation and stability. The front detection algorithms were also applied to high-resolution bathymetry data which serves as a new technique for analyzing bottom topography. The spatial relationships between catch data collected through 415 angler interviews, frontal boundaries and stability, bathymetric gradients, bottom structure, and baitfish presence were identified using ESRI ArcGIS.

Fishing success and fishing effort were highly variable regarding the distance of fishing activity to the nearest front. This was attributed to non-persistent winds. Intermediate water clarity (0.7 to 1.0 mW $cm^{-2}$ $\mu m^{-1}$ $sr^{-1}$), the presence of baitfish, and the side of the front with relatively less chlorophyll showed the greatest influence on the king mackerel catch rates. Fishing success was found to be significantly higher at fishing locations where baitfish were reported present compared to where they were not reported. Concurrent with the 2005 harmful algal bloom event, a significant decrease in king mackerel catch occurred in the fall of 2005 (208 fish) compared to fall 2004 (818) and spring 2005 (538). Additionally, fishing locations with baitfish present were observed about 15% less often during the fall of 2005 than the preceding seasons. From this, a model can be developed to diagnose the environmental conditions that can be used by resource managers to better understand variations in catch, which result from naturally occurring phenomena or man-induced overfishing.

# Chapter 1
# Automated Detection of Surface Oceanic Fronts in Coastal Waters off West-Central Florida

## 1. Introduction

One objective of this study was to apply an automated technique suitable for detecting oceanic fronts on the inner west Florida Shelf (WFS) waters, specifically off Tampa Bay, Florida. Prior to this study, published maps where oceanic fronts are likely to occur along the inner WFS did not exist. This study aims to identify where stable spring and fall fronts occur along the coastal waters off west-central Florida. The goal was to better understand the spatial distribution of frontal features in this region which may lead to improved resource management decisions, such as those regarding fisheries commonly associated with frontal regions.

Oceanic fronts are relatively narrow zones of enhanced horizontal gradients of physical, chemical, optical, and/or biological parameters which may have an expression at the ocean's surface (e.g., see Bowman and Esaias, 1978; Le Fevre, 1986). Frontal systems in coastal seas can be dynamically very active and can indicate water mass boundaries (e.g., Blanton, 1986). They can be established through action of wind-driven upwelling or river discharge along the coast, and their surface expression can be marked or muted depending on the strength of temperature, salinity and ocean color gradients. Upwelling regions and the associated frontal zones result in the vertical flux of nutrients which contribute to high concentrations of phytoplankton biomass (e.g., Marra*, et al.*, 1990). Convergence at fronts can also lead to the accumulation of materials creating surface biological features (e.g, Polovina*, et al.*, 2001). Both of these events can have marked gradients in ocean color that may or may not be coincident with the surface expression of a thermal front. The characterization of frontal boundaries can lead to a better understanding of the dynamic physical and biological processes occurring in the ocean. Oceanic front location, duration and intensity have been analyzed by fisheries scientists to understand variations in fish abundance, based on the hypothesis that the availability of prey increases at fronts (Sund*, et al.*, 1981; Roffer, 1987; Olson*, et al.*, 1994; Bigelow*, et al.*, 1999; Lutcavage*, et al.*, 2000; Polovina*, et al.*, 2001; Schick*, et al.*, 2004).

### 1.1 Front Detection

Visual frontal analysis can be more accurate but it is highly labor intensive and subjective. The development of automated algorithms has allowed for the relatively quick detection fronts for large data sets. Detecting biological (color) and thermal fronts automatically by computer image processing methods requires a series of statistical analyses. A variety of algorithms exist to automatically detect oceanographic fronts using satellite data. These algorithms range from using a simple statistic to characterize the gradient of, for example, the thermal field (Van Woert, 1982; Cornillon and Watts,

1987) to more complex methods such as a cluster-shade technique (Holyer and Peckinpaugh, 1989), semivariogram analysis (Franklin*, et al.*, 1996; Diehl*, et al.*, 2002), histogram analysis (Cayula and Cornillon, 1992; Cayula and Cornillon, 1995; Saraceno*, et al.*, 2005), and entropic histogram analysis based on the Jensen-Shannon divergence (Vázquez*, et al.*, 1999).

The histogram analysis developed by Cayula and Cornillon (1992; 1995) was chosen for this study as it reliably detects verified thermal fronts and ignores false fronts or frontal features not identified with in situ observations (Ullman and Cornillon, 1999; Mavor and Bisagni, 2001; Ullman and Cornillon, 2001; Belkin and Cornillon, 2003; Belkin and Cornillon, 2004). In addition, a comparative study of the cluster-shade technique and the single image edge detection (SIED) histogram analysis by Cayula*, et al.* (1991) found the performance of the SIED to be superior. The SIED histogram method has been applied to detect satellite-derived chlorophyll *a* concentration gradients, the proxy indicator for phytoplankton biomass, for the Long Island Sound (Stegmann and Ullman, 2004). It has also been used to examine gradients and fronts of normalized water-leaving radiance, a proxy indicator for water clarity, for the South Atlantic Bight (Bontempi and Yoder, 2004). Prior applications of the histogram algorithm were mainly for lake or shelf-break environments; this study adapts the Cayula and Cornillon (1992) algorithm for coastal waters off west-central Florida.

### 1.2 Characteristics of the West Florida Shelf

The WFS extends from the Florida Keys north to the Mississippi River and over 200 miles out from the coast creating a wide, gently sloping shelf. The WFS is less influenced by the Gulf of Mexico (GOM) Loop Current (LC) than by local wind regimes and local heat flux and freshwater inputs (Koblinsky, 1981; Del Castillo*, et al.*, 2000; Lenes*, et al.*, 2001; Hu*, et al.*, 2003; Weatherly*, et al.*, 2003; Oey*, et al.*, 2005; Weisberg*, et al.*, 2005, and references therein). The LC controls the circulation in and near the shelf-slope and -break regions (Huh*, et al.*, 1981; Weisberg*, et al.*, 1996; Sturges and Leben, 2000). Over the middle and inner shelf, the circulation is controlled by local wind forcing, seasonal heating and cooling, stratification, and freshwater inputs by rivers (Schmidt*, et al.*, 2001; Virmani and Weisberg, 2003; Hu*, et al.*, 2004; Virmani and Weisberg, 2005; Weisberg*, et al.*, 2005, and references therein). These processes generate cross-shelf transport of nutrients and plankton (Gilbes*, et al.*, 1996; Del Castillo*, et al.*, 2000; Del Castillo*, et al.*, 2001; Gilbes*, et al.*, 2002; Paramo and Viana, 2002; Hu*, et al.*, 2003; Hu*, et al.*, 2004; Weisberg*, et al.*, 2005).

Tampa Bay is the largest of Florida's estuaries and is located on the west-central coast of Florida. To a first order, semi-diurnal and diurnals tides control sea level and the circulation within Tampa Bay (He and Weisberg, 2002). In addition, a non-tidal gravitational convection known as "estuarine circulation" also operates in the bay. Wind and rivers influence sea level at the mouth of Tampa Bay (Weisberg and Zheng, 2005). Water flows from Tampa Bay to the GOM in complex ways, and is modified by the intracoastal waterway, deep shipping channels, bridge causeways, and keys and shoals located at the mouth (Weisberg and Zheng, 2005). Estuarine outflow to the inner WFS (depths < 50 m) affects the establishment and duration of fronts within the region of interest, and while this study focuses on detection and assessment of the short-term

duration of coastal fronts, the circulation inside Tampa Bay and Charlotte Harbor, another large estuary located on the west-central coast, are outside the scope of the study.

Physical and biological water-column processes are related to bottom topographic features, such as slopes, ridges, and canyons (Killworth, 1978; Huh*, et al.*, 1981; Pingree and Mardell, 1981; Pingree*, et al.*, 1982; Molinari and Morrison, 1988; Pingree and Le Cann, 1991; Vlasenko, 1992; Harris*, et al.*, 1997; Fratantoni*, et al.*, 1998; Hamilton*, et al.*, 2000; Weisberg and He, 2003; Fan*, et al.*, 2004). Enhanced mixing due to internal waves or tidal action in areas associated with a topographic feature is attributed to increased phytoplankton growth under improved light conditions and wind-induced upwelling (Pingree and Mardell, 1981; Franks, 1992). Topographic features and the resulting nutrient upwelling events therefore will likely influence the establishment and duration of oceanic fronts off the west-central coast of Florida.

## 1.3 Objectives and Approach

The objective of this study was to apply an automated technique suitable for detecting surface oceanic fronts on the inner WFS, specifically off Tampa Bay, Florida. This led to the adaptation of two automated algorithms to identify fronts for remotely sensed thermal and sea spectral reflectance (ocean color) parameters. The results were compared with local winds estimated from a University of South Florida (USF) Coastal Ocean Monitoring and Prediction System (COMPS) observing station, in an attempt to examine factors that influence oceanic frontal formation and stability. This is part of another study involving king mackerel (*Scomberomorus cavalla*) catch rates and proximity to oceanic fronts.

## 2. Methods

### 2.1 Study Area

This study focuses on the inner shelf off west-central Florida between 28°30' N, 81°30' W to 26° N, 84°30' W (Fig. 1-1). This area extends from Pasco County south to Collier County and approximately 180 km into the Gulf of Mexico (GOM) from the coast. Tampa Bay and Charlotte Harbor are two large estuaries located within the study area whose outflow may influence the location of some fronts. Satellite data recorded within the estuaries were not incorporated into the analysis due to the different environmental conditions of estuaries and infrequency of complete satellite coverage.

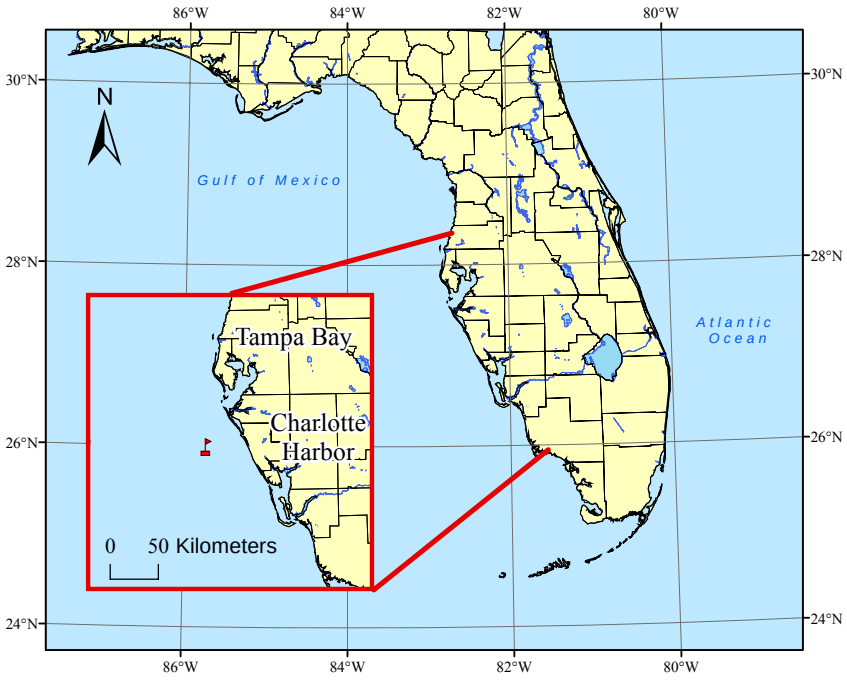


Figure 1-1. Study area located between 28°30' N, 81°30' W to 26° N, 84°30' W (inset). This area extends from Pasco County south to Collier County on Florida's west-central coast and approximately 180 km into the Gulf of Mexico. The study area does not include processes within Tampa Bay or Charlotte Harbor. The red flag represents where wind and current buoy data were recorded.

### 2.2 Oceanographic Data

Meteorological data and satellite imagery were collected for the week leading up to recreational king mackerel (kingfish) tournaments held around the Tampa Bay area during the spring and fall 2004 to 2005. Kingfish are a coastal pelagic species related to the tuna, and the tournaments are timed for their biannual migration through this area.

Tournament dates for this study included:

2004 (10 tournament days): April 3 and 4; May 1, 2, and 8; October 23 and 30; November 6, 7, and 13.

2005 (12 tournament days): March 26; April 3, 9, 16, 17, 23, and 30; October 15 and 29; November 5, 6, and 12.

Coincident with the fisheries data collection, wind and 4 m depth current velocity data were collected from the (COMPS), specifically at Station C10 located at 27°10' N, 82°56' W. A 36 hour low-pass filter was applied to the one hour resolution data to remove high anomalous speeds and directions. The wind data collected at the buoy were supplemented with NASA's Quick Scatterometer (QuikSCAT) satellite derived wind data. For the inner WFS, persistent winds and currents were defined as 24 hours in which the direction did not oscillate greater than approximately +/- 22.5° and wind and current speed did not change more than 5 m $s^{-1}$ and 5 cm $s^{-1}$, respectively (Virmani, 2006). These calculations were based on the raw wind and current data, not the low-pass filtered data.

Full resolution (1.1 $km^2$ per pixel at nadir) real-time and retrospective infrared (IR) and ocean color data derived from NASA's Moderate Resolution Imaging Spectoradiometer (MODIS) sensors on the Terra and Aqua satellites, ocean color data derived from ORBIMAGE's Sea-viewing Wide Field-of-View Sensor (SeaWiFS) carried on the SeaStar spacecraft, and IR data derived from the Advanced Very High Resolution Radiometer (AVHRR) sensors on NOAA polar orbiting environmental satellites NOAA-12, NOAA-15, and NOAA-17 were used to quantify the daily changes in sea surface temperature (SST), chlorophyll *a* concentrations, normalized water-leaving radiance at 443 nm (nLw_443), and fluorescence line height (FLH) within the study area. In total, 468 MODIS and AVHRR thermal images and 90 MODIS and SeaWiFS ocean color images were used to analyze the surface ocean features for the three days leading up to and including the tournament days. Anomalous SSTs were calculated from the difference between a weekly 10 year mean (1995-2005), excluding 1998 (an El Niño year), and the corresponding weekly SST mean. The satellite data were provided for free by the USF Institute for Marine Remote Sensing (IMaRS). While temporally longer climatology maps currently exist, they do not posses the spatial resolution comparable to that of this research or the ability to be easily georeferenced for further spatial analysis.

In coastal areas and areas downstream from upwelling regions, colored dissolved organic matter (CDOM), detritus, and bottom reflectance can lead to errors in satellite-derived estimates of chlorophyll *a* by over 130% (Carder*, et al.*, 1991). Semi-analytical algorithms have been developed for the data derived from the MODIS sensor in an attempt to remove some of these interferences (Morel and Prieur, 1977; Garver and Siegel, 1997; Carder*, et al.*, 1999; Garcia*, et al.*, 2006). In addition, empirical algorithms applied to SeaWiFS data were improved, namely the Ocean Color 4 band algorithm (OC4), to better derive the chlorophyll *a* concentration in coastal waters (O'Reilly*, et al.*, 2000; Gohin*, et al.*, 2002). These methods implement a band ratio of 412, 443, 490, or 510 to 555 nm to calculate chlorophyll *a* estimates. However, satellite-derived coastal chlorophyll *a* estimates remain contaminated by a combination of optically active constituents (O'Reilly*, et al.*, 1998; Hu*, et al.*, 2000, 2000; Liew*, et al.*, 2001; Hu*, et al.*, 2003; Carder*, et al.*, 2004) and will be referred to as "chl+". This parameter is an index of biomass or how much food is in the water. It is not a measure of productivity.

Normalized water leaving radiance (nLw) is derived after correcting for atmospheric radiance, atmospheric light scattering, and the solar zenith angle. The remaining estimate indicates the measured radiance exiting the flat surface of the ocean without the influence of the atmosphere or solar angle, therefore observations from different days can be compared with each other (Gordon and Wang, 1994; Gordon, 1997; Hu*, et al.*, 2000). The nLw_443 observations show the overall effects of phytoplankton, CDOM, and suspended sediments on light absorption and scattering at 443 nm within the water column. This single wavelength product may show different spatial patterns than the chl+ product, as ocean color gradients may be less apparent if the corresponding bio-optical constituents influence both wavelengths used in the chl+ ratio algorithm (Hu*, et al.*, 2003). Similar to the methods of Hu*, et al.* (2003), nLw_443 will be used as a relative index of water clarity as it was found to be the best indicator of the ocean color gradients for the inner WFS.

MODIS imagery was processed using the NASA SeaDAS (version 4.8) software to obtain the FLH data. This is a new product that uses solar stimulated phytoplankton fluorescence to remotely sense phytoplankton concentrations in the surface ocean. FLH represents the height of nLw at 678 nm in reference to a baseline. In the study area, FLH data have been used successfully to identify areas of high concentrations (Chl > 1.0 mg $m^{-3}$) of *Karenia brevis*, the toxic dinoflagellate associated with harmful algal blooms in the GOM (Cannizzaro*, et al.*, 2004; Hu*, et al.*, 2005; Hu*, et al.*, 2006).

Daily SST composites were derived by combining cloud-filtered images from MODIS and AVHRR passes prior to 1700 EST into a daily mean of pixels with valid and cloudless data. The later passes were discarded in an attempt to represent ocean features during the kingfish tournaments, which typically end at 1700 EST. Daily MODIS or SeaWiFS passes with the least cloud cover and image banding (Seemann*, et al.*, 2003) were incorporated into the daily ocean color composites. These composites were derived from combining the cloud-filtered images into a daily mean of pixels with valid and cloudless data.

Daily SST and ocean color composites were qualitatively evaluated based on the extent of the spatial coverage and the limitation of clouds. Since 97% of the fishing locations occurred within 100 km from Tampa Bay, this is the region of most interest for clear satellite coverage and thus complete frontal contours. A clear view of this region is desired to detect fronts and especially the gradients, which are not calculated properly in the presence of fronts. Daily composites with no cloud cover in this particular area of concern were defined as “Good”. Composites defined as “Fair” contained less than 25% cloud cover and less than 25% of gradients within the area of concern were affected by artifacts, typically due to banding, cloud vapor or compositing, not present in the previous days. Composites defined as “Poor” contained less than 50% cloud cover and less than 50% of the gradients within the area of concern were affected by artifacts. Composites defined as “Bad” contained greater than 50% cloud cover, which covered greater than 75% of the area of concern. Composite images with hybrid definitions contained a combination of the criteria, e.g. “Fair-Poor” images contained less than 50% cloud cover and less than 25% of the gradient within the area of concern affected by artifacts.

Prior to applying an algorithm to detect fronts on the imagery, the composite SST data were preprocessed by rescaling the 256-color image linearly to the minimum and

maximum SST values in the scene to enhance the thermal gradients. The chl+, nlw_443, and FLH composite data were log-transformed to enhance the ocean color gradients because these parameters tend to have log-normal distributions more frequently or pronounced than SST. Three by three pixel median value filters were applied consecutively one to five times to determine the extent of gradient smoothing and noise reduction. Analysis of the results when using one to three median value filters showed little loss of detected oceanographic features, yet small, fragmented fronts were deleted (data not shown). Applying the median value filter one to three times also appeared to enhance frontal detection and led to longer fronts by linking neighboring features. As a result three separate median value filters were applied to the images to decrease noise and minimize the detection of false fronts.

## 2.3 Frontal Detection Algorithms

### *2.3.1 Cayula and Cornillon (1992) Algorithm*

Cayula and Cornillon (1992) developed a single-image edge detection (SIED) algorithm to statistically determine the presence of an oceanic front. A front is represented as the separation line between a bi-modal histogram distribution within a specific area of an image. The distance between the two modes in geophysical units (°C, mg Chl $m^{-3}$, etc.) determines the strength of the front as defined by the surrounding gradient; the farther away the modes, the greater the difference in the mean values of the populations and thus the larger the frontal gradient.

This algorithm is composed of six steps using three "region of interest" levels: picture, window, and local. Steps one through three are cloud detection algorithms to reduce the effect of gradients corrupted by clouds that could lead to the detection of false fronts. Step four calculates the histogram within a roving window of 64 x 64, 32 x 32 or 16 x 16 pixels. In a roving window, each window overlaps at the midpoint of the previous pixel box as the window roams across the entire image. The histograms computed within each window identify significant changes in SST populations in the window level processing. This step has two requirements for an edge to be identified; the ratio between the variance of the two populations to the variances within the populations in the histogram must be greater than 0.76 and the difference between the mean temperature of the two populations in the histogram must be more than three digital counts. The USF IMaRS AVHRR and MODIS processing defines a digital count as 0.1992°C. Comparatively, the digital count for the Cayula and Cornillon (1992) SST images was defined as 0.125°C.

Step five applies a cohesion algorithm at the window level to determine spatial distinction between the two populations identified in the histogram calculated in step four. "High cohesion" predicts that for a pixel close to an edge, surrounding pixels are likely to belong to the same population. For each detected edge, this algorithm creates a spatial segmentation between the two populations to verify the existence of a true front. The objective is to discard false fronts by accounting for noisy distributions. Spatial distinctness is defined as the ratio of the number of comparisons between center and neighbor pixels both within the first population to the total number of comparisons between center pixels in the first populations and neighboring pixels of either population, $C_1$. This is repeated for the second population, $C_2$, and for the two populations combined, C. Cayula and Cornillon (1992) suggest a minimum value of 0.90 for $C_1$ and $C_2$ and 0.92

for C. For $C_n$ less than the given thresholds, the segmentation is invalid and not classified as a front. If both requirements are met, an edge is marked at the pixels defining the center line located between the two populations in the histogram.

Step six applies a contour-following function at the local level to link spatially close fronts. This step connects adjacent edges, eliminates weak, typically false, edges, and removes isolated front pixels from the final image. Contours extend and connect isolated pixels if the gradient in the neighborhood of (adjacent to) an edge pixel is coherent. This is completed by calculating the ratio of gradients, the sum of gradient vectors to the sum of the absolute gradient vectors within a 3 x 3 pixel window, centered at the edge pixel. Detected fronts less than 10 pixel edges long are removed. Complete details of this algorithm are described in Cayula and Cornillon (1992).

*2.3.2 Modifications to the Cayula and Cornillon* (1992) *Algorithm*

Due to relatively weak ocean surface gradients found on the inner WFS compared with the shelf break fronts that Cayula and Cornillon (1992) investigated, the following modifications to their algorithm helped to optimize frontal detection for this region. The Cayula and Cornillon (1992) algorithm, which uses a default 32 x 32 pixel roving window, was re-applied with a 16 x 16 pixel roving window to produce a final image of fronts. Weaker, smaller fronts undetected by the 32 x 32 pixel window should be identified with the 16 x 16 pixel window since the histogram is calculated for a smaller area. However, it was found that the Cayula and Cornillon (1992) algorithm sensitivity decreased with the application of smaller window sizes, as also seen by Ullman (2005).

Despite combining the results of both pixel box sizes, it was apparent that the algorithm did not detect all fronts perceptible by visual evaluation of SST images. In step 4 above, the ratio of variance between the populations of the histogram to the variance within the populations was therefore changed from the default 0.76 to 0.72 to increase the frontal detection sensitivity. However, this adjustment may only compensate for the increased digital count value due to different image processing methods. Adjustments within step five did not produce a difference in the front detection results so the original values were maintained.

Two changes were applied to the contour-following thresholds in step six. First, the minimum length for a valid front was increased from 10 to 20 pixels so that isolated edges less than 20 pixels were removed. This consequently increased the spatial range in which front segments are considered part of the same feature. Second, the threshold of the ratio of gradients was changed from 0.90 to 0.95 to increase the coherence between the fronts. This resulted in longer, smoother fronts with fewer occurrences of dendritic fronts. Since long, jagged edges are often the result from noise and not true thermal fronts (Cayula and Cornillon, 1992), the results of the changes in the contour-following function appear to produce more realistically-shaped fronts. The Cayula and Cornillon (1992) algorithm with the threshold adjustments described above were applied to the SST, nLw_443, and FLH daily composite data.

*2.3.3 Canny (1986) Algorithm*

Another frontal detection method was tested to characterize the chl+ fronts. The "Canny method" developed by Canny (1986) was applied because it was able to better detect nearshore gradients for this parameter. The Canny method for edge detection

consists of four steps. First, to smooth the image, noise suppression using linear filtering with a Gaussian mask is applied to the image. The size of the mask depends on the parameter sigma ($\sigma$), the standard deviation of the Gaussian filter. Increasing the value of sigma and thus the width of the Gaussian mask reduces the detector's sensitivity to noise. However, this results in a loss of some of the finer detail in the image. The probability of error in the detected edges also increases as the Gaussian width is increased. In this study, a sigma value of 1.0, corresponding to a 7 x 7 pixel mask, was applied.

Second, the edge gradient (strength and direction) for each pixel is computed using a 3 x 3 pixel window in the smoothed image. Third, the edges which contain two or more adjacent pixels in the gradient image are thinned to a one pixel edge through non-maximal suppression. In this thinning process, the magnitude of the edge gradient of each candidate edge pixel is set to zero if it is weaker than the two adjacent pixels in the gradient direction. Fourth, hysteresis (double) thresholding is applied to the thinned edge gradient image to determine the significance of the edge gradient. Chains of candidate edge pixels below the lower gradient hysteresis threshold are labeled as non-edges. Only those pixels above the lower threshold and connected through a chain to any pixel above the upper gradient hysteresis threshold are labeled as edge pixels. In this study, thresholds of 0.05 and 0.08 were applied. Both threshold values are set to small values in order to increase the detector's sensitivity to identify inshore chl+ fronts without increasing the detection of noise. These thresholds also produce the most visually accurate edge detection results for the chl+ fronts.

Both edge detection algorithms described above were also applied to an ~ 90 $m^2$ resolution digital bathymetry grid of the inner WFS obtained from NOAA (Divins and Metzger) to identify areas of significant depth gradients. These areas were investigated to determine their role in the establishment and stability of the detected thermal and ocean color fronts. These data were also used to identify regions where bottom reflectance was accentuating the ocean color gradients.

The Cayula and Cornillon (1992) algorithm is a FORTRAN program that was embedded in the Interactive Data Language (IDL; Research Systems, Inc.) software for processing. The Canny algorithm was implemented using Matlab$^{TM}$ software (Mathworks, Inc.). The final frontal images were georeferenced and remapped in the standard North American Datum 1983 projection for spatial analysis. This was carried out using ArcGIS developed by Environmental Systems Research Institute (ESRI$^{TM}$).

## 2.4 Sustained Fronts

Frontal features of SST, chl+, nLw_443, and FLH were sequentially analyzed to identify frontal duration for up to four days. Scales of oceanographic variability on the WFS are typically driven by inertial oscillation (He and Weisberg, 2002). Therefore, the radius of inertial motions was used to determine the width scale of the fronts. This is defined as:

$$r = \frac{v}{f}, \qquad (1)$$

where $v$ is the current velocity, m $s^{-1}$, and $f$ is the Coriolis parameter, 6.67E-5 $s^{-1}$. Weisberg and He (2003) showed average current velocities to be 20 cm $s^{-1}$ for this region.

Therefore, the area in which a front would rotate due to the Coriolis force over one inertial period, 25.9 hours at 27° N latitude, would have a radius of ~ 3 km.

The internal Rossby radius of deformation is another scale of physical processes (Rossby, 1937) that potentially influence frontal features in the WFS:

$$L_D = \frac{N * D}{f}, \qquad (2)$$

where $N$ is the Brunt-Väisälä buoyancy frequency ($s^{-2}$) and $D$ is the water depth (m). The Rossby radius of deformation is mainly used to estimate scales in open ocean conditions where two-layer geostrophic flow influences the circulation and pressure patterns (Tang and Weisberg, 1993; Chelton*, et al.*, 1998; Wang and Weisberg, 1998). Although the physical processes driving the boundary depths in coastal shallow waters are more complex due to the influence of friction from surface and bottom Ekman layer interaction (Mitchum and Clarke, 1986, 1986; Weisberg*, et al.*, 2001), geostrophic flow remains the dominant process influencing circulation when considering periods longer than 24 hours. The specific region of interest on the inner WFS lies mainly within the 30 m isobath. Rossby radius calculations corresponding to this depth were between 2 to 5 km (Liu, 2005). These values are consistent with the ~ 3 km radius of inertial motions.

Sustained fronts were determined by identifying the frontal pixels present on the tournament day and up to three days prior to within 3.3 km (3 pixels) as defined by the radius of inertial motions (He and Weisberg, 2002) and the Rossby radius of deformation (Liu, 2005) for this region. The number of frontal pixels identified in the sustained frontal image was divided by the number of frontal pixels in the corresponding tournament day frontal image. This represents the percentage of frontal pixels that were spatially sustained for up to four days on that tournament day.

2.5 Gradient Vector

The gradient vector for each frontal image was calculated by applying a gradient magnitude algorithm:

$$\text{Gradient magnitude} = \sqrt{(\partial T / \partial x)^2 + (\partial T / \partial y)^2}, \qquad (3)$$

where $\partial T$ equals the change in the parameter value in the vertical (y) and horizontal (x) direction; $\partial$x and $\partial$y equal 3 pixels or about 3 km (Van Woert, 1982; Emery*, et al.*, 1986). It is suspected that stronger chl+ fronts, or those with a higher gradient magnitude, have increased surrounding concentrations of chlorophyll *a* and thus abundance of biomass compared to weaker fronts. This response may be reflected in thermal and water clarity fronts as well. Equation (3) was applied to the SST, chl+, nLw_443, and FLH daily composites prior to filtering and gradient enhancements. The gradient magnitude surrounding the daily and sustained front pixels were calculated for each tournament day. Equation (3) was also used to identify the presence of false fronts detected by the front detection algorithms. A false frontal pixel is identified in the frontal image if it does not spatially coincide with a gradient pixel within the gradient image. The percentages of false frontal pixels in each image were calculated for the four parameters to help determine the accuracy of the front detection algorithms.

# 3. Results

## 3.1 Satellite Data

Image quality was often a limiting factor as four consecutive cloudless days were infrequent during the spring and fall seasons studied. Banding artifacts also limit the applicability of ocean color imagery, specifically passes from the MODIS Terra sensor. Also, a higher number of IR satellite passes available were available, up to eight per day, compared to ocean color passes per day, up to two per day, due to its ability to obtain data at night.

Appendix A lists the images available and the qualitative assessment of images. The images with "Poor" or inferior quality were not incorporated into this study unless no better data were available. The AVHRR and MODIS SST combined data provided useable imagery for 75% of the study days. This is in comparison to both MODIS and SeaWiFS ocean color images, which yielded only 25% and 20% of coverage for chl+ and nlw_443, respectively. FLH imagery were analyzed for only the fall of 2005 due to the lack of adequate imagery for the preceding seasons. Ocean color data were unavailable for the tournament held on May 2, 2004. Data were not analyzed for the tournaments held on March 26 and October 15, 2005 due to a small sample size of surveys collected at the kingfish tournaments. .

## 3.2 Oceanographic Data

### *3.2.1 Winds and Currents*

Atmospheric fronts and wind changes were observed in the wind data throughout the study period (Figs. 1-2 to 1-7). Spring 2004 and fall 2005 each recorded six wind rotations, defined as ~ 360° rotation from pre-atmospheric front to post-atmospheric front occurring on time scales of four to 10 days (Fernandez-Partagas and Mooers, 1975); fall 2004 and spring 2005 each recorded five. This coincides with the mean of five to six frontal systems estimated to occur over the study area in the spring and fall (DiMego*, et al.*, 1976). Wind direction, described as the direction toward which the wind is blowing, was predominantly to the south (either southward, southeastward or southwestward). The wind direction during April 2004 (Fig. 1-2a) shows a mainly southeastward direction while May 2004 (Fig. 1-3a), October 2004 (Fig. 1-4a), October 2005 (Fig. 1-7a), and November 2005 (Fig. 1-7b) tended to be south-southwestward. In the three days prior to and including the tournaments days only November 6, 2004 recorded persistent winds (Fig. 1-5a), however, the wind strength was strong (> 8 m $s^{-1}$) during this time. Persistent winds were not recorded throughout any consecutive four-day period associated with all of the tournaments. Gaps in wind data collected at the buoy occurred from November 16 to 30, 2004, April 1 to 4, 2005, and November 24 to 30, 2005.

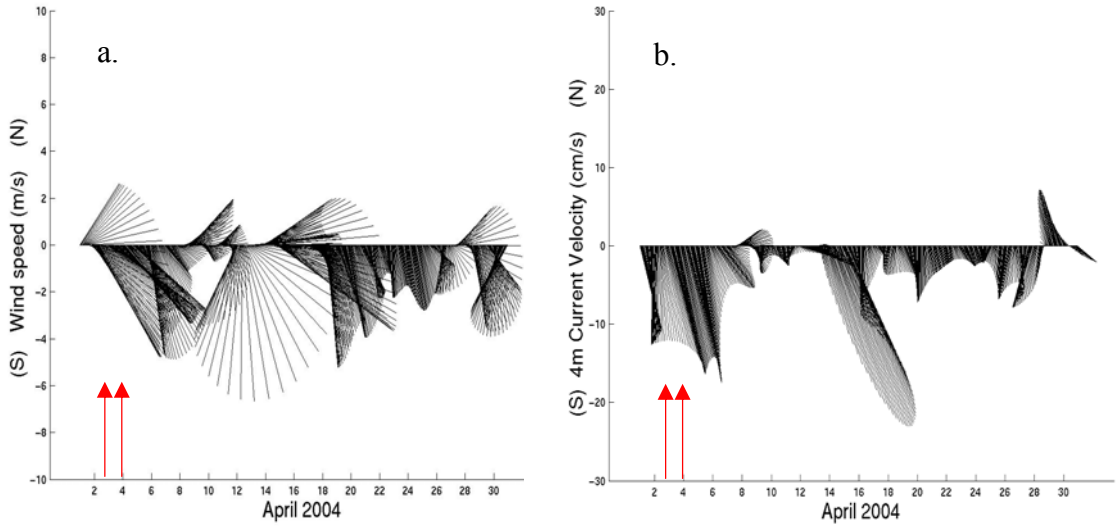


Figure 1-2. April 2004 (a) wind and (b) current velocity data. Data recorded from the USF COMPS C10 buoy, 27°10' N, 82°56' W, see figure 1-1 for location. Tournament dates are highlighted by the red arrows.

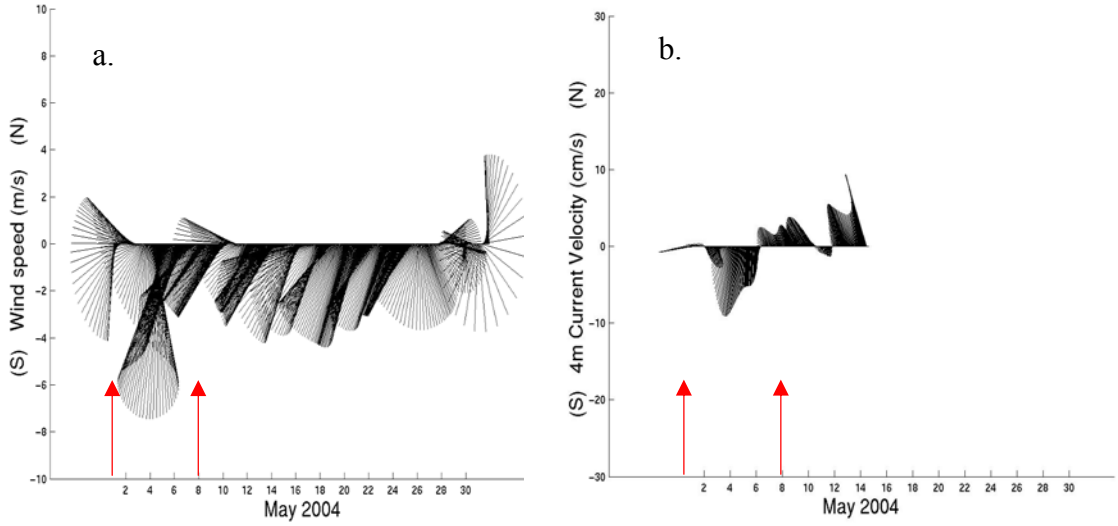


Figure 1-3. May 2004 (a) wind and (b) current velocity data. Data recorded from the USF COMPS C10 buoy, 27°10' N, 82°56 W', see figure 1-1 for location. Tournament dates are highlighted by the red arrows.

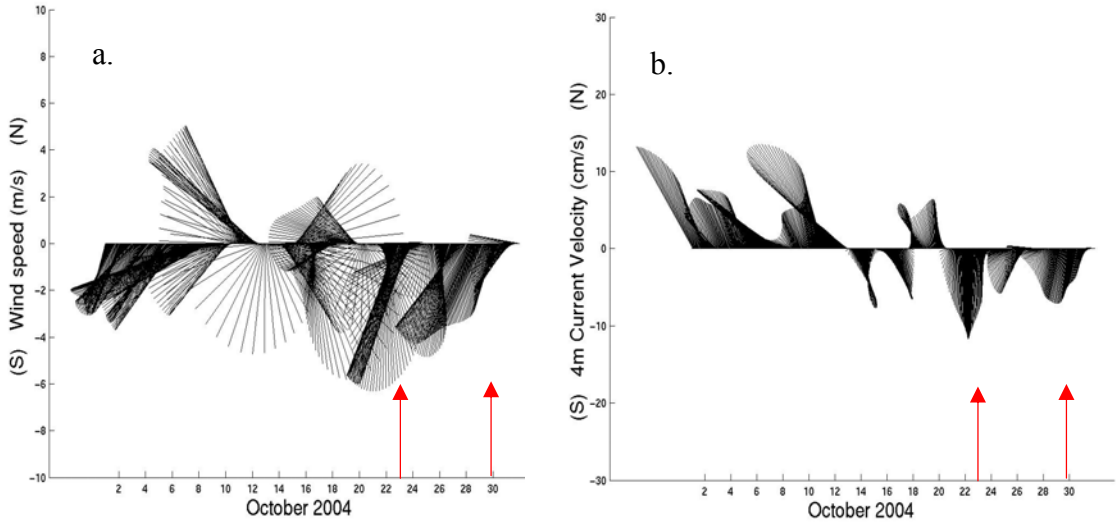


Figure 1-4. October 2004 (a) wind and (b) current velocity data. Data recorded from the USF COMPS C10 buoy, 27°10' N, 82°56' W, see figure 1-1 for location. Tournament dates are highlighted by the red arrows.

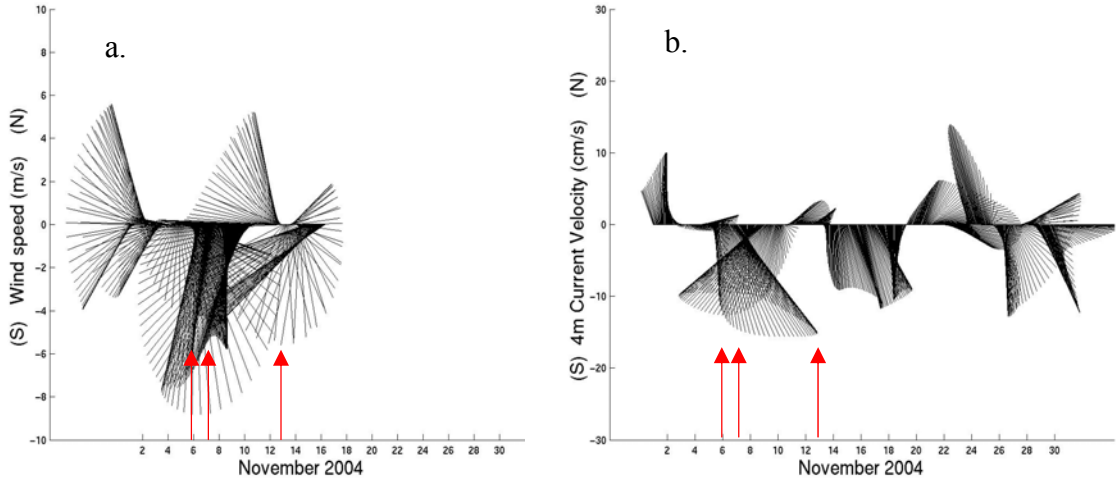


Figure 1-5. November 2004 (a) wind and (b) current velocity data. Data recorded from the USF COMPS C10 buoy, 27°10' N, 82°56' W, see figure 1-1 for location. Tournament dates are highlighted by the red arrows.

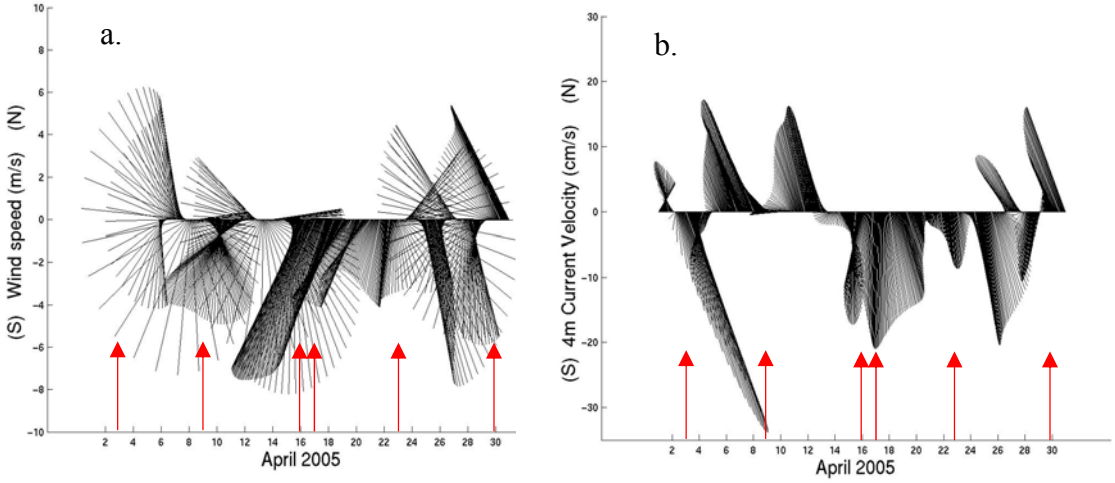


Figure 1-6. April 2005 (a) wind and (b) current velocity data. Data recorded from the USF COMPS C10 buoy, 27°10' N, 82°56' W, see figure 1-1 for location. Tournament dates are highlighted by the red arrows.

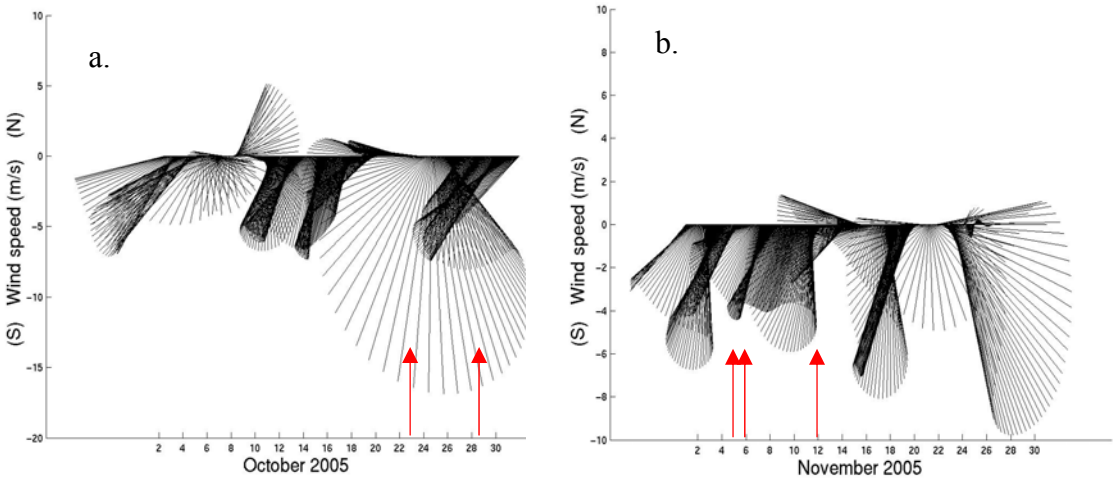


Figure 1-7. Wind velocity data for (a) October 2005 (Note the change in scale) and (b) November 2005. Data recorded from the USF COMPS C10 buoy, 27°10' N, 82°56' W, see figure 1-1 for location. No current velocity data is available for these months. Tournament dates are highlighted by the red arrows.

Highly variable wind directions, or those that exceeded 90° changes in 24 hours, were recorded on 79% of the tournament days and the three days prior. These four-day periods in 2004 include April 1 to 4 when winds changed from northeastward at 3 m $s^{-1}$ to southeastward at nearly 5 m $s^{-1}$; April 28 to May 1 when winds changed from southward to northwestward decreasing from 4 to 2 m $s^{-1}$; October 20 to 23 when winds changed from southward to eastward at 4 m $s^{-1}$ and then south-southwestward at 7 m $s^{-1}$; November 3 to 6 and 4 to 7 when winds shifted from southwestward at 3 m $s^{-1}$ to southeastward decreasing from 8 to 2 m $s^{-1}$ then returning to south-southwestward near 8 m $s^{-1}$; and November 10 to 13 when winds circled clockwise from southward near 6 m $s^{-1}$ to northward reaching 8 m $s^{-1}$ and then returning to the south at 6 m $s^{-1}$. Note the change in wind velocity from November 3 to 7, 2004. Despite persistent winds recorded on November 6, this was preceded by changes in wind speed up to 5 m $s^{-1}$ and wind direction over 45°. Periods during April 1 to 4, 2004 recorded alongshore upwelling favorable winds, southeastward over 5 m $s^{-1}$. April 3 and 4 recorded approximately 15 and 10 consecutive hours of upwelling favorable winds, respectively. Upwelling is confirmed on these dates by 4 to 22 m current velocity data collected from the C10 buoy (OCG, 2006). Periods during May 1, October 26 and 27, 2004 recorded offshore upwelling favorable winds for approximately 9, 11, and 19 hours, respectively. Weak upwelling is confirmed on these dates (OCG, 2006).

In 2005, four-day periods of highly variable wind directions coinciding with the tournament dates included March 31 to April 3. During this time winds changed from south-southwestward at 10 m $s^{-1}$ to northwestward at 5 m $s^{-1}$. These observations were obtained from QuikSCAT data as buoy-based wind data were not available. April 6 to 9 showed a counterclockwise change in wind direction from northward at 6 m $s^{-1}$ to eastward at 5 m $s^{-1}$ then returning southward; on April 13 to 16 and 14 to17 winds changed from southwestward at 8 m $s^{-1}$ to northeastward decreasing from 8 to 2 m $s^{-1}$ and then ending southwestward at 8 m $s^{-1}$; on April 27 to 30 winds changed from south-southeastward winds at 8 m $s^{-1}$ to west- , southwest- and then northwestward at 5 m $s^{-1}$; on November 2 to 5 and 3 to 6 winds shifted from southward to southwestward with speeds ranging from 2 to 7 m $s^{-1}$; and on November 9 to 12 winds changed from southward at 4 m $s^{-1}$ to eastward increasing to 8 m $s^{-1}$.

The remaining 21% of the four-day tournament periods had less variable, but still not persistent, wind velocities. This includes May 5 to 8, 2004 when winds remained mainly south-southwestward at 8 m $s^{-1}$ then shifted southwestward decreasing to 3 m $s^{-1}$; October 27 to 30, 2004 when winds remained southwestward decreasing from 5 to 2 m $s^{-1}$; April 20 to 23, 2005 winds changed from south-southwestward to south-southeastward remaining at 4 m $s^{-1}$; and October 26 to 29, 2005 when winds remained mainly southwestward but strong at 8 m $s^{-1}$.

A total of nine hurricanes affected Florida and the eastern GOM in 2004 and 2005. However, Hurricane Wilma, impacted the area near the time of a tournament. Highly variable wind direction and strong wind speeds over 15 m $s^{-1}$ observed on October 23, 2005 shows the passage of Hurricane Wilma (Fig. 1-2k). Hurricane Wilma moved eastward from the eastern GOM across Florida near 26° N latitude, over 200 km south of Tampa Bay, the southern part of the study region. Vertical mixing as a result of the strong winds during Wilma and an adjacent atmospheric cold front expressed in the wind data by continuous and strong southward winds, overlapping the tournament held on

October 29. This resulted in anomalously low SSTs (~ 2°C) from the week of October 22, 2005 to the week of November 5, 2005.

Current speed and direction mostly followed patterns similar to that of the wind speed and direction. However, mid May 2004 (Fig. 1-3b), early October 2004 (Fig. 1-4b), and early April 2005 (Fig. 1-6b), show opposing current and wind directions. In these events, the current direction is mainly northward, while the wind is directed southward. No current data are available for May 14 to May 31, 2004, October and November 2005.

## 3.3 Fronts

### *3.3.1 Frontal Detection Algorithms*

A comparison of the original and adjusted thresholds applied to the Cayula and Cornillon (1992) edge detection algorithm for an SST daily composite image is shown in figure 1-8. The results obtained using the original Cayula and Cornillon (1992) algorithm with the 32 x 32 pixel box are depicted in figure 1-8, left panel. The adjusted algorithm thresholds (step 4: histogram sensitivity 0.76 to 0.72; step 6: ratio of gradients 0.90 to 0.95, minimum front length 10 to 20 pixels) with the 32 x 32 pixel box detect more fronts for this study area (Fig. 1-8, middle panel). The addition of the 16 x 16 pixel box results appear to identify weaker fronts (Fig. 1-8, right panel).

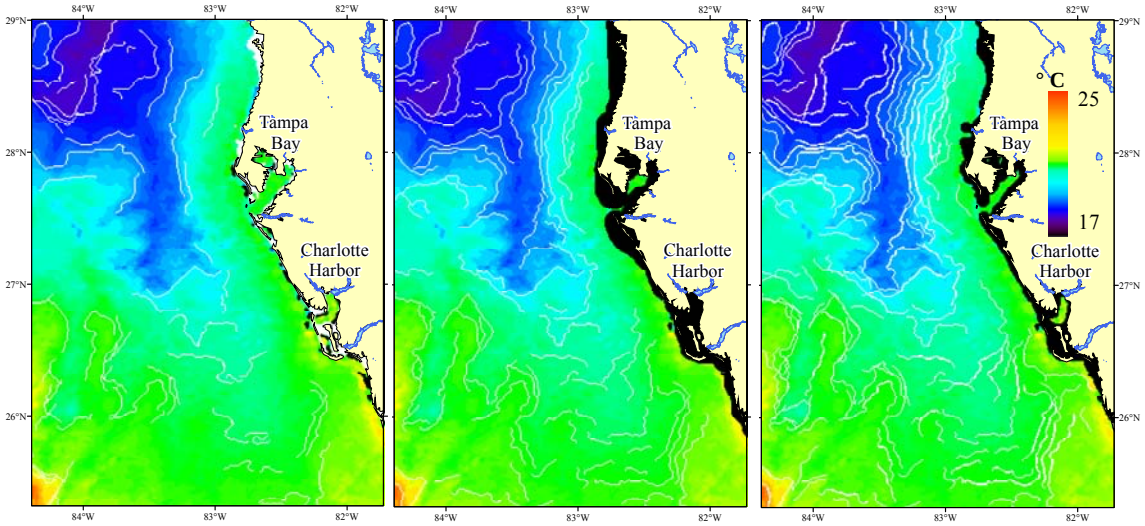


Figure 1-8. Comparison of SST edge detection images for April 9, 2005. (left) The original Cayula and Cornillon (1992) algorithm and 32 x 32 pixel box results, (middle) the Cayula and Cornillon (1992) algorithm with adjusted thresholds (step 4: histogram sensitivity 0.76 to 0.72; step 6: ratio of gradients 0.90 to 0.95, minimum front length 10 to 20 pixels) and 32 x 32 pixel box results, and (right) the 16 x 16 pixel box results combined with (middle). White lines delineate detected fronts.

Figure 1-9a shows the results of applying the Canny method to the chl+ data. The Canny method is able to detect more nearshore fronts, specifically at the mouth of Tampa Bay, compared to the Cayula and Cornillon (1992) algorithm. While the Cayula and Cornillon (1992) algorithm is able to identify offshore chl+ fronts, it also seems to

trace fronts where gradients are not visually apparent, therefore possibly falsely identifying fronts (Fig. 1-9b).

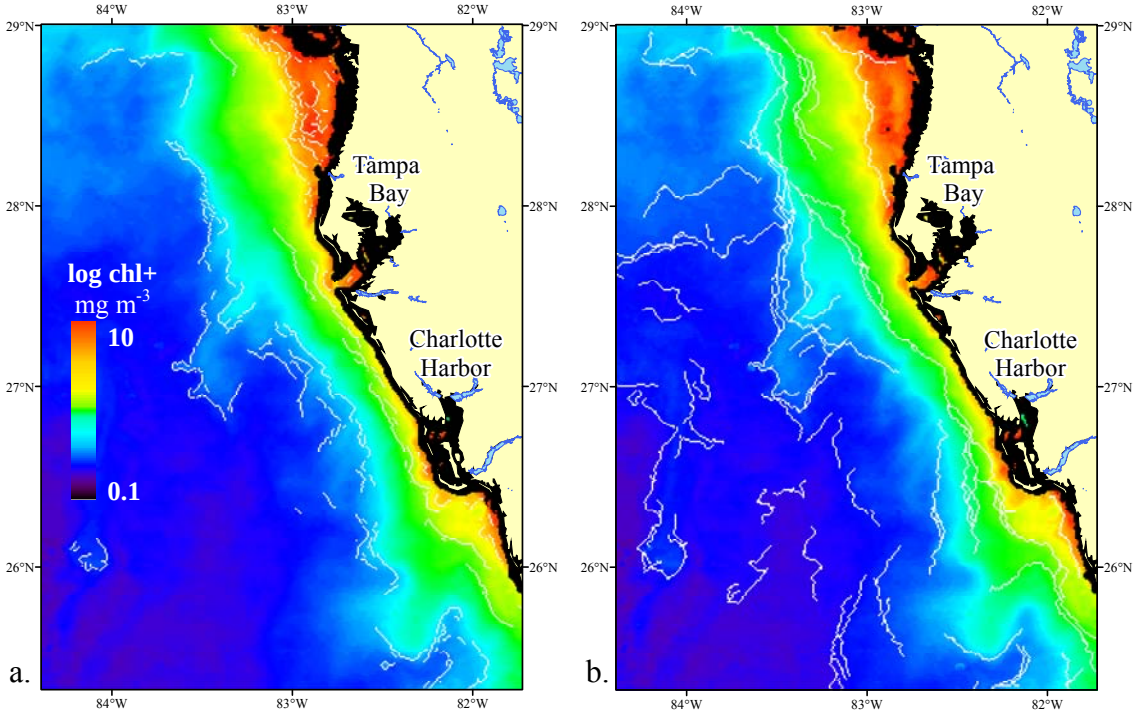


Figure 1-9. April 9, 2005 chl+ composite with (a) Canny (1986) algorithm and (b) Cayula and Cornillon (1992). White lines delineate the detected fronts.

The mean gradient magnitude obtained using the 32 x 32 pixel box compared to the 16 x 16 pixel box in the adjusted Cayula and Cornillong (1992) algorithm for the SST and nLw_443 images was 0.03°C and 0.04 mW $cm^{-2}$ $\mu m^{-1}$ $sr^{-1}$ higher per km, respectively. Therefore, the addition of the 16 x 16 pixel box results does identify weaker fronts. The difference in mean gradient magnitude between the pixel box sizes in the FLH imagery was negligible (2.3E-4 mW $cm^{-2}$ $\mu m^{-1}$ $sr^{-1}$ per km).

Using a Student's *t*-test analysis, the use of both 32 x 32 pixel and 16 x 16 pixel boxes within the Cayula and Cornillon (1992) algorithm was not found to significantly increase the percentage of falsely identified thermal fronts compared to using only the 32 x 32 pixel box result ($p > 0.05$). The thermal fronts detected using the adjusted Cayula and Cornillon (1992) algorithm thresholds showed a mean 0.60 ± 0.40%, N = 19 of the pixels identified as false fronts. Mean percentages of falsely identified front pixels were 1.28 ± 1.38%, N = 18 for nLw_443 and 0.05 ± 0.06%, N = 4 for FLH. The percentage of falsely identified fronts using the Canny (1986) for chl+ data was 1.41 ± 1.45%, N=18. Differences in sample size per parameter result from limited data available on tournament days. This indicates that the frontal detection methods do not identify a significant amount of false frontal pixels.

*3.3.2 Bathymetric Gradients*

Although the continental shelf is typically characterized as gently sloping, areas of transition to a steeper gradient, represented by the red lines, were identified with the

adjusted Cayula and Cornillon (1992) algorithm (Fig. 1-10a). Well-defined bathymetric gradients, which follow some of the bathymetric contours, were also identified with the Canny method (Fig. 1-10b).

Relatively stronger bathymetric gradients were detected by both algorithms along the 20 m and 40 m isobath between Tampa Bay and Charlotte Harbor, Florida, and north of 28° N near the 9 m isobath. The Canny method specifically identified a strong bathymetric gradient coinciding with the 30 m isobath.

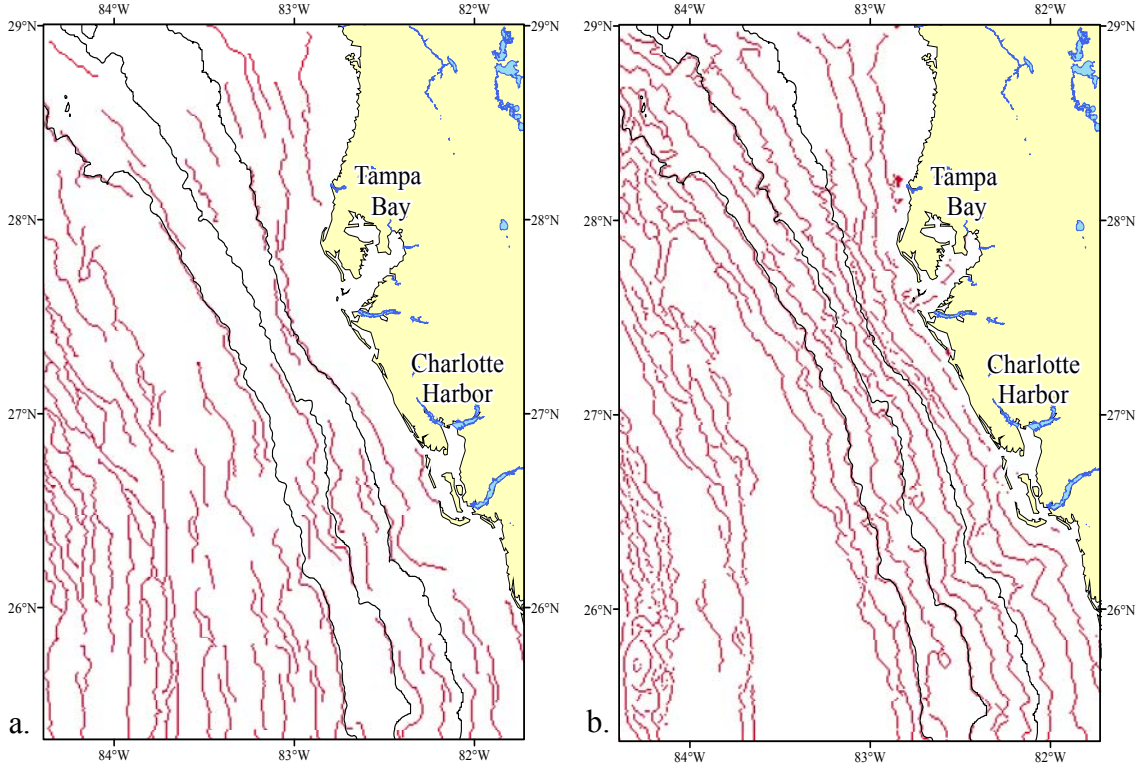


Figure 1-10. Bathymetric gradients (red lines) detected using (a) the adjusted Cayula and Cornillon (1992) algorithm and a 32 x 32 pixel box histogram and (b) the Canny method (Canny, 1986). The 20 m, 30 m, and 40 m isobaths are outlined in black.

*3.3.3 Detected Harmful Algal Blooms*

Harmful algal blooms (HAB) caused by the toxic dinoflagellate *Karenia brevis* were present off central Florida from January through at least November 2005. The frontal detection algorithms applied to the nLw_443, chl+, and FLH fall 2005 data outline the boundaries of water masses that contain relatively high counts of HAB organisms (Fig. 1-11). These results coincide with the *K. brevis* counts reported by researchers at the Florida Fish and Wildlife Research Institute (FWRI) (FWRI, 2005) (Fig. 1-12).

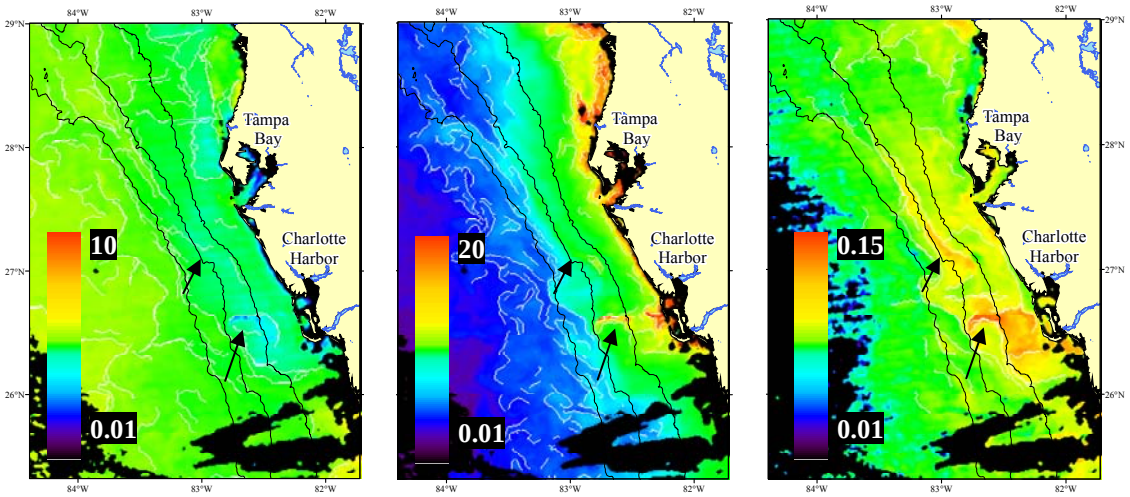


Figure 1-11. Front detection results for (left) nLw_443, (middle) chl+, and (right) FLH on November 12, 2005. The ocean data is log scaled and expressed in mW $cm^{-2}$ $\mu m^{-1}$ $sr^{-1}$ for both nLw_443 and FLH and mg $m^{-3}$ for chl. White lines delineate fronts. The 20 m, 30 m, and 40 m isobaths are outlined in black. Black arrows indicate coinciding areas of detected extreme HABs.

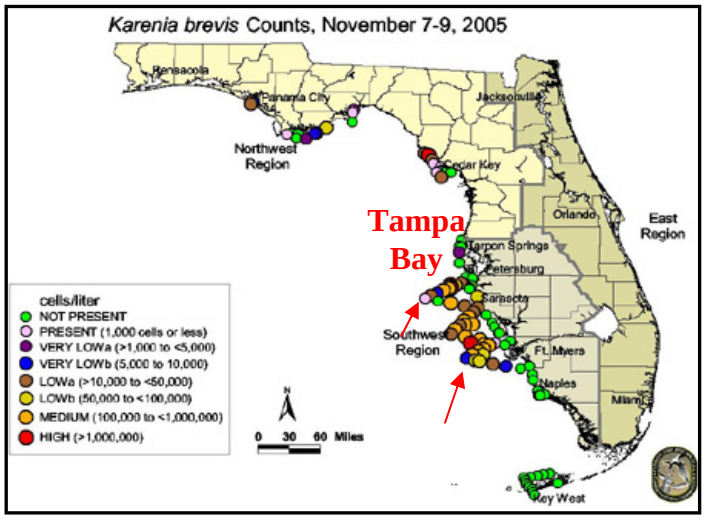


Figure 1-12. *Karenia brevis* in situ counts from November 7 - 9, 2005 reported by FWRI. Red arrows indicate coinciding areas of observed extreme HABs.

*3.3.4 Daily Fronts*

Daily thermal fronts detected in spring 2004 and 2005 show a cold-water tongue, dark blue in color, (Fig. 1-13a) consistent with the predominant southward direction of the currents and winds recorded during this time. Thermal fronts detected in fall 2004 and 2005 show an alongshore pattern reflecting the bathymetric contours of the inner WFS (Fig. 1-13b). Colder water (green color) fringing the cloud (black areas towards the mid-left) represents water vapor related to clouds that was not identified during the pre-front detection processing. However, the cloud detection and cohesion algorithms within

the Cayula and Cornillon (1992) frontal detection notably did not mark the boundaries of these areas as "fronts".

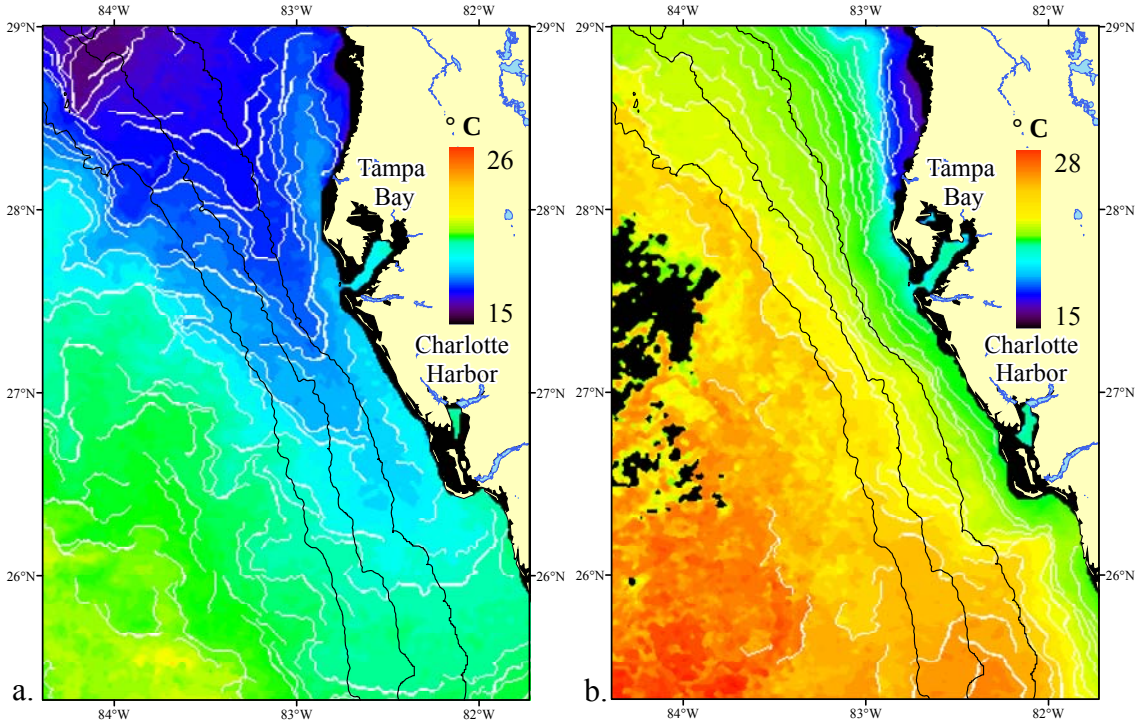


Figure 1-13. Thermal fronts detected on (a) April 3, 2004 as an example of spring and (b) October 29, 2005 as an example of fall. White lines delineate fronts. The 20 m, 30 m, and 40 m isobaths are outlined in black. Areas of black represent the land mask or clouds.

The Cayula and Cornillon (1992) algorithm with adjusted thresholds was also applied to the nLw_443 and FLH data. In general, nLw_443 fronts coincide with the 10 m, 20 m, and 40 m isobath offshore of Tamp Bay, however, additional fronts identified throughout the imagery do not appear to be related to the bathymetry (Fig 1-14). Since only fall 2005 FLH imagery was available for analysis, a seasonal comparison is not possible. However, FLH data clearly identified chlorophyll patches and were not influenced by darker, more turbid waters related to river discharge along the coast (*see* Fig. 1-11, right panel).

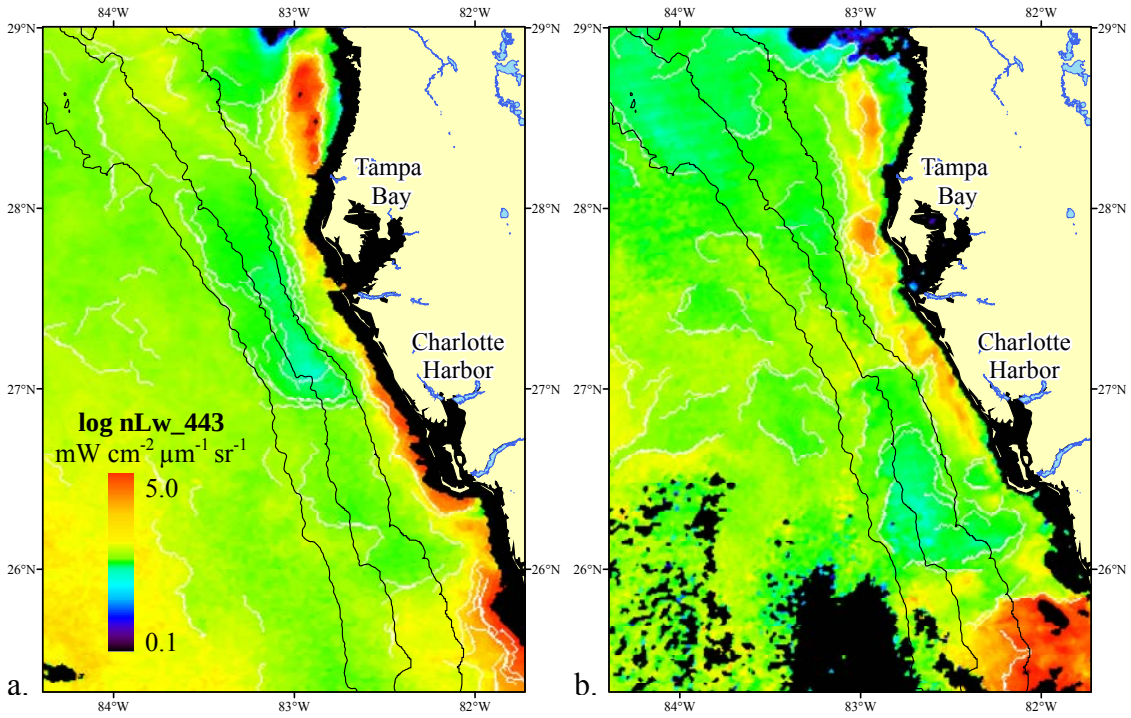


Figure 1-14. NLw_443 fronts detected on (a) April 3, 2004 as an example of spring and (b) November 6, 2004 as an example of fall. White lines delineate fronts. The 20 m, 30 m, and 40 m isobaths are outlined in black. Areas of black represent the landmask or clouds.

The daily spring 2004 fronts detected in chl+ images were primarily shoreward of the 40 m isobath (Fig. 1-15a). In fall 2004, increased nearshore chl+ gradients were apparent near the mouth of the estuaries and nearby rivers (outlined in blue) suggesting these fronts were mainly linked to riverine outflow (Fig. 1-15b). Some frontal features identified in the spring 2005 chl+ frontal data coincided with the 20 m and 30 m contours between Tampa Bay and Charlotte Harbor (*see* Fig. 1-9a). Fall 2005 chl+ fronts traced the boundaries of high chl+ concentrations (> 5 mg $m^{-3}$) up to 70 km off the coast of the study area (*see* Fig. 1-11, middle panel).

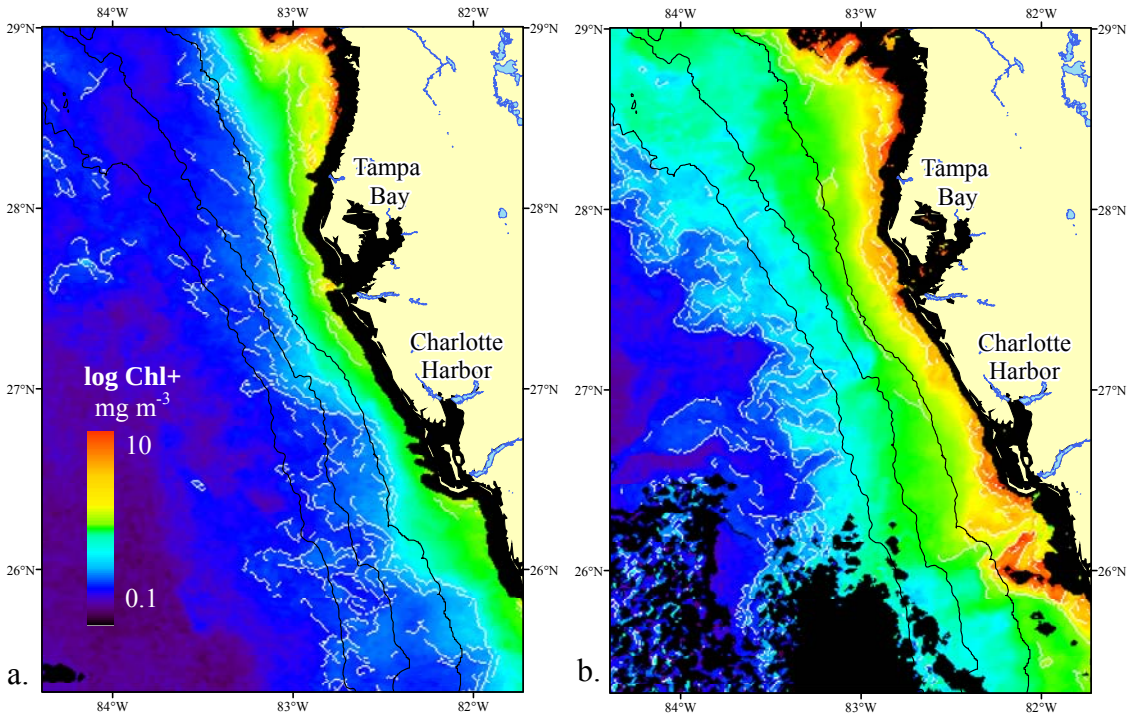


Figure 1-15. Chl+ fronts (red lines) on (a) April 3, 2004 as an example of spring and (b) November 6, 2004 as an example of fall. The 20 m, 30 m, and 40 m isobaths are outlined in black. Areas of black represent the land mask or clouds.

Fronts experienced displacement up to 15 km over a 24 hour period when wind and current speeds were strong (> 8 m $s^{-1}$ and >10 cm $s^{-1}$, respectively) and wind direction was not persistent. This was observed between April 2 to 4, 2004, April 2 to 3, and 29 to 30, 2005. Figure 1-16 shows the displacement of fronts from April 2 to 3, 2005. Note the change in position of the left arrow on April 3, 2005 (Fig. 1-16b). This corresponds to ~ 10 km southward movement of this frontal feature. Comparatively, 3 to 5 km frontal displacement was observed on October 29 to 30, 2004, which corresponded to weaker (< 5 m $s^{-1}$) and more persistent wind velocities, and on October 28 to 29, 2005 when mainly southwestward winds between 5 and 8 m $s^{-1}$ were recorded (Fig. 1-17). In situ current velocity data were unavailable during these periods. The parallel positions of corresponding frontal features in both images indicate little change or movement (≤ 3 km) in the features. The remaining days within this study period exhibited between 3 and 10 km daily frontal displacement. Similar frontal displacement was observed for the ocean color data (not shown).

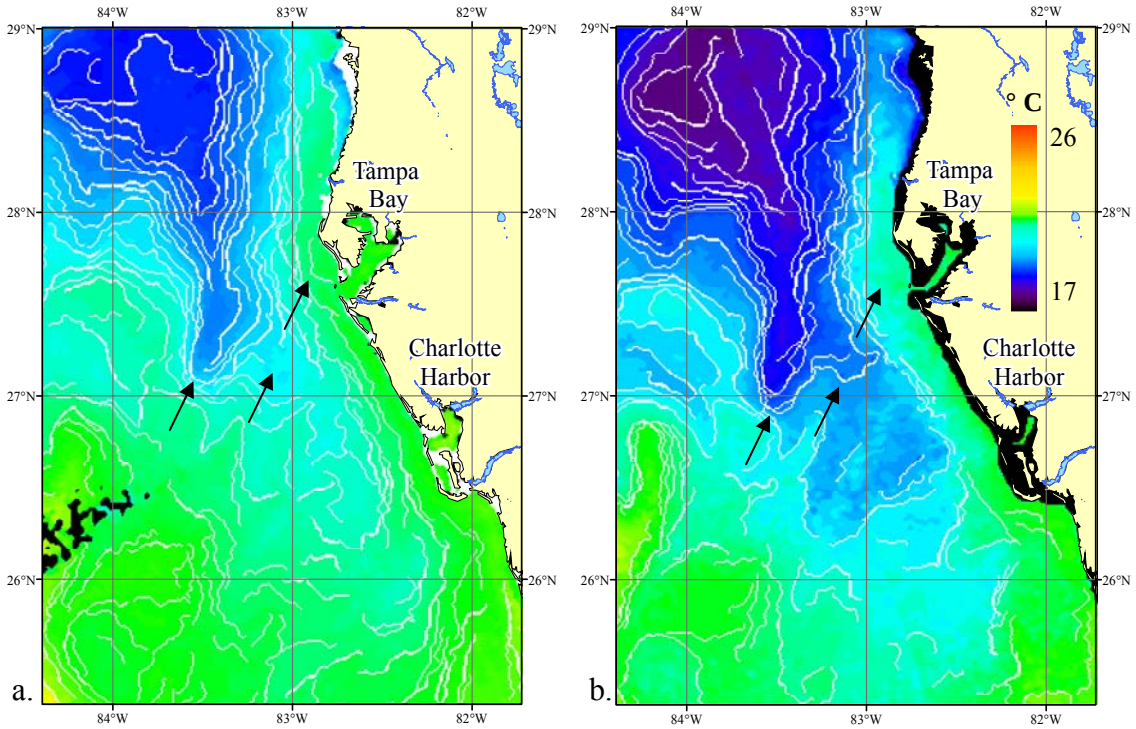


Figure 1-16. Sea surface temperature fronts detected on (a) April 2, 2005 and (b) April 3, 2005. The black arrows on the images correspond to regions of frontal displacement or dissipation/establishment. Areas of black represent the land mask or clouds.

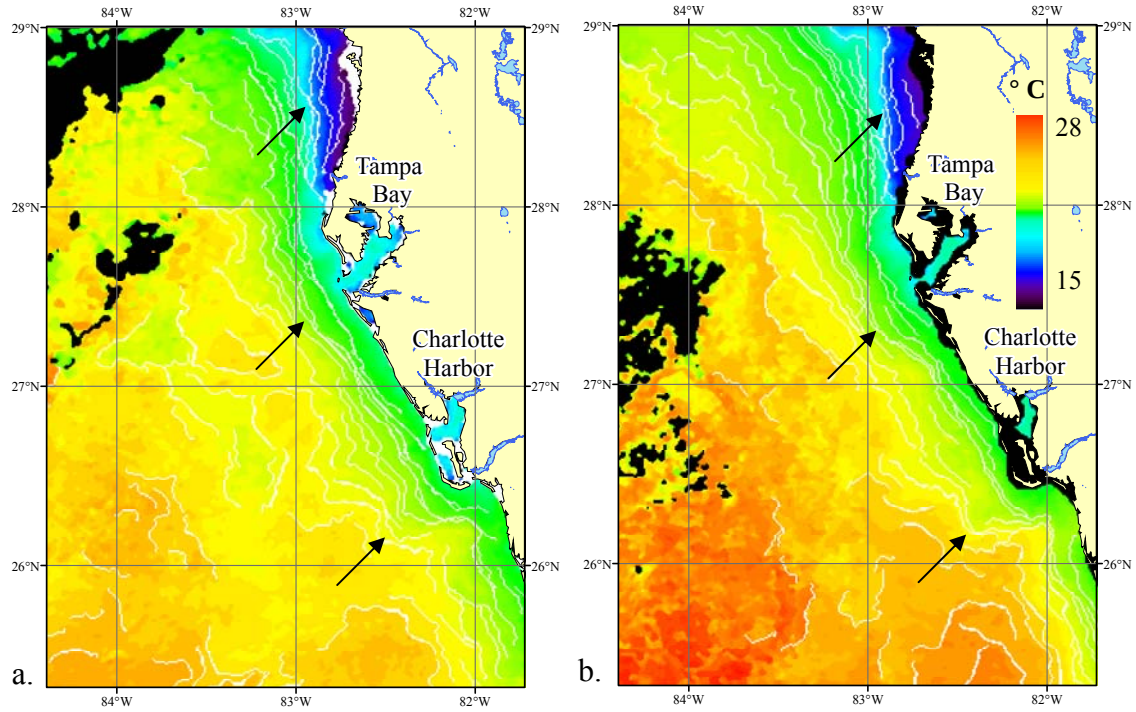


Figure 1-17. Sea surface temperature fronts detected on (a) October 28, 2005 and (b) October 29, 2005. The black arrows indicate regions where fronts showed little change or movement over 48 hours. Areas of black represent the land mask or clouds.

*3.3.5. Sustained Fronts*

Sustained SST, nLw_443, chl+, and FLH fronts were identified on the tournament days; however, they represented only a small fraction of the daily fronts. Of all frontal pixels identified in each tournament day, ~18 ± 14% SST, ~25 ± 18% chl+, ~25 ± 13% nLw_443, and ~17 ± 11% FLH pixels were spatially sustained for up to three days prior (Table 1-1).

Table 1-1. Percent of sustained frontal pixels relative to total number of daily frontal pixels observed on the tournament day. NA denotes data is not available for that tournament day.

| 2004 | SST | chl+ | nLw | FLH |
|---|---|---|---|---|
| 3-Apr | 11.5% | 25.5% | 21.1% | NA |
| 4-Apr | 15.1% | 28.4% | 7.7% | NA |
| 1-May | 45.4% | 23.6% | 29.8% | NA |
| 8-May | 17.4% | 36.1% | 18.5% | NA |
| 23-Oct | 9.6% | 10.6% | 5.8% | NA |
| 30-Oct | 11.4% | 25.2% | 30.8% | NA |
| 6-Nov | 7.6% | 34.8% | 15.6% | NA |
| 7-Nov | 10.7% | 51.4% | 27.6% | NA |
| 13-Nov | 11.0% | NA | NA | NA |

| 2005 | SST | chl+ | nLw | FLH |
|---|---|---|---|---|
| 3-Apr | 10.8% | 44.9% | 33.8% | NA |
| 9-Apr | 12.9% | 14.0% | 13.0% | NA |
| 16-Apr | 21.6% | 5.1% | 21.0% | NA |
| 17-Apr | 8.9% | 10.7% | 6.0% | NA |
| 23-Apr | 31.8% | 27.9% | 27.5% | NA |
| 30-Apr | 10.4% | 55.9% | 35.6% | NA |
| 29-Oct | 32.9% | 6.2% | 21.9% | 9.8% |
| 5-Nov | 58.8% | 5.5% | 51.2% | 25.5% |
| 6-Nov | 15.0% | 0.2% | 49.8% | 4.9% |
| 12-Nov | 30.4% | 46.0% | 25.9% | 26.8% |

Figure 18 shows the combined sustained frontal pixels in the spring (black lines) and fall (blue lines) identified for the 19 tournament days during 2004 and 2005 for SST, nLw_443, and chl+. Sustained fall 2005 FLH pixels are shown in black. Sustained frontal gradients represent the mean magnitude for that pixel for that season. The sustained frontal pixels identified were seasonally located over areas where the steepness of the shelf bathymetry changed near the 20 m and 30 m isobaths, specifically off the mouth of Tampa Bay and to the north. Sustained SST frontal gradients appear to be stronger nearshore, ~9 m depth north of 28° N, and off the mouth of Tampa Bay (Fig. 1-18a) specifically during the fall. Sustained nLw_443 frontal gradients were consistently strong both near and offshore (Fig. 1-18b). Sustained chl+ fronts of relatively stronger gradient were observed nearshore, north of 28° N and outside the mouth of Tampa Bay and Charlotte Harbor (Fig 1-18c). Offshore fall chl+ fronts reflect the increased chl+ gradients observed in the fall of 2005. Sustained FLH fronts were within 10 km of the 30 m or 40 m isobath where HABs were present (Fig. 1-18d). The gradient magnitude of the sustained frontal pixels were compared to the gradient magnitude of the daily frontal pixels using an analysis of variance (ANOVA). No significant difference ($p > 0.05$) between the gradient magnitudes was identified for any of the four parameters.

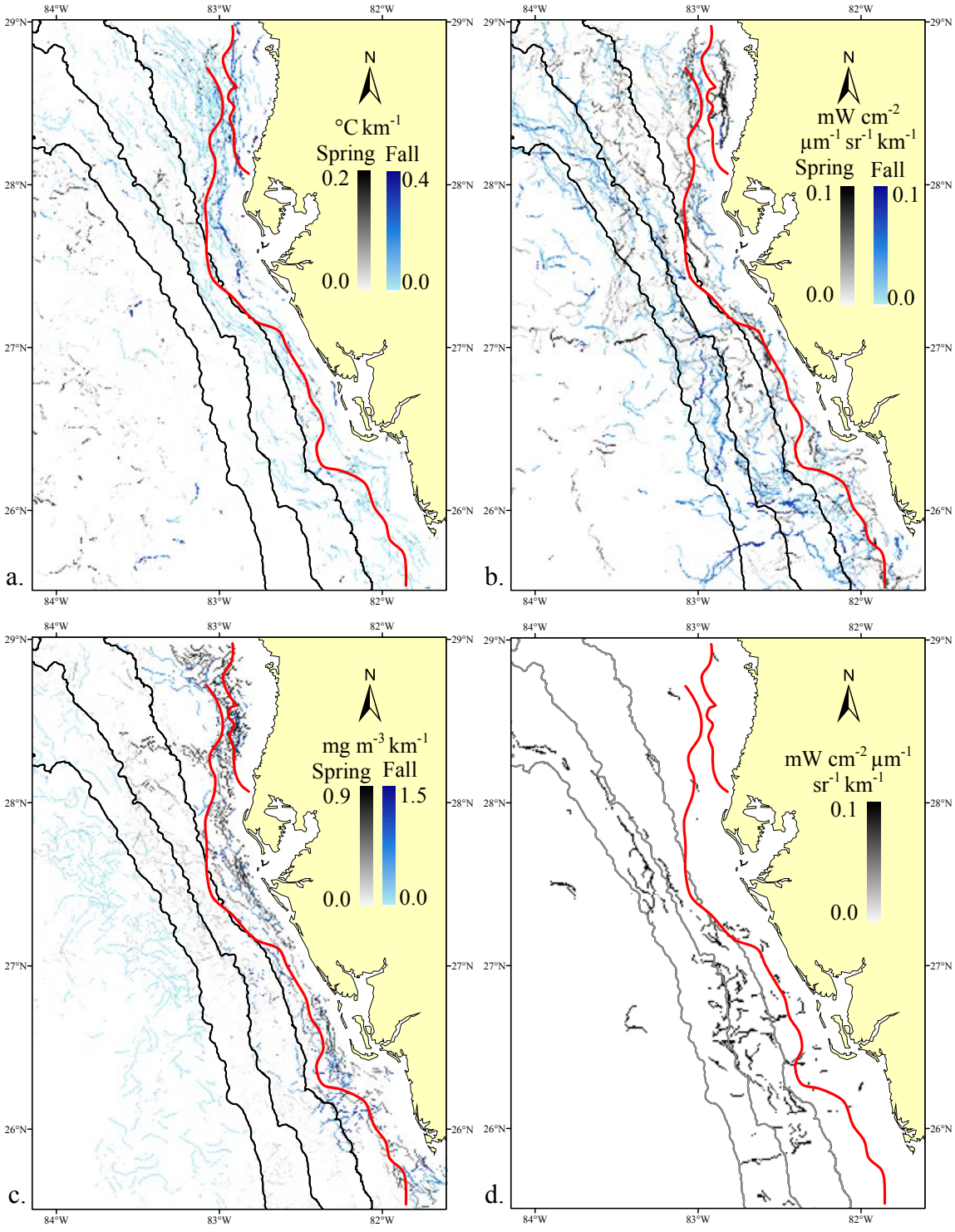


Figure 1-18. Combined sustained fronts detected during this study for (a) SST, (b) nLw_443, (c) chl+, and (d) FLH. Frontal gradients are depicted by the frontal line darkness. Red lines indicate nearshore bathymetric gradients extracted from figure 1-5a. The 20 m, 30 m, and 40 m isobaths are outlined in solid grey lines.

## 4. Discussion

Oceanic fronts were detected over the inner WFS for four remotely sensed parameters, SST, chl+, nLw_443, and FLH, using automated methods adapted for the coastal environment during periods coinciding with recreational kingfish tournaments. The threshold adjustments made to the Cayula and Cornillon (1992) algorithm appeared to produce realistically-shaped fronts for the SST, nLw_443, and FLH data in this region. This algorithm has previously been applied to lake or shelf-break environments. With the threshold modifications developed in this research, it has proved to be useful in detecting coastal surface thermal, water clarity, and fluorescence fronts.

The ability of the Canny method to identify nearshore features (< 10 m depth), specifically at the mouth of Tampa Bay, is shown throughout the chl+ frontal imagery. Detection of weak offshore (> 70 km) features seemed to be more limited. The Canny method analyzes a 3 x 3 pixel box to identify fronts whereas the Cayula and Cornillon (1992) algorithm incorporates at least a 16 x 16 pixel box. The application of the smaller pixel box may allow the Canny method to increase its ability to detect fronts closer to land. However, the sensitivity to detect offshore features within the hysteresis thresholds is lessened in order to decrease the noise detected closer to shore. Additional adjustments to this algorithm are necessary to improve frontal detection across the shelf, though sensitivity to noise may consequently increase. Although this method was originally developed for arbitrary edge profiles, it shows promise for future applications of coastal satellite data when studying coastal chl+ fronts from satellite data. The low (< 2%) percentages of false frontal pixels identified for each parameter demonstrates that the algorithms applied rarely detect false fronts, those associated with insignificant gradients identified by equation (3), and are potentially viable methods for the detection of coastal surface oceanic fronts. While these percentages appear to be low, in situ data, such as coinciding ship tracks, are required to more accurately validate the frontal detection algorithms.

The application of the edge detection algorithms to bathymetry data is a new technique to identify bathymetric gradients and appears to be effective for bottom topography mapping. The Canny method is able to detect gradients closer to shore including within Tampa Bay, and the results mimic the isobaths. The wider spread depth gradients identified by the Cayula and Cornillon (1992) algorithm are more indicative of the characteristic gently sloping shelf and therefore may provide a better representation of the inner WFS bathymetry. Variations in the results of the algorithms results from the technique in how a front is determined. Although, the detected bathymetry gradients have not been ground truth data, those identified by both front detection algorithms, specifically nearshore north of 28° N (< 10 m depth), and along the 20 m and 40 m isobaths, support their statistical significance and spatial location. The application of the edge detection algorithms to a relatively stable environment, such as bathymetry, may be a better subject than dynamic ocean currents to verify the algorithm results.

The thermal fronts detected from the daily satellite data show only the distribution of oceanographic features on the surface ocean. However, the movement of a front over an inertial period, ~26 hours, can be attributed to surface advection or a subsurface movement. A surface "tongue" shaped pool of cold water was evident throughout the spring SST frontal data. This is attributed to vertical stratification controlled by vertical mixing and increased surface heat flux (Virmani and Weisberg, 2003). As the surface heats, differential warming of the nearshore waters cause an offshore temperature gradient (Li and Weisberg, 1999). The cold tongue results as the colder North Eastern GOM (NEGOM) offshore water moves southeastward along the WFS and the inshore waters move northwestward, the predominant circulation pattern during the spring (Weisberg*, et al.*, 1996; Li and Weisberg, 1999; Weisberg*, et al.*, 2005). This feature is also associated with increased salinity and a chlorophyll plume, deemed the "green river" by Gilbes*, et al.* (1996). Fall SST frontal data were consistently detected mirroring the isobaths. This is attributed to ocean dynamics, large heat flux changes, and passing storms that cool the shelf water in a series of step-like temperature decreases from fall to early winter (Virmani and Weisberg, 2003). Stronger winds and cooler air create strong vertical mixing, destratification, and cooling with shoaling depth during this period (Virmani and Weisberg, 2003). With this understanding of the thermodynamics of the circulation, I can better infer the processes driving the establishment and movement of surface thermal fronts.

Interpreting the nLw_443 data for coastal environments proves challenging due to the number of optically active constituents influencing the signal (Hu*, et al.*, 2003). For example, the gradients of lower water clarity off of Tampa Bay in the nLw_443 spring image (April 3, 2004), represented by dark green / blue colors, suggest a patch of light absorbing phytoplankton or CDOM was detected and, in this example, is suspected to be related to upwelling and decreased water clarity. This is strongly supported by the upwelling favorable winds and current depth profiles data concurrently recorded near this region by the USF COMPS C10 observing station (OCG, 2006). Whereas the gradients of higher water clarity detected closer inshore along the coast (near 10 m depth) north of 28° N, represented by red / orange colors, more likely corresponds to bottom reflectance, which impacts all visible wavelengths from 400 to 740 nm (Tolk, 2000). Further inshore (< 9 m depth) in this area, where the color again progresses to green, the increased absorbance of this wavelength is apparent and is most likely due to the presence of seagrass beds. Increased discharge from freshwater systems rich in nutrients and organic matter from tropical systems and storms reduced bottom interference in the fall (Gilbes*, et al.*, 1996; Del Castillo*, et al.*, 2001) and a wider spread influence of the dark green / blue color is apparent directly along the coast in this region. Due to increased backscattering of light, suspended inorganic sediments, apparent at all wavelengths from near 400 to 900 nm (Ritchie*, et al.*, 1976; Tolk, 2000), are also considered to influence coastal nLw_443 estimates resulting in higher water clarity values with increased sedimentation (Hu*, et al.*, 2003). Frontal boundaries of high water clarity off the mouth of Charlotte Harbor and near the Everglades, the bottom right region of this study area, are suspected to be related to suspended sediments in addition to discharge related CDOM. Despite the complications in interpreting this parameter, nLw_443 fronts can be used to distinguish boundaries between masses with varying water clarity.

The occurrence of chl+ fronts at the mouth of Tampa Bay and Charlotte Harbor, most likely reflects the convergence of river plume outflow and marine water inflow. These water masses have been found to influence the development and sustainability of phytoplankton biomass and the production of CDOM formed as a result of biological activity (Del Castillo*, et al.*, 2000). Coinciding with the nLw_443 image, the April 3, 2004 chl+ image also shows a patch of higher chl+ concentrations southwest of Tampa Bay suspected to be related to upwelling. However, the nLw_443 data appeared to portray this event more effectively than the chl+ data and could be an important tool for future analysis of remotely sensed upwelling events.

Highly variable winds were observed throughout this study and the variable current velocities and movements of daily oceanic fronts reflect the influence of the local wind regime. Varying wind speed and direction resulted in an ~80% loss of surface oceanic SST, chl+, nLw_443, and FLH fronts that had been present over the previous 48 to 72 hours. The few days in which winds were less variable showed less movement and dissipation of fronts, and a nearly three-fold increase in the percentage of sustained fronts for each parameter. Wind events alter the shape and relative production of modeled chlorophyll *a* patches at fronts and the wind direction largely dictates the future patch characteristics (Franks and Walstad, 1997). A significant phytoplankton response from an upwelling event is estimated to be at least one day (Franks, 1992). Although few upwelling events corresponded to the study period, the convergence of water masses likely results in a similar delay of trophic-level response. This may also play a role in the impact of non-persistent winds on the stability of a front. Alternatively, the lack of a significant difference between the daily and sustained frontal pixel gradient magnitudes could be due to the transportation of the biomass with the movement of the front. Therefore, while a front moves 10 km over a 24 hour period, it may still retain the same magnitude of biomass suggesting an alternative method for analyzing sustained fronts may be needed. Periods greater than 24 hours over which current velocities were inconsistent with wind velocities may reflect the response of the current to both the wind and other forces such as, but not limited to, continental shelf waves (Buchwald and Adams, 1968; Adams and Buchwald, 1969). Although the local wind regime is the dominant process driving coastal WFS circulation, currents in deeper areas of the WFS can be of oceanic origin, not just wind-driven (Meyers*, et al.*, 2001).

The remaining 20% of the SST, chl+, and nLw_443 fronts that were sustained showed seasonal frequency with the detected bathymetric gradients, specifically along the 20 m and 30 m isobaths. The influence of the bathymetric features on physical processes, such as internal waves, tidal fronts, and wind-induced upwelling (Killworth, 1978; Pingree and Mardell, 1981; Pingree*, et al.*, 1982; Pingree and Le Cann, 1991; Vlasenko, 1992; Franks and Chen, 1996; Harris*, et al.*, 1997) will likely influence the position of the sustained fronts. Additionally, bathymetric gradients within the inner WFS largely impact the Ekman-geostrophic responses to wind-forcing (Li and Weisberg, 1999) and the consequent upwelling events (Weisberg*, et al.*, 2000). Sustained SST fronts were more strongly influenced by bathymetric gradients in the fall than in the spring, which shows more dispersed sustained frontal pixels. This is consistent with the expected seasonal heat flux and circulation patterns described above, and supports the conclusion that bathymetric gradients can influence the establishment and stability of fronts.

Although nearshore chl+ and nLw_443 sustained fronts are consistently detected north of 28° N, water depth is very shallow (~9 m) and bathymetry contours are close together. Therefore, ocean color fronts frequently detected in this region may reflect bathymetric gradients in addition to chl+ and nLw_443 gradients. Bottom reflectance and gradients (up to the 30 m isobath) appear to play a larger role in the spring for chl+ and nLw_443 sustained fronts, which may result from increased river discharge typical of the fall. Use of additional remote sensing products, such as the nLw 412 nm and the nLw 412 nm to nLw 670 nm ratio, will help to identify the extent of seasonal bottom interference on nLw_443 and chl+ frontal data, respectively (Cannizzaro and Carder, 2006). Due to the limited number of passes available for analysis, it is difficult at this point to identify linkages between detected FLH fronts and bathymetry or the surrounding physical processes. However, this does provide an initial understanding of the location, often seasonal, where fronts are more likely to occur.

The review by Weisberg*, et al.* (2005) clearly establishes that the inner WFS is a fully three dimensional system. While this is supported by the frequently coinciding bathymetric gradients and surface features observed in this study, the remotely sensed synoptic observations do not provide a comprehensive understanding of the physical processes, namely stratification of the water column which plays a major role in driving both surface and bottom circulation (Weisberg*, et al.*, 2001; Weisberg*, et al.*, 2004). Additional in situ research incorporating water column and remotely sensed surface observations is needed to confirm the location of stable oceanic fronts and bathymetric gradients detected, and their subsequent influence on marine organisms.

Remote sensing data provides a tool to synoptically analyze large-scale areas with concurrently recorded environmental parameters. The new FLH data product effectively characterized the spatial distribution of surface phytoplankton concentrations for coastal waters off west-central Florida. When supplemented with the in situ observations conducted by FWRI, the extent of phytoplankton concentrations related to the HABs may be identified from the FLH frontal data. The ability to easily detect and track these features daily will aid scientists and resource managers to better understand the processes driving HABs and could potentially lead to identifying their cause and reducing the impact to coastal communities, both marine and terrestrial.

Cloud cover, the ability of the algorithms to correct for unwanted optical constituents, such as water vapor, bottom reflectance, and CDOM present within the signal, and sensor calibration affect satellite data quality and limits the use of the data. Despite these limitations, remote sensing data provided valuable information on how the linkages of physical processes and biological characteristics on the WFS. The maps of sustained fronts and bathymetric gradients, and the relationship observed between the local wind regime, the bottom topography, and the establishment and duration of coastal fronts provides the framework for defining ecosystem relationships in this area. This is likely to help improve our understanding of the influence of the environment on surrounding living marine organisms. Of particular interest is the migratory coastal pelagic fish (e.g. king mackerel), affected by circulation dynamics and the availability of prey. The frontal and bathymetric regions identified in this study are likely to be linked to the accumulation of phytoplankton biomass and higher trophic level organisms such as the prey of king mackerel. This and the effect of bottom relief, and biomass accumulation on king mackerel are considered in the succeeding chapter.

# Chapter 2
# Linkages Between Environmental Conditions and Recreational King Mackerel Catch off West-central Florida

## 1. Introduction

### 1.1 King Mackerel

King mackerel (*Scomberomorus cavalla*) are members of the family *Scombridae*, which also includes tunas. They are a highly migratory pelagic fish that inhabit coastal marine waters from the Gulf of Maine to Brazil, the Gulf of Mexico (GOM) and the Caribbean (Briggs, 1958; Godcharles and Murphy, 1986). Migration patterns extend northward in the Gulf of Mexico and the U.S. east coast in the spring. They congregate both off Texas and the Carolinas in the summer, and move southward along the Florida coasts again in the fall (Sutherland and Fable, 1980; Godcharles and Murphy, 1986; Nakamura, 1987). King mackerel (kingfish) are found off west-central Florida from April to May and from October to November. Their migration route has been reported to remain within coastal ocean temperatures of 20ºC to 26ºC (Manooch, 1979) and a salinity range of 32 to 36 (Godcharles and Murphy, 1986). While their habitat extends to the edge of the continental shelf (200 m), kingfish are most commonly found at depths less than 80 m (Manooch, 1979; GOM and SAFMC, 1985). They seem to prefer areas of hard bottom and reefs (Collette and Nauen, 1983).

Since February 1983, the GOM Fishery Management Council and South Atlantic Fishery Management Council have jointly managed kingfish under the Coastal Pelagic Management Plan (Anon, 1983). Despite numerous studies implementing a variety of techniques for genetic testing, the size and territory of kingfish stocks have not been conclusively delineated (May, 1983; Sutter*, et al.*, 1991; Johnson*, et al.*, 1994; Schaefer and Fable, 1994; DeVries and Grimes, 1997; Gold*, et al.*, 1997; Roelke and Cifuentes, 1997; Broughton*, et al.*, 2002; DeVries*, et al.*, 2002; DeVries and Magnum, 2002; Gold*, et al.*, 2002). Thus, the two management councils (GOM and South Atlantic) continue to use the Atlantic and GOM stocks as definitions of separate populations.

Tagging studies of kingfish populations from 1975 to 1979 by the Florida Department of Environmental Protection identified separate stocks or “migratory groups" in the Atlantic and GOM waters of the U.S. (Williams and Godcharles, 1984; Sutter*, et al.*, 1991). Those caught south of the Volusia-Flagler county border off northeast Florida (29°26’ N, 81°6’ W) from November to March are allocated to the Gulf group since the study suggested more than half of the fish in that zone originated from the GOM migratory group. Throughout the rest of the year, the Monroe-Collier county border off southwest Florida (25°48’ N, 81°19’ W) is considered the dividing line between the two stocks (DeVries, 2003). The water between these two areas is referred to as the mixing zone. In addition to the two groups, the possibility of a residential population of larger kingfish (> 85 cm forklength) in the northwest GOM, that mix with the smaller schooling kingfish (< 85 cm forklength) that migrate to and from Mexico and south Florida, has

been suggested (Collette and Nauen, 1983; Fable, *et al.*, 1987; Trent, *et al.*, 1987). A split in the GOM group, creating an eastern and western stock, was also proposed (Fable, *et al.*, Unpublished).

Collectively termed "baitfish", several coastal clupeids (Spanish sardine *Sardinella aurita*, Atlantic thread herring *Opisthonema oglinum,* and gulf menhaden *Brevoortia patronus*) and small carangids (round scad *Decapterus punctatus*, and blue runner *Caranx crysos*) support large and varied fish stocks in Florida (Mahmoudi, *et al.*, 2002). Baitfish fishery assessment studies (Mahmoudi, *et al.*, 2002) identified pinfish *Lagodon rhombodes*, tomtate *Haemulon aurolineatum*, round scad, Atlantic bumper *Chlorosombrus chrysurus*, mojarra *Eucinostomus spp.*, and Spanish sardine as the most abundant species collected along the west-central coast of Florida from 1994 to 2002. Atlantic thread herring and scaled sardine *Harengula jaguana* comprised 1.8 to 13.9% of the total catch from 1994 to 2002 and scaled sardine was the third most abundant species collected in 1996 (Pierce, 2002). These two latter baitfish species are considered primary prey for the kingfish in waters off Florida (Beaumarriage, 1973).

Clupeids are abundant in surface waters within 6 m to 60 m depth off west-central Florida (Klima, 1971; Pierce and Mahmoudi, 2001). However, thread herring and scaled sardine were typically collected in shallow (< 12.7 m) water (Mahmoudi, *et al.*, 2002). Clupeids are closely associated with the spatial and temporal patterns of phytoplankton biomass (Odum and Heald, 1972; Carr and Adams, 1973; Pierce, 2002) as well as a salinity of ~31 and temperature of ~20°C (Mahmoudi, *et al.*, 2002).

In the mid 1970s, the aggregate potential yield of scaled sardine, thread and round herring, *Etrumeus teres*, and Spanish sardine was estimated to be 545 million kg in the eastern GOM (Houde, *et al.*, 1976; Houde, 1977a, 1977b, 1977c). Despite decreased baitfish landings due to the 1995 net limitation, 7.3 million kg of coastal clupeids were caught of west-central Florida in 1997 making the Tampa Bay region an important producer of baitfish in the GOM (Pierce, 2002). As these are the primary food source for kingfish, the baitfish fishery in the eastern GOM are linked to predator aggregations, such as kingfish, that are drawn to sources of prey.

The focus of this study is to evaluate linkages between oceanographic features and kingfish aggregations. There have been no reported studies in the scientific literature on this topic. Determining the driving oceanographic processes behind movements of pelagic fish is of interest to fisheries managers (Block, *et al.*, 1998; Lutcavage, *et al.*, 1999; Maravelias, 1999; Block, *et al.*, 2000; Brill and Lutcavage, 2001; Palumbi, 2004; Stokesbury, *et al.*, 2004; Block, 2005). Laboratory and field observations identified temperature as a primary factor limiting the range of tunas (Blackburn, 1965; Dizon, *et al.*, 1977; Brill, *et al.*, 1998; Brill, *et al.*, 1999). Salinity, ocean color, dissolved oxygen, and turbidity also affect the distribution of pelagic fish (Sharp and Dizon, 1978; Sund, *et al.*, 1981; Laurs, *et al.*, 1984; Maul, *et al.*, 1984; Brill, 1994; Fréon and Misund, 1999; Sharp, 2000; Brill and Bushnell, 2001).

Similar to other migratory pelagic fish like tuna, swordfish, and sharks (Sund, *et al.*, 1981; Olson, *et al.*, 1994; Bigelow, *et al.*, 1999; Lutcavage, *et al.*, 2000), kingfish are opportunistic feeders and their local daily distribution is likely linked to sources of available prey and the processes driving prey abundance. These processes could include local oceanographic circulation and primary productivity (productivity). Kinesis models (i.e. reaction to ambient conditions) applied to Atlantic bluefin tuna (*Thunnus thynnus*

*thynnus*) migrating from the GOM to the Gulf of Maine suggest that foraging behavior plays a role in the short-term concentration of tuna schools outside their optimum temperature (Humston*, et al.*, 2000).

Upwelling regions and the associated frontal zones result in the vertical flux of nutrients, this leads to high concentrations of near-surface phytoplankton biomass. Convergence at fronts can also lead to the accumulation of materials, creating surface biological features, which will attract forage and apex predators. The influence of oceanic fronts on the distribution of large pelagic fish has been widely studied (Yuen, 1970; Sund*, et al.*, 1981; Maul*, et al.*, 1984; Fiedler and Bernard, 1987; Roffer, 1987; Power and May, 1991; Brill*, et al.*, 1993; Block*, et al.*, 1997; Lutcavage, 1997; Brill*, et al.*, 1999; Block*, et al.*, 2000; Lutcavage*, et al.*, 2000; Brill and Lutcavage, 2001; Schick*, et al.*, 2004; Block, 2005).

Roffer (1987) found that the location and persistence of the frontal mixing zone in coastal waters off Virginia was dependent on local and regional winds and positively correlated with the catch of juvenile Atlantic bluefin tuna (ABT). In the Pacific, the Transition Zone Chlorophyll Front is as an important migration and forage habitat for a variety of large pelagic species (Polovina*, et al.*, 2001; Polovina*, et al.*, 2004; Polovina and Howell, 2005). In addition to oceanic fronts, bathymetric features, such as fish aggregating devices (FADS), seamounts, and submarine canyons have also influenced aggregations of pelagic species (Roffer, 1987; Holland*, et al.*, 1990; Maravelias, 1999; Josse*, et al.*, 2000; Sedberry and Loefer, 2001; Sedberry*, et al.*, 2001). For example, Campana, *et al*. (2002) found higher catch per fishing effort for porbeagle sharks *Lamna nasus* in well-defined areas near the continental shelf edge, where fronts are common.

## 1.2 Gulf of Mexico Circulation

See Chapter 1, Section 1.2 for details of the characteristics and physical processes driving the Gulf of Mexico (GOM) circulation, specifically the inner west Florida shelf.

## 1.3 Objective and Approach

The core hypothesis of this study is that oceanic fronts yield a higher relative catch of kingfish by recreational anglers. A corollary to this hypothesis is that if fronts are spatially sustained for three days or longer before fishing occurred, then they will serve to aggregate kingfish more effectively due to the accumulation of forage, and thus fishing success will be higher at these locations.

Remote sensing techniques have been successfully used in studying the apparent relationship between seasonal tuna distributions and the location, size and condition of pelagic habitats (Laurs*, et al.*, 1984; Maul*, et al.*, 1984; Fiedler and Bernard, 1987; Roffer, 1987; Zuenko*, et al.*, 1992; Kirby*, et al.*, 2000; Brill and Lutcavage, 2001; Schick*, et al.*, 2004). In this study, frontal location and duration will be examined using satellite images of sea surface temperature and sea spectral reflectance (ocean color), local wind and current data. The relative apparent abundance of kingfish, defined by the abundance as affected by availability or number of fish accessible to a fishery relative to similar measures for other periods (Marr, 1951), will be examined using recreational kingfish catch and fishing effort during particular days in spring and fall of 2004 and 2005 and compared with the physical oceanographic observations.

## 2. Methods

### 2.1 Study Area

This study focused on the inner shelf off west-central Florida between 28°30' N, 81°30' W to 26° N, 84°30' W (Fig. 2-1). This area extends from Pasco County south to Collier County, and approximately 180 km into the Gulf of Mexico (GOM) from the coast. Tampa Bay and Charlotte Harbor are two large estuaries located within the study area whose outflow influences coastal water color and buoyancy. While large natural coral reefs do not occur on the inner west Florida shelf, artificial reefs and wrecks provide structure and cover for fish within the study area. Fishing locations recorded within Tampa Bay and Charlotte Harbor and outside the study area are discarded.

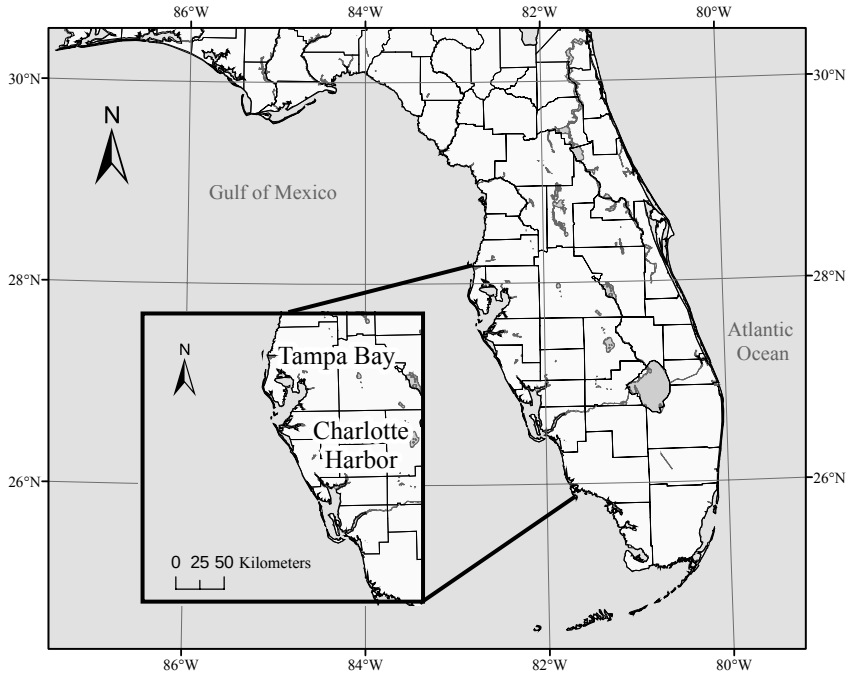


Figure 2-1. Study area located between 28°30' N, 81°30' W to 26° N, 84°30' W (inset). This area extends from Pasco County south to Collier County on Florida's west-central coast and approximately 180 km into the Gulf of Mexico but not Tampa Bay or Charlotte Harbor.

### 2.2 Oceanographic Data

Meteorological data (wind and current velocity data) and satellite imagery, namely sea surface temperature (SST), chlorophyll *a* (chl+), normalized water leaving radiance at 443 nm (nLw_443), and fluorescence line height (FLH, available for fall 2005 only), were collected for the week leading up to the kingfish tournaments. These data were analyzed to assess the influence of the local wind regime on the formation and duration of oceanic fronts, and the relative apparent abundance of kingfish. Oceanic

fronts were determined from the satellite imagery using Cayula and Cornillon (1992) and Canny (1986) frontal detection algorithms adjusted for coastal waters off west-central Florida. The frontal detection algorithms were also applied to high-resolution bathymetry grid data (Divins and Metzger) to identify steep bathymetric gradients (*see* Chapter 1 of this thesis).

Positive or negative signs for the frontal gradient values were identified depending on which side of the nearest front the fishing occurred, i.e. fishing located on the cold side of a thermal front would be reflected by a negative gradient. Daily fronts are defined as the fronts detected within the tournament day composite satellite imagery. Sustained fronts are defined as the frontal pixels that were located within 3.3 km (or 3 pixels) of the frontal imagery three days leading up to and including the tournament day. Distance from fishing activity to the nearest daily and sustained SST, chl+, nLw_443, and FLH front was determined using Euclidean distance. This was carried out using ArcGIS developed by Environmental Systems Research Institute (ESRI$^{TM}$).

A weekly 10-yr mean, 1995-2005, excluding 1998, an El Niño year was compared with the weekly mean for October 28 to November 3, 2004 and October 29 to November 4, 2005 to identify anomalous SSTs coinciding with a strong southward wind and vertical mixing event in the fall of 2005. FLH data was only available in the fall of 2005. Also, mean daily salinity readings coinciding with the tournaments were calculated from a USF Physical Oceanographic Real-Time System (USF PORTS) station located within Tampa Bay, 27°40' N, 82°36' W.

## 2.3 Recreational Kingfish Catch Data

Kingfish catch data were collected during recreational kingfish tournaments held between Clearwater and Sarasota, Florida with the collaboration of participating recreational anglers. Tournaments for this study occurred on:

2004 (10 tournament days): April 3 and 4; May 1, 2, and 8; October 23 and 30; November 6, 7, and 13.

2005 (12 tournament days): March 26; April 3, 9, 16, 17, 23, and 30; October 15 and 29; November 5, 6, and 12.

Dockside interviews were conducted with one angler per boat who returned to the official tournament weigh station. Data on the location, number, and time of kingfish catch; observed presence of baitfish; fishing method; fishing effort, and catch of other, incidental species were collected. Fishing success is defined as the number of kingfish hooked and landed per boat, per fishing location, per tournament day (catch). Fishing effort is defined as the number of kingfish hooked and landed per hour, per line, per boat, per fishing location, per tournament day (CPUE). If the number of lines used was not recorded during the interview, four lines was substituted into the dataset as this is the mean and median number of lines recorded for the entire, yearly, and seasonal study periods, with a standard deviation of $< 1$. Zero catch data were recorded and used for spatial correlation analyses. Normalized catch, CPUE, were used in an attempt to standardize fishing success.

The fisheries data obtained from the surveys depend on the recreational anglers' honesty and cooperation. Telephone interviews were sometimes necessary to obtain additional data on effort, and to clarify or verify information provided at the tournament.

Surveys were discarded if the accuracy of the fishing effort and locations were not verified.

Fishing power of a boat or fishing gear depends on the area or volume affected by the gear, relative to the area covered by the stock, the number of animals present in that area or volume relative to the total stock, and the proportion of the animals in that area or volume that can effectively be captured by the gear (Gulland, 1969). Fishing methods were recorded during the dockside interviews to analyze the effect of fishing power, if any, on the catch rates.

The bottom type over which fishing occurred was determined by fishing directly over a known artificial reef or wreck (bottom structure), directly in the shipping channel (channel), or an undocumented bottom relief (flat). Fishing locations less than 1 km from a bathymetric gradient (*see* Figure 1-10a) were classified as bottom structure. For the statistical analyses, baitfish presence and bottom structure were analyzed as a non-parametric index (1 = high or present, 0 = low or not present, and -1 = not recorded; 1 = over bottom structure, 2 = in the channel, and 3 = over flat bottom). FLH data was not included because it was only available for fall 2005.

## 2.4 Statistical Analyses

Multivariate statistical techniques were used to interpret the results of this study and assess the correlation between the observed environmental conditions (distance of fishing to nearest daily and sustained SST, chl+, and nLw_443 fronts; the corresponding frontal gradients; the derived values of SST, chl+, and nLw_443; baitfish presence; bottom structure; distance of fishing from land, and latitude and longitude of fishing) and the kingfish catch data (Johnson and Kotz, 1972; Anderson, 1984; Zar, 1999). The initial approach consists of solving the linear regression problem between the response variable and the predictor variables:

$$y = xB \qquad (1)$$

where y is the vector of kingfish catch data (response), x is the matrix of environmental conditions (predictor), and B is the matrix of coefficients, or weights, that reflect the effect of each predictor on the response. The magnitude of the weights indicates the relative importance of the predictor variables on the response. To obtain the weights, a principal component regression analysis (PCA) was used,

$$B_{PCA} = u*[x'*x'*x*u]^{-1}*x'*x'*y \qquad (2)$$

where x' defines the transposed predictor matrix and u is the matrix of eigenvectors corresponding to x'*x. This technique is applied when high correlation (collinearity) in the predictor variables results in ill-conditioning of the x'*x matrix and an inverse of the matrix cannot be obtained. The advantage of using PCA is that a subset of the principal components can be used to reduce the collinearity and to obtain adequate estimates of the coefficients, B. For an outline of the eigenvalue problem and PCA, see Appendix B.

In addition to high collinearity, high variability was also present in the dataset such that the variance of the catch observations were similar to the mean, $\sigma^2 \sim \mu$. While this condition impedes simple comparisons of means, an analysis of a counting process

was applied. The result of each recorded fishing location is binomial; kingfish were either caught or not caught. Therefore, the catch data may be represented as a binomial distribution, with a discrete probability distribution of the number of successes in a sequence of *n* independent yes/no events. A good approximation to the binomial distribution under certain conditions is the Poisson distribution, defined as:

$$f(\mathrm{x};\lambda) = e^{-\lambda}\frac{\lambda^{x}}{\mathrm{x!}} \quad \text{for x = 0, 1, 2, …} \qquad (3)$$

where $\lambda$ is a single parameter (Miller and Freund, 1965; Johnson and Kotz, 1969). The Poisson distribution applies when low probability and randomness are inherent in the data, and when a counting process is involved. This method is advantageous for this study's dataset because the two center moments of the distribution, mean and variance, are expressed independently but relate to the same single parameter that characterizes the Poisson, $\mu = \lambda$ and $\sigma^2 = \lambda$. The maximum likelihood estimate (MLE) of the parameter ($\lambda$) of the Poisson and the 95% upper and lower confidence intervals were also calculated. MLE is the sample average of $\lambda$, defined as:

$$\hat{\lambda} = \frac{1}{n}\sum_{i=1}^{n}\mathrm{x}_i \qquad (4)$$

MLE was used to determine significant difference, if any, among Poisson distributions. Kingfish hooked and landed per hour, per fishing location, per tournament day (CPUE) were incorporated into this statistical analysis instead of catch per line, per hour to identify significant relationships. These values were rounded to the nearest whole value in order to more effectively illustrate the Poisson distribution (3). However, the exact values were used to determine the MLE and the corresponding confidence intervals (4).

A balanced one-way analysis of variance (ANOVA) was applied to the environmental data (SST, chl+, and nLw_443 values at the fishing locations) to determine significant differences among the means by season. Reduced variability ($\mu > \sigma^2$) of the SST and nLw_443 data allow for the application of this test. Although the chl+ values were highly variable, the Poisson distribution is not a good representation since the data were not binomial and therefore ANOVA was implemented. ANOVA determines a p-value from the seasonal environmental values. If the p-value is near zero, this suggests at least one season's mean is significantly different from the other seasons' means. For the purpose of this study, p-values less than 0.05 were considered significant (Hogg and Ledolter, 1987). ANOVA assumes all sample populations are normally distributed, have equal variance, and all observations are mutually independent. However, this test is known to be robust to modest violations of the first two assumptions (Hogg and Ledolter, 1987). Box plots representing the lower quartile value (25%), median, upper quartile value (75%), 95% confidence interval for the median, whiskers (extent of data range), and outliers (values more than 1.5 times the interquartile range, the difference between the upper and lower quartile values, away from the top or bottom) (McGill, *et al.*, 1978) were created to show which season, if any, was significantly different.

To determine if significant changes occurred between the seasonal baitfish indices, a Monte Carlo analysis and randomization test were applied. The percent difference of baitfish presence was determined by subtracting the observed baitfish fraction, the number of fishing locations where baitfish were reported present divided by

the total number of fishing locations, of spring 2004 from the observed baitfish fraction of fall 2005. The randomization test consisted of randomly extracting values from zero to one for the total number of fishing locations in spring 2004, and fall 2005. This process was repeated 10,000 times. Values less than 0.49 represented no baitfish present and were set to 0; values greater than 0.49 represented baitfish present and were set to 1. The value 0.49 was chosen since, overall, 51% of the fishing locations recorded baitfish present. The fraction of baitfish present was calculated for each season's random baitfish data. The percent difference was calculated for each of the 10,000 pairs of baitfish fraction. A histogram of the 10,000 percent difference results was created. The probability of the observed percent difference to occur based on the outcome of 10,000 random samples determined the significance between the two seasons. These steps were repeated to compare baitfish indices for all seasons. This method was applied because this parameter does not involve a counting process and does not have reduced variability, and therefore does not meet the conditions of the Poisson distribution nor the ANOVA.

The Monte Carlo analysis assumes the all fishing locations with bait are independent. However, as baitfish are known to school and aggregate under certain environmental conditions this assumption does not hold. Since the extent of spatially dependent fishing locations with baitfish present are unknown, this is simulated in the randomized baitfish data. The modeled occurrence of bait (random values > 0.49) was normalized with a reduced number of fishing locations until an 80% confidence interval was obtained. By systematically reducing the number of locations included in the analysis, I determined the size of the dataset that accounts for spatially dependent fishing locations, i.e. the degrees of freedom or the number of independent observations, without significantly altering the outcome. In more classical statistical tests, this is important when calculating the variance of the mean, defined as the variance ($\sigma^2$) divided by the degrees of freedom (N minus 1 or in this case N minus the number of dependent observations). All statistical analyses outline above were completed using Matlab™ software (Mathworks, Inc.).

# 3. Results

## 3.1 Oceanographic Data

### *3.1.1 Wind and Current Velocity*

Cyclical patterns of changes in wind direction, defined as ~360° rotation from pre-atmospheric front to post-atmospheric front wind direction (Fernandez-Partagas and Mooers, 1975), were observed throughout the study period (*see* Figs. 1-2a, 1-3a, 1-4a, 1-5a, 1-6a, and 1-7a, b). Of the groups of four days preceding and including the tournaments, only November 6, 2004 recorded persistent winds. However, wind strength was greater than 8 m $s^{-1}$ on this date and variable during the three days prior. April 2004 recorded mainly southeastward wind directions during these groups of days, while May 2004, October 2004, October 2005, and November 2005 tended to blow south-southwestward. Persistent winds, defined as 24 hours in which the wind direction did not oscillate greater than approximately +/- 22.5° and wind speed did not change more than 5 m $s^{-1}$ (Virmani, 2006), were not recorded throughout any consecutive four-day period associated with the tournaments. Instead, non-persistent wind directions that changed greater than 90° per day were recorded on 79% of the tournament dates and the three days prior. The remaining 21% of these tournament periods recorded less variable, but still not persistent, wind velocities.

Current direction and speed mostly followed the wind direction and speed, reflecting the influence of the local wind regime on the circulation (*see* Figs. 1-2b, 1-3b, 1-4b, 1-5b, and 1-6b). However, there were several events of opposing current and wind directions over periods greater than 24 hours. In these events, the current direction was mainly northward, while the wind was directed southward.

Mean daily salinity readings at the USF PORTS observing station in Tampa Bay on April 3 and 4, 2004 were 29.3, standard deviation of 0.6, and 30.0, standard deviation of 0.5, respectively. On May 2 and 8, 2004, mean daily salinity were 30.5, standard deviation of 0.6, and 29.4, standard deviation of 1.0, respectively. On October 30, 2004, mean daily salinity was 24.3, standard deviation of 0.2. April 16 and 17, 2005 mean daily salinity were 34.9, standard deviation of 1.1, and 34.5, standard deviation of 1.5, respectively. Kingfish catch were reported within Tampa Bay during these tournament days.

### *3.1.2 Fronts*

Non-persistent winds resulted in an ~80% loss of surface oceanic SST, chl+, nLw_443, and FLH fronts that had been present over the previous 48 to 72 hours. Fronts experienced displacement in excess of 6 km over a 24 hour period when the wind and current speeds were strong (> 8 m $s^{-1}$ and > 10 cm $s^{-1}$, respectively). These displacements occurred when changes in wind direction exceeded 90° over a 24 hour period. This was observed between April 2 to 4, 2004, April 2 to 3, and 29 to 30, 2005. Comparatively, 3 km to 5 km frontal displacement was observed on October 29 to 30, 2004 and on October 28 to 29, 2005, which corresponded to weaker (< 8 m $s^{-1}$) and more persistent wind

velocities in terms of direction. The remaining days within this study period exhibited between 3 km and 10 km daily frontal displacement. The few days in which winds were more persistent corresponded to a nearly three-fold increase in the percentage of sustained fronts.

*3.1.3 Harmful Algal Bloom Events*

Harmful algal blooms (HAB) caused by the toxic dinoflagellate *Karenia brevis* were present off the central west Florida shelf from January through at least November 2005 (FWRI, 2005). The brevetoxin produced by *K. brevis* can be fatal to birds, fish, and other marine organisms. Mass mortalities of fish and marine mammals due to the HAB were reported in Pinellas County from March to November (FWRI, 2006). "Dead zones", anoxic or hypoxic areas which depleted the bottom of respiring organisms, were detected 15 to 25 km off the west-central Florida coast in August (FWRI, 2006). Anglers reported a scarcity of baitfish within the study region throughout the fall of 2005 season. The frontal detection algorithms applied to the nLw_443, chl+, and FLH fall 2005 data identify the boundaries of extreme HAB (*see* Figs. 1-11 and 1-12).

3.2 Detected Bathymetric Gradients

Bathymetric gradients were identified by the oceanographic front detection algorithms formulated by Cayula and Cornillon (1992) and Canny (1986) (*see* Fig. 1-10). Sharp gradients were detected by both algorithms following the 20 m and 40 m isobaths between Tampa Bay and Charlotte Harbor, Florida, and north of 28° N near the 9 m isobath. The Canny method also identified a bathymetric gradient coinciding with the 30 m isobath between the two estuaries.

3.3 Kingfish Survey Data

Surveys were conducted at 22 tournaments over the course of the spring and fall of 2004 and 2005. A total of 666 interviews were completed, 591 of which were deemed useable for the analysis based on the reliability of the angler reporting and the completeness of the survey data. The anglers reported 2,008 kingfish hooked or landed at 792 fishing locations. A total catch of 37 kingfish were reported within Tampa Bay at tournaments held on April 3 and 4, 2004, May 2 and 8, 2004, October 30, 2004, and April 16 and 17, 2005. Since ocean color data were commonly not available less than 5 km from land due to decreased daily satellite coverage, ocean color fronts could not be detected. Therefore, fishing locations in this area were discarded. While SST data were available closer to shore, statistical analysis calculations would have failed due to gaps in the matrix of environmental variables caused by available SST data but no ocean color data. Surveys conducted at tournaments held on March 26, 2005 and October 15, 2005 were not incorporated due to small sample size (N = 2 and 3, respectively). Survey data collected during May 2, 2004 were not incorporated into the frontal analyses due to gaps in ocean color satellite data. Although SST data were available for this date, it was limited to one AVHRR image identified as 'Fair' in Appendix A and statistical analysis calculations would have failed as described above. This reduced the total number of interviews to 415 and the fishing locations analyzed with the frontal data to 579 with 1,599 kingfish reported hooked or landed over 19 tournament days (Fig 2-2).

Trolling was the predominant fishing method used at 74% of the fishing locations and it accounted for 70% of the kingfish catch. Anchoring accounted for 17% of the fishing locations and 22% of the catch, drifting accounted for 4% of the fishing locations and 2% of the catch, and a combination of fishing methods accounted for 3% of the fishing locations and 4% of the catch.

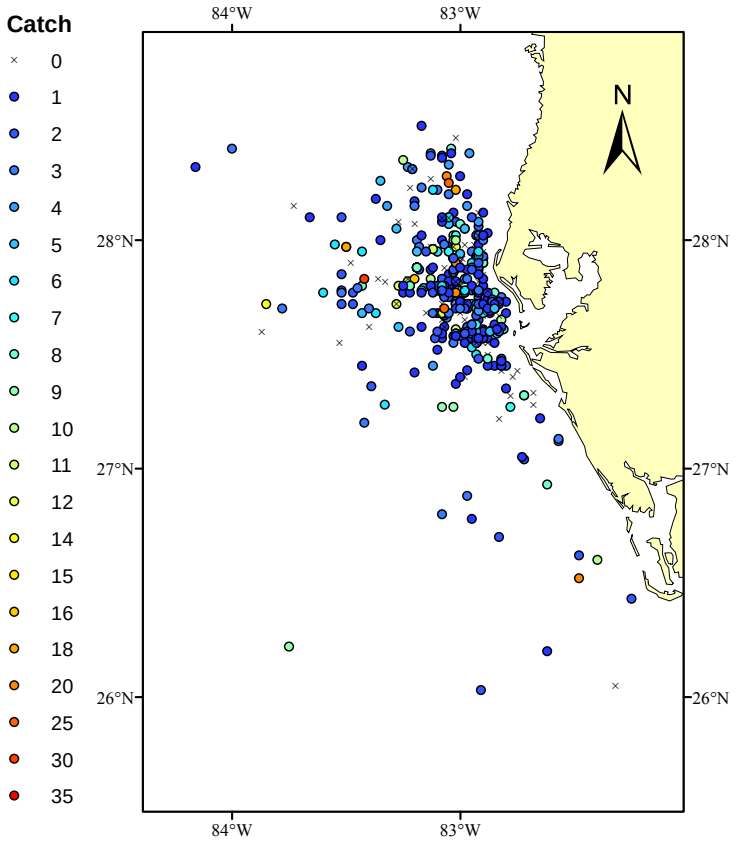


Figure 2-2. Fishing locations and associated kingfish catch from the tournament surveys.

The total number of kingfish caught in the fall of 2005 (208) was much lower than in the preceding seasons (444 for spring 2004, 818 for fall 2004, and 538 for spring 2005). However, the mean number of boats registered for the fall of 2005 tournaments (165) was not significantly lower than the preceding seasons (241 for spring 2004, 122 for fall 2004, and 136 for spring 2005; $p < 0.05$). The Poisson distribution shows the probability of a CPUE value occurring, P(CPUE), for each season (Fig. 2-3a). A smoothed line was interpolated for each Poisson distribution to better illustrate the distributions, however, as this is a discrete probability function the probability values, represented by the symbols, are of most importance. The MLE shows the CPUE value of the Poisson distribution most likely to occur with corresponding confidence intervals for each season (Fig. 2-3b).

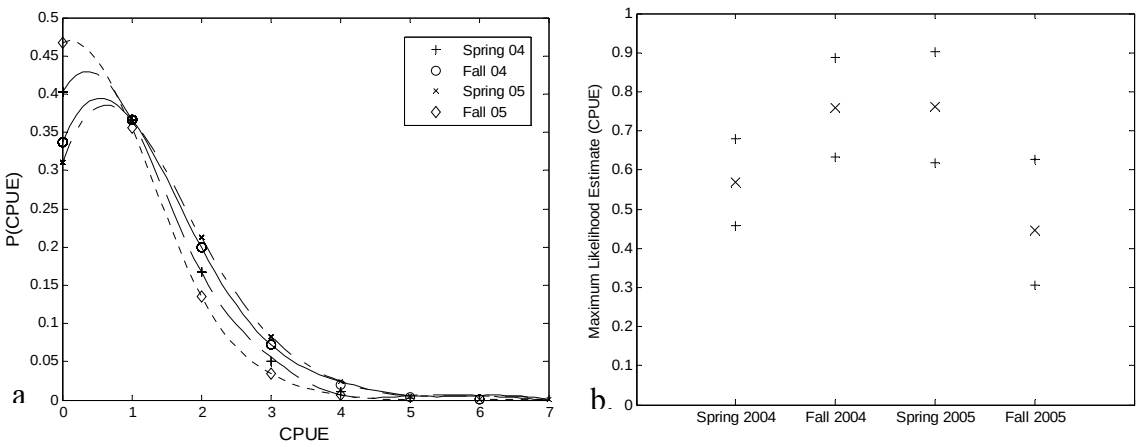


Figure 2-3. Analysis of CPUE recorded by season. (a) Poisson distribution: spring 2004 (+, long dash line), fall 2004, (o, solid line), spring 2005 (x, long and short dash line), and fall 2005 (◊, short dash line). Probability is represented on the y-axis, P(CPUE). (b) Maximum likelihood estimate of the CPUE (x) with 95% confidence intervals (+).

The spring 2004 Poisson distribution (+) shows the probability of catching zero fish (CPUE = 0) to be near 40%. The probability for catching one kingfish per hour (CPUE = 1) is ~36% with decreasing probability for increased catch rates. The fall 2004 Poisson distribution (o) shows the probability of catching zero fish to be near 34%, and the highest probability, ~36%, corresponds to catching one kingfish per hour. The probability for increased catch rates also gradually declines. The spring 2005 Poisson distribution (x) shows the lowest probability of catching zero fish for all seasons, near 30%, and, similar to spring and fall 2004, the highest probability, ~36%, corresponds to catching one kingfish per hour with gradually decreasing probability with increased catch rates. Lastly, the fall 2005 Poisson distribution (◊) shows the highest probability of all seasons for fishing effort when no fish were caught, near 47%. The fall 2005 CPUE data did not exceed four kingfish per hour and showed the lowest probabilities of successfully fishing (CPUE > 0). MLE of CPUE for spring 2004, fall 2004, spring 2005, and fall 2005 were 0.57, 0.76, 0.76, and 0.45, respectively. Within a 95% confidence interval, the fall of 2005 MLE for CPUE is significantly lower than the fall 2004 and spring 2005 MLE but not the spring of 2004.

Table 2-1 summarizes the environmental satellite observations detected at the fishing locations by season. Mean and median values were calculated to identify the influence of overestimations derived from the standard bio-optical algorithms in this coastal environment (Carder, *et al.*, 1991) and potentially skewed data. Figure 2-4 shows the environmental conditions at the fishing locations relative to the corresponding CPUE.

Table 2-1. Summary of environmental conditions at the fishing locations.

| **SST** (°C) | | | | | | |
|---|---|---|---|---|---|---|
| | Mean | Median | Min | Max | SD | N |
| Spring 2004 | 22.5 | 23.0 | 19.0 | 24.6 | 1.5 | 172 |
| Fall 2004 | 24.6 | 24.8 | 22.2 | 26.2 | 1.0 | 183 |
| Spring 2005 | 21.2 | 21.2 | 19.4 | 22.2 | 0.4 | 149 |
| Fall 2005 | 22.9 | 22.6 | 20.4 | 24.8 | 1.0 | 80 |

| **Chl+** (mg $m^{-3}$) | | | | | | |
|---|---|---|---|---|---|---|
| | Mean | Median | Min | Max | SD | N |
| Spring 2004 | 1.1 | 0.9 | 0.1 | 3.7 | 0.7 | 172 |
| Fall 2004 | 2.2 | 2.1 | 0.2 | 9 | 1.3 | 183 |
| Spring 2005 | 2.2 | 1.7 | 0.2 | 5.5 | 1.4 | 149 |
| Fall 2005 | 5.4 | 4.3 | 0.3 | 16.4 | 4.1 | 80 |

| **nLw_443** (mW $cm^{-2}$ $\mu m^{-1}$ $sr^{-1}$) | | | | | | |
|---|---|---|---|---|---|---|
| | Mean | Median | Min | Max | SD | N |
| Spring 2004 | 0.8 | 0.8 | 0.4 | 1.6 | 0.2 | 172 |
| Fall 2004 | 0.8 | 0.8 | 0.3 | 1.9 | 0.3 | 183 |
| Spring 2005 | 0.9 | 0.9 | 0.1 | 3.4 | 0.5 | 149 |
| Fall 2005 | 0.3 | 0.3 | 0.1 | 1.1 | 0.2 | 80 |

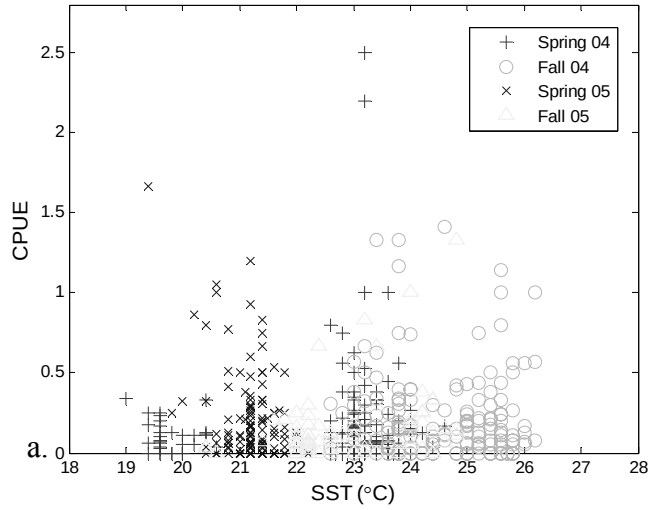


Figure 2-4. Remotely sensed environmental conditions at each fishing location *vs.* CPUE. Data are separated by season: spring 2004 (black +), fall 2004 (dark grey o), spring 2005 (black x), and fall 2005 (light grey Δ) for (a) SST, (b) chl+, and (c) nLw_443.

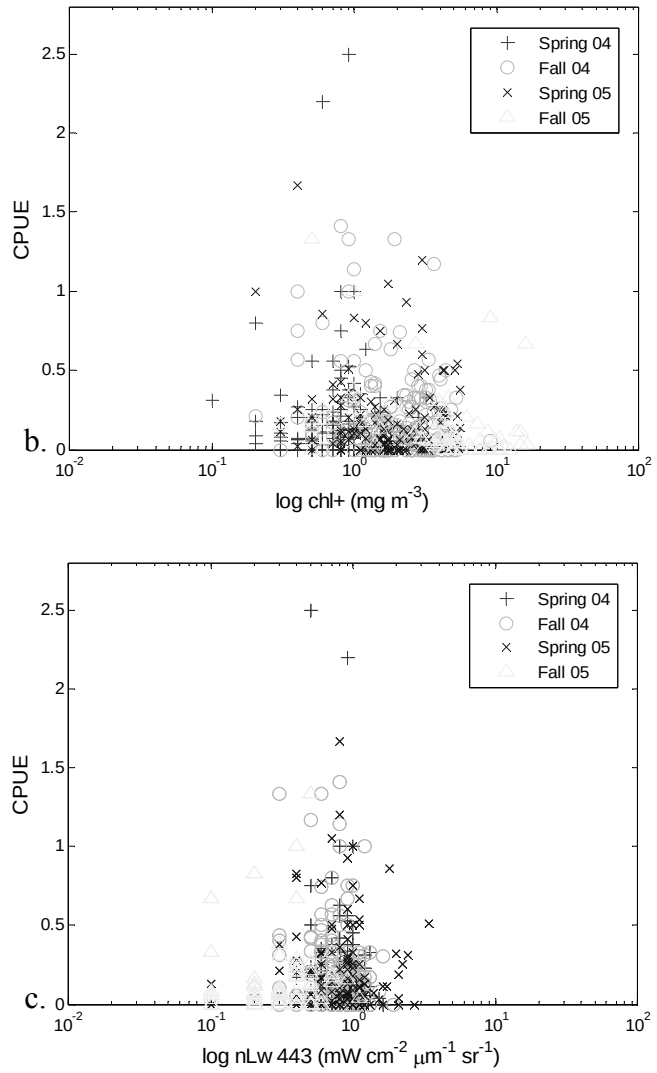


Figure 2-4 (Continued)

The gap of fishing effort between 21°C and 23°C in the spring 2004 data represents the lag in tournaments between April 4, 2004 and May 1, 2004 (*see* Fig. 2-4a). All spring 2005 tournaments took place in April, when recorded SST values appear continuous and in between the spring 2004 temperature gap. Sea surface temperature values recorded at fall 2005 fishing locations were approximately 2°C with a standard deviation less than 1°C lower than in fall 2004.

Weekly SST anomaly images were evaluated with the combined 2004 and 2005 fall fishing locations, N = 266 (Appendix C). Fall 2005 thermal data recorded 1° to 2°C anomalously colder SST compared to fall 2004 over the same locations. This is most likely due to the passage of Hurricane Wilma south of Tampa Bay and an adjacent atmospheric cold front in late October 2005. Spring 2004 and 2005 temperatures were lower than those of fall 2004 and 2005 due to the cooler GOM waters present after the winter, negative heat flux, and warmer waters present after the summer, positive heat flux.

ANOVA demonstrated that all tournament seasons recorded significantly different (p = 0) median SST values (Fig. 2-5). However, the catch for each season did not differ significantly with surface temperature and is attributed to the SSTs for all seasons remaining within the preferred kingfish temperature range, 20 – 26°C (*see* Fig. 2-4a).

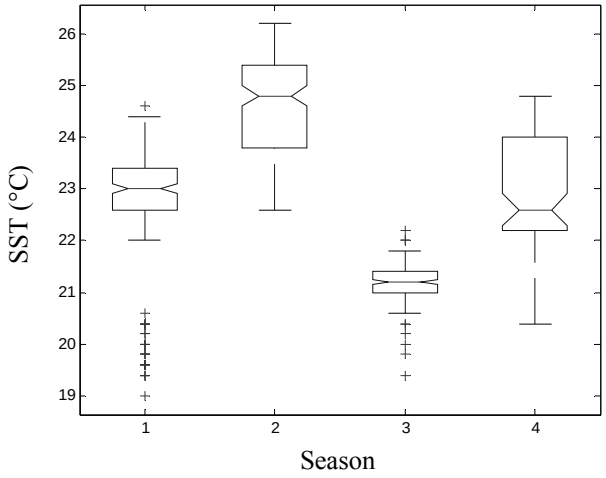


Figure 2-5. Box plot of SST values by season, calculated by ANOVA. Spring 2004 = 1, fall 2004 = 2, spring 2005 = 3, fall 2005 = 4. The median, upper and lower quartile values, and extent of data range are shown; + = outliers.

Chl+ values in spring 2004 ranged from 0.1 to 3.7, fall 2004 and spring 2005 showed a slightly larger range reaching up to 9.0 mg $m^{-3}$, whereas, fall 2005 showed the highest median and maximum chl+ values, 4.3 and 16.4 mg $m^{-3}$, respectively (*see* Table 2-1). However, catch rates varied for all chl+ values (*see* Fig. 2-4b). ANOVA identified significantly different (p = 0) median chl+ values in spring 2004 and fall 2005 (Fig. 2-6).

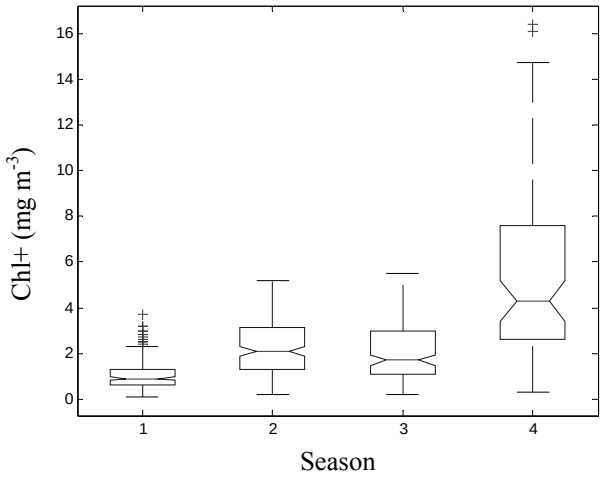


Figure 2-6. Box plot of chl+ values by season, calculated by ANOVA. Spring 2004 = 1, fall 2004 = 2, spring 2005 = 3, fall 2005 = 4. The median, upper and lower quartile values, and extent of data range are shown; + = outliers.

Intermediate water clarity values, 0.7 to 1.0 mW $cm^{-2}$ $\mu m^{-1}$ $sr^{-1}$, were associated with the highest mean catch (2.7 kingfish fishing $location^{-1}$ ± 3.9, max: 30) and the highest mean CPUE rates (0.7 kingfish $h^{-1}$ ± 1, max: 6.67; *see* Fig. 2-4c). Catch and CPUE in fall 2005 coincided with areas of lower water clarity (2 kingfish fishing $location^{-1}$ ± 2.8, max: 18; 0.5 kingfish $h^{-1}$ ± 0.8, max: 4; at < 0.5 mW $cm^{-2}$ $\mu m^{-1}$ $sr^{-1}$). ANOVA identified the fall 2005 median nLw_443 value was significantly different (p = 0; Fig. 2-7).

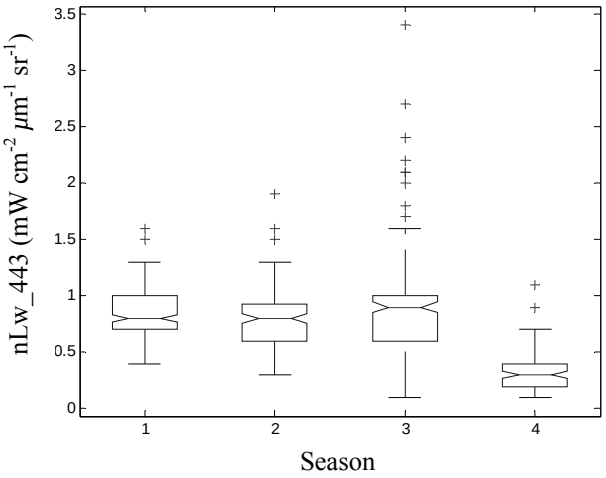


Figure 2-7. Box plot of nLw_443 values by season, calculated by ANOVA. Spring 2004 = 1, fall 2004 = 2, spring 2005 = 3, fall 2005 = 4. The median, upper and lower quartile values, and extent of data range are shown; + = outliers.

Reports where observed baitfish abundance was low or not present accounted for 51% of the fishing locations and represented 31% of the fish caught for all seasons. For fall 2005, 62% of the fishing locations reported baitfish as low or not present and represented 38% of the fish caught. The preceding seasons showed only 46%, 46%, and 48% of the fishing locations with little to no baitfish reported for spring 2004, fall 2004 and spring 2005, respectively. Fishing where baitfish were present occurred 15%, 17%, and 14% more often in spring 2004, fall 2004, and spring 2005 than in the fall of 2005, respectively.

The Monte Carlo analysis identified a significant difference in the baitfish indices between fall 2005 and the three preceding seasons: spring 2004, fall 2004, and spring 2005. The probability of the baitfish indices to have no difference among the seasons was 3% for spring 2004 compared to fall 2005, 1.5% for fall 2004 compared to fall 2005, and 5% for spring 2005 compared to fall 2005. Comparatively, the probability of the baitfish indices to not be significantly different between spring 2004 and fall 2004, when HAB were not present, was 78.7%.

This analysis also identified that if only one third of the fishing locations with baitfish present were incorporated into the randomization test, statistical significance would remain at an 80% confidence interval. This value, ~33%, represents an estimated number of independent observations. Since it is unlikely that two thirds of the fishing locations with baitfish present were dependent considering the temporal scale and the daily oceanographic dynamics, the fishing locations are assumed to be independent. The

overall occurrence of fishing where baitfish were not reported present (49%) was approximately equal to where baitfish were reported present (51%). Therefore, fishing locations where bait were not reported present, which are equally likely to occur as those with baitfish present, are also assumed to be independent. Therefore, the statistical calculations are completed with confidence that the unknown number of dependent observations do not change the significance of the statistical result.

Environmental conditions at fishing locations where CPUE was greater than zero were compared with conditions where CPUE equaled 0 using a Student's *t*-test. The *t*-test values do not show a significant difference between environmental conditions. A list of the environmental variables analyzed and the corresponding *t*-test values are provided in Appendix D with the mean and standard deviation for kingfish fishing effort (CPUE > 0 and CPUE = 0).

The Poisson distribution of CPUE sorted by bottom types (over bottom relief, in the channel, and over flat bottom) was calculated for all fishing locations (Fig. 2-8a). The Poisson distribution for locations over bottom structure (o) shows the lowest probability (30.0%) for catching zero fish (CPUE = 0) and a relatively higher probability for successful fishing (CPUE > 0) compared to the other bottom types. Conversely, the Poisson distribution for locations in the channel (x) showed the highest probability for zero catch (41.0%) and a relatively lower probability for successful fishing compared to the other bottom types. The Poisson distribution for fishing over flat bottom (◊) showed the central probability for zero catch (36.0%), and for successfully fishing. The Poisson distribution was also calculated for fishing locations where baitfish were present and excluded fall 2005 to reduce the influence of the HAB (Fig. 2-8b).

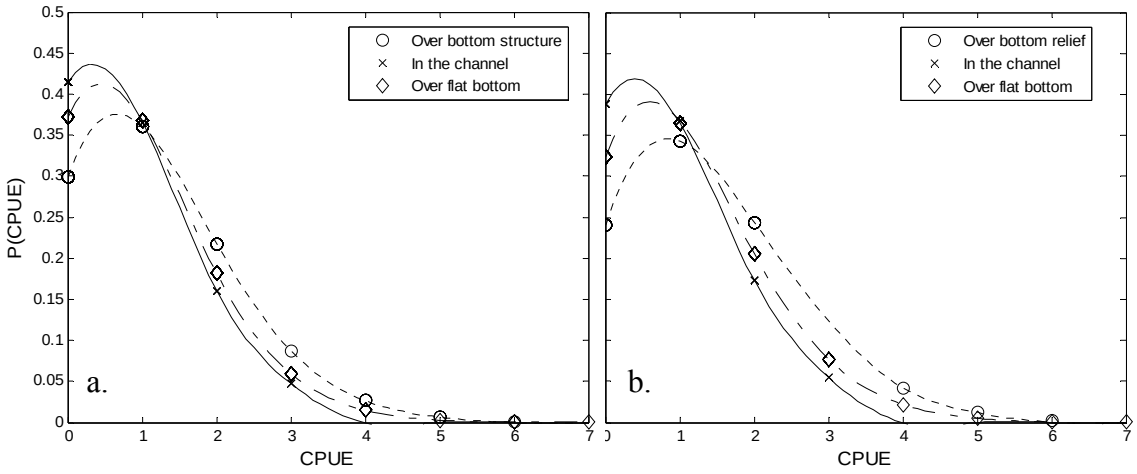


Figure 2-8. Poisson distribution of CPUE by bottom type. Data includes (a) all fishing locations and (b) fishing locations where baitfish were present and not influenced by HAB for fishing over bottom relief (o, short dash line), in the channel (x, long dash line), and over flat bottom (◊, solid line). Probability is represented on the y-axis, P(CPUE).

With 95% confidence, no significant difference is determined between the MLE of the CPUE values by bottom type or between the two datasets, all fishing locations and fishing locations with bait, excluding fall 2005 (Fig. 2-9). This suggests kingfish catch rates and observed baitfish presence were influenced by factors independent of the bottom structure or relief. This is consistent with the positive correlation identified

between the bottom index and the kingfish catch (0.63), CPUE (0.67), which reflects an increase in fishing success and effort with an increase in the bottom index (the highest value was associated with "over flat bottom"). The baitfish index was also positively correlated (0.93) with the bottom index reflecting an increase in the observed presence of baitfish at the fishing locations (the highest value was associated with baitfish present) with fishing locations recorded over flat bottom.

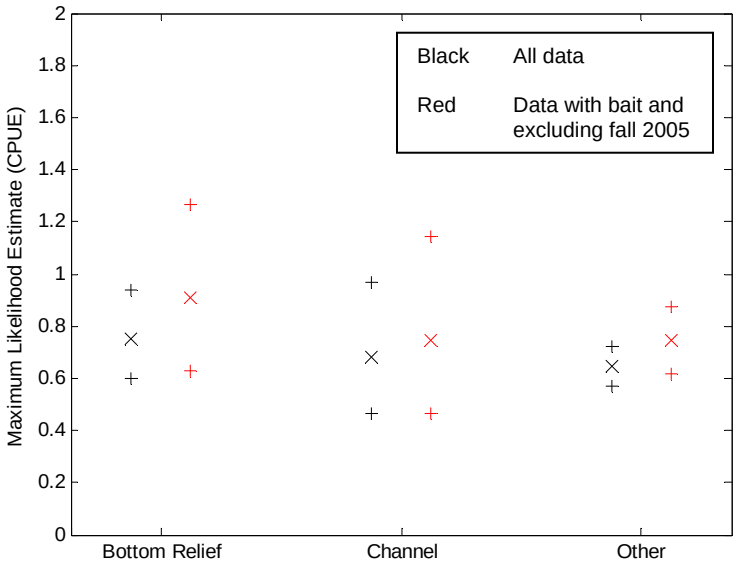


Figure 2-9. Maximum likelihood estimates for CPUE of the Poisson (x) and the 95% confidence interval (+) by bottom type. Black symbols included all fishing locations; red symbols included fishing locations where baitfish were present and excluded fall of 2005.

Fishing locations where baitfish were not reported had the highest probability (0.43) where no fish were caught (CPUE = 0) (Fig. 2-10). The highest probability (0.37) for fishing locations where baitfish were reported present were associated with the catching one kingfish per hour (CPUE = 1). The MLE and 95% confidence intervals show a significantly higher CPUE associated for fishing locations where baitfish are reported present compared to where they are not presents (Fig. 2-11). There was not a significant difference in the distributions when the fall 2005 fishing locations were removed, the likelihood of catching kingfish remained significantly higher where baitfish was present (data not shown). This reflects the connection between the low catch rates and decreased baitfish presence reported in the fall of 2005.

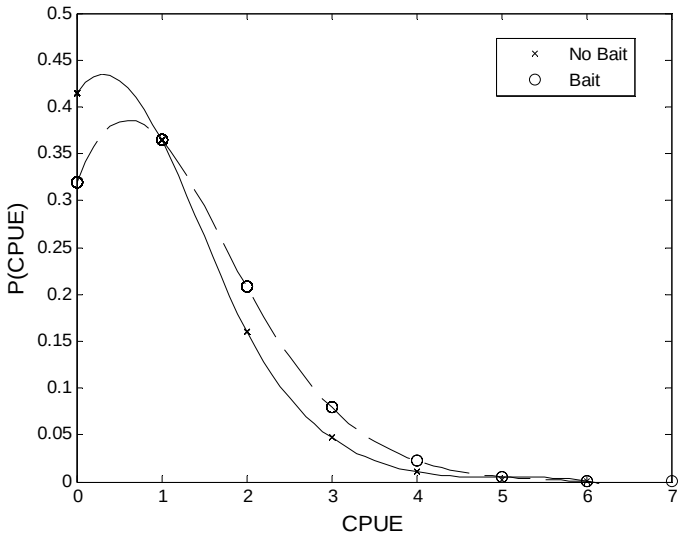


Figure 2-10. Poisson distribution of CPUE by bait presence. Data is separated by fishing locations where bait were present (o, solid line) and not present (x long dash line). Probability is represented on the y-axis, P(CPUE).

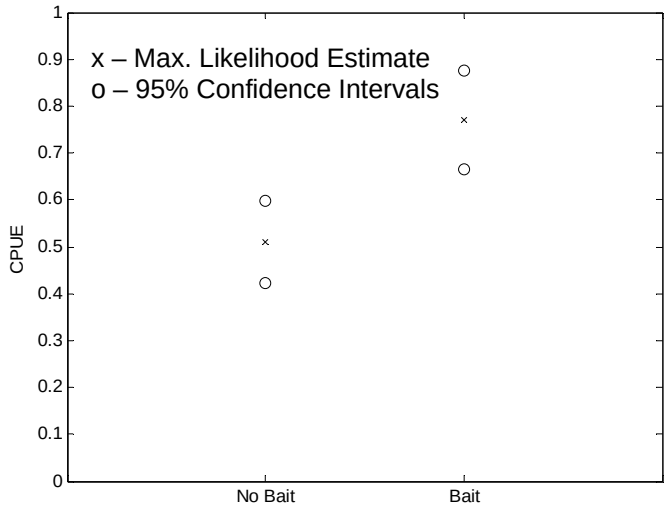


Figure 2-11. Maximum likelihood estimates for CPUE of the Poisson (x) and the 95% confidence interval (+). Data is separated by fishing locations where bait was and was not reported present.

3.4 Kingfish Catch and Proximity to Fronts

For the purposes of this study, catch at distances greater than 10 km from a front were not considered to be related to that front. There is little (or no) documentation on the range of Scombridae sensory perception in the ocean for prey searching, much less account for the effects of varying, short-term wind-driven circulation, depth, and light attenuation on the movements of kingfish. Directional hearing and olfaction (Gooding, 1962; Atema, *et al.*, 1980) may aid the visual sensors to respond to more favorable conditions (Nakamura, 1969, 1972). However, the distances over which these senses

perceive stimuli in the ocean remain undetermined. Unpublished kingfish tracking data in the GOM (Edwards, 2006) recorded ~1 km $h^{-1}$ swimming rates, which defines an estimated radius of 24 km the kingfish may cover per day. During the periods covered by this study, fronts that moved were displaced between 3 km and 10 km per day (*see* Chapter 1 Section 3.3.4), but not having any other information on how fish would detect fronts at large distances, 10 km was chosen as the radius within which a kingfish may be or have been affected by a shifting front.

The Poisson distribution calculated for the distance of fishing locations to the nearest daily front shows the highest probability of fishing occurred ~5 km away from the nearest SST and chl+ fronts, and greater than 10 km away from the nearest nLw_443 and FLH fronts (Fig. 2-12). Therefore, fronts and gradient vectors defined by nLw_443 and FLH data were not included in the PCA.

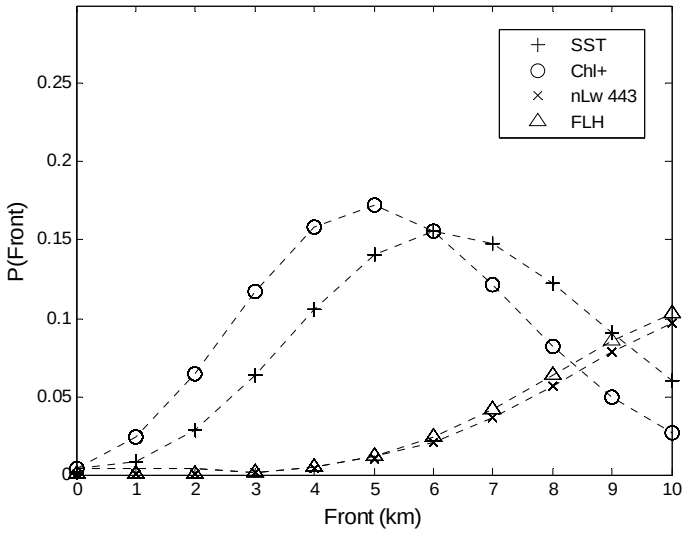


Figure 2-12. Poisson distribution for fishing distances to nearest daily front by parameter: SST (+), chl+ (o), nLw_443 (x), and FLH (Δ). Probability is represented on the y-axis.

The Poisson distribution calculated for distances to nearest sustained SST, chl+, nLw_443, and FLH fronts identified the highest probability of fishing occurred ~25 km away and therefore the sustained frontal data was not incorporated into the analysis (data not shown). Fishing success and fishing effort were highly variable with distance of fishing activity to the nearest daily and sustained front. The influence of additional and potentially synergetic variables driving the observed relative apparent abundance of kingfish was explored.

The PCA and eigenvalue analysis identified five linearly independent environmental variables: distance to nearest daily SST front, distance to nearest daily chl+ front, baitfish presence, nLw_443 value, and chl+ gradient vector. Linear regression of these environmental variables and kingfish catch, CPUE, and CPUE per line found the highest variance in the catch was explained by the nLw_443 value or the distance to nearest daily chl+ front, followed by baitfish presence, distance to nearest daily SST front, and chl+ gradient vector (Table 2-2). Despite slight changes in the weights associated with the variables depending on the response variable incorporated into the

PCA (i.e. catch, CPUE or CPUE per line), this shows a strong correlation between the relative apparent abundance of kingfish and the clarity of the water. A positive coefficient for the distance to the nearest front variables represents increasing distance with increasing catch rates. The influence of the chl+ gradient vector suggests that higher fishing success is associated with fishing on the side of the nearest front with less chl+ where water clarity is relatively higher. Due to the similar relationship identified between the predictor variables and their relative contribution to the response variable, further PCAs will report the results incorporating CPUE per line (CPUE) as the response variable.

Table 2-2. Percentage of weights for the independent variables determined by PCA and linear regression analysis. Results are provided for kingfish catch, CPUE, CPUE per line.

| | Contribution to Kingfish Catch | | |
|---|---|---|---|
| Variable | Catch | CPUE | CPUE per line |
| Chl+ gradient vector | -15.6% | -14.7% | -15.7% |
| Distance to nearest SST front | 20.9% | 9.4% | 10.5% |
| Baitfish index | 16.3% | 10.5% | 11.8% |
| Distance to nearest chl+ front | 22.3% | 42.2% | 38.0% |
| nLw_443 value | 24.9% | 23.3% | 24.0% |

In an attempt to account for the various fishing methods implemented by the anglers, a PCA was calculated for the fishing data where trolling, the predominant fishing method, was used. The five linearly independent variables and corresponding weights identified by PCA and linear regression analysis from this subset of data were distance to nearest daily chl+ front (44.3%), nLw_443 (31.0%), bait presence (14.8%), chl+ gradient vector (-6.2%), and distance to nearest daily SST front (3.9%). Again, decreasing proximity to the chl+ front and increased water clarity at fishing locations on the less chl+ side of the front, and with baitfish present have the most influence on the CPUE.

To reduce the effect of the extreme HABs that occurred in the fall of 2005, a PCA was calculated for data excluding this time period. The five linearly independent variables influencing CPUE and their associated weights were distance to nearest chl+ front (43.9%), chl+ gradient vector (-22.8%), distance to nearest SST front (13.7%), nLw_443 value (12.5%), and bait presence (7.2%). Notably, the variability in the catch data attributed to nLw_443 values here is less than for the overall data (24.0%).

To better define the relationship between kingfish, baitfish and the surrounding environment only the data corresponding to fishing locations where baitfish were reported present were included into the PCA. The results of the five linearly independent variables and their associated weights are as follows: SST gradient vector (41.7%), distance to nearest chl+ front (26.7%), nLw_443 value (-17.1%), distance to nearest SST front (-7.2%), and chl+ gradient vector (7.2%). The majority of the variance in the kingfish catch rates appears to be attributed to the strength of the nearest SST front and increasing proximity to the nearest chl+ fronts. The negative nLw_443 value weight corresponds to decreasing nlw_443 values or those associated with phytoplankton or

CDOM concentrations with increasing fishing success where baitfish are reported present on the side of the front with more chl+ and relatively higher temperature.

Wind speed also affected fishing behavior. Tournament days in which strong wind speed (> 8 m $s^{-1}$) and variable wind direction were recorded, notably on April 4, 2004, April 16, 17 and 30, 2005, and November 12, 2005, corresponded to decreased mean fishing distance from land (< 20 km), decreased mean CPUE (< 50%), and/or increased percentage of fishing effort in the Egmont Channel (>20%) (Appendix E). To remove the influence of strong and highly variable wind velocities, only the data recorded on May 8, October 30, and November 6, 2004; April 23 and October 29, 2005 were incorporated into the PCA analysis. These tournament days correspond to lower wind speeds with more persistent direction. The five independent factors influencing fishing effort were the nLw_443 value (46.0%), SST gradient vector (34.6%), baitfish presence (8.8%), chl+ gradient vector (-6.5%), and distance to nearest SST front (4.2%).

Data recorded at tournaments with more persistent winds (May 8, October 30, and November 6, 2004; April 23 and October 29, 2005) were compared tournaments with highly non-persistent winds (the remaining tournament days) to determine if there was a significant difference in SST, chl+, and nLw_443 values, and the distance of fishing from land. ANOVA and the corresponding box plots identified a significantly higher median chl+ value ($p = 0$), and a significantly lower median SST value ($p = 0$) for the highly non-persistent wind subdataset compared to the more persistent winds subdataset (data not shown). Poisson distributions and the corresponding MLE with confidence intervals were calculated for these two subdatasets to determine if there was a significant difference in CPUE and distance to the nearest SST and chl+ front. The MLEs identified a significantly closer distance to the nearest SST front for the data recorded during more persistent winds. However, CPUE and distance to the nearest chl+ front did not significantly differ with the wind conditions.

## 4. Discussion

The hypothesis proposed, namely that higher fishing success will be observed closer to oceanic fronts, and especially closer to those fronts sustained for periods greater than 48 hours, was not proven. However, relatively strong winds from varying directions and varying current velocities seemed to displace fronts by distances greater than the estimated radius of inertial motion, 3.3 km over 24 hours, and it is likely that the location of catches was offset from the original front by at least these distances. This suggests a time lag of at least 24 hours for the development of a front to affect the location and concentration of the apex predator kingfish. This is consistent with Franks (1992) where research conducted off northwest Africa, and the western coast of the U.S. reported significant phytoplankton responses to occur at least one day after a wind-driven upwelling event. Murphy and Shomura (1958) observed similar patterns in yellowfin tuna *T. albacares*. The displacement of their abundance from the center of the upwelling regions was attributed to the development of each trophic level between zooplankton and tuna with respect to time. Thus, "the geographical distribution of tuna reflects this time lag by showing spatial displacement from the source of the enrichment" (Murphy and Shomura, 1958). Instability and movement of the fronts resulted in a low correlation with catch rates. Re-establishment of a front for at least 24 hours after it moved was found to be an important factor for concentrating baitfish and juvenile ABT (Roffer, 1987). The lack of observed kingfish catch at a front likely reflects the lack of forage concentration due to the constantly moving and weaker frontal gradients. This coincides with the findings of Polovina, *et al.* (2001) and Napp and Hunt (2001). Additionally, Roffer (1987) identified higher juvenile ABT catch rates with well-defined oceanic fronts if they were stable over bottom relief for at least 18 hours.

Bathymetric gradients identified by the frontal detection algorithms were found to influence the position of sustained SST, chl+, and nLw_443 fronts (*see* Fig. 1-18). Benthic topographic features along the coast, 1-2 m high, have been found to influence the movements of skipjack and yellowfin tunas around the main Hawaiian Islands (Yuen, 1970; Holland*, et al.*, 1990; Brill*, et al.*, 1999). However, Brill and Lutcavage (2001) argue the apparent aggregation of these pelagic species with the topography is purely coincidental with the preferred productivity and clarity of the water mass. As a result of the present study, it is proposed that areas of increased bathymetric gradient lead to frontal enhancement as suggested by Pingree and Mardell (1981) and are more likely to have increased forage density, when this enhancement occurs. Apex predators, such as kingfish, concentrate in these zones due to the increased abundance and availability of food. The occurrence of productive water masses in the study zone were shown to be related to bathymetric gradients. Pelagic fish and their prey are also known to aggregate near bottom structures, such as a reef or wreck (Collette and Nauen, 1983; Holland*, et al.*, 1990; Dagorn*, et al.*, 2000; Fromentin and Powers, 2005). Although these regions are highly preferred by anglers, the CPUE, and thus the baitfish, did not differ significantly with bottom type. This is again suspected to be due to the frequently unstable fronts

observed throughout this study. Improved digital databases of validated bottom indices may help to better identify the influence of bottom structure on the surrounding organisms.

Water clarity substantially influenced kingfish catch and effort. Intermediate water clarity values, 0.7 to 1.0 mW $cm^{-2}$ $\mu m^{-1}$ $sr^{-1}$, were associated with the highest CPUE (~7 kingfish per hour) and high catch (up to 30 kingfish per fishing location). This is consistent with Brill and Lutcavage (2001), Roffer (1987), and Fiedler and Bernard (1987) who found movements of juvenile ABT related to chlorophyll concentrations and the consequent forage density, and intermediate water clarity values sufficient for visual predation. Additionally, fishing locations associated with increased nLw_443 values, on the side of the front with less chl+ where baitfish were present, accounted for the greatest variance in the kingfish catch and catch rates. This suggests kingfish avoid more turbid regions as they are visual predators (Blackburn, 1965; Abrahams and Kattenfeld, 1997; Brill and Lutcavage, 2001) or because areas of low water clarity (< 0.5 mW $cm^{-2}$ $\mu m^{-1}$ $sr^{-1}$) observed in the fall 2005 coincided with the extreme HAB.

Previous controlled investigations in the visual acuity of several Scombrids identified the maximum horizontal distance of resolution of prey or body marks in "brightly-lit" surface waters to be up to 40 m (Nakamura, 1968; Brill, *et al.*, 2005). A review of recent research in the visual function in bigeye tuna (Brill, *et al.*, 2005), noted their ability to distinguish different spectrums within the water, confirming the presence of color vision, which enables the tuna to more effectively detect and capture prey particularly in a clear pelagic habitat. The tuna species examined in these visual sensory studies mainly inhabit the open ocean. However, the coastal waters where kingfish are most commonly found are more seldom "brightly-lit". Very little is known of the visual acuity of king mackerel but it is likely to be comparative if not equally developed as in other tunas (Tamura and Wisby, 1963). Therefore, their visual acuity is suspected to be less than the maximum distance of 40 m based on the characteristics of their coastal environment.

The clarity of the water has an ostensible impact on the visual range in which Scombrids are able to detect prey. Decreasing water clarity will further decrease this distance (Utne-Palm, 2002), suspected to be less than 40 m, however the exact relationship is unknown. Additionally, the contrast of the prey against increasingly turbid water may limit visual recognition (Brill, *et al.*, 2005). Despite previous efforts, the current understanding of the visual capabilities of Scombrids is still largely limited. Future investigations into the capacity and sensitivity thresholds of the tuna eye along with characterizing the contrasts of their prey, inherent and apparent, are desired (Kirby, *et al.*, 2000). In general, a smaller nLw_443 value relates to increased turbidity, or a smaller Secchi disk depth. However due to the complications interpreting the nLw_443 product (*see* Chapter 1, Section 4), the exact correlation between nLw_443 and turbidity levels is unknown. Future work supplementing this satellite data with in situ measurements using a Secchi disk will help define this relationship. The in situ data will also identify areas that could interfere with accurately deriving the nLw_443 values, such as shallow or grassy areas.

The influence of baitfish presence on fishing success was evident throughout the study. This is supported by the statistically significant decrease in probability of successful fishing where baitfish were not reported present. This was especially apparent

when HABs were present. During fall 2005, baitfish were observed ~16% less frequently than the previous seasons. Decreased baitfish abundance coincided with the HAB; this was also observed in pinfish surveys conducted from October 30 to November 5, 2005 by FWRI off west-central Florida (Mahmoudi, 2006) (Fig. 2-13). Presumably, the lack of baitfish led to an absence of kingfish, and caused the 53% to 75% decrease in kingfish catch compared to the preceding seasons.

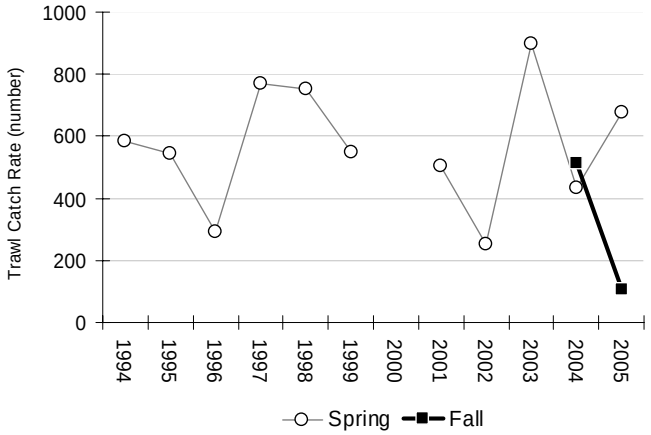


Figure 2-13. FWRI trawl survey catch rates for pinfish along the west-central coast of Florida, 1994 – 2005 (Mahmoudi, 2006).

The abundance of prey, which is driven by the growth or convergence of phytoplankton biomass at a frontal zone, is coupled with the physical processes at oceanic fronts in understanding the distribution and relative apparent abundance of pelagic fish (Fiedler and Bernard, 1987; Olson*, et al.*, 1994). This is consistent with Schick, *et al.* (2004) who suggested that prey data are needed to help understand ABT distribution patterns associated with oceanic fronts. Also, Bigelow, *et al.* (1999) found a greater response of pelagic fish to concentrations of prey species along fronts than just the SST fronts. However, when frontal duration and location is transient, the mechanism to aggregate predators cannot be explained by their proximity to fronts and the resulting prey abundance alone. This was observed in the kingfish catch data where due to non-persistent wind and circulation patterns, the correlation of nearby surface ocean fronts to increased CPUE was insignificant. Therefore, an additional mechanism(s) drove baitfish aggregations, which increased kingfish catch rates.

Intermediate water clarity from chl+ fronts indicative of increased chlorophyll concentrations but not completely turbid waters are suggested to play a significant role in understanding the baitfish index. This is supported by the lower nLw_443 values associated with phytoplankton or CDOM at fishing locations on the higher chl+ concentration side of the front with the observed presence of the filter feeding baitfish. These areas of less clear but suspected productive waters are proposed to be the preferred condition for kingfish catch rates at fishing locations where baitfish were observed. Notably, water clarity affects the accuracy of anglers reporting the presence of baitfish, which is often observed visually. Unfortunately, the effect decreased water clarity had on the ability of the angler to confirm the baitfish presence is unknown but is expected to be insignificant given the sonar technology developed to help anglers find subsurface

schools of bait. The proximity of thermal fronts and their gradient magnitude also influenced the kingfish catch rates (48% of the variance) where baitfish were reported. Therefore, this study was able to quantify the relationships between the relative apparent abundance of kingfish and its forage, which serves as an essential step in forming ecosystem-based management strategies.

For all fishing locations, proximity to thermal fronts and gradient magnitude did not appear to have a strong influence on the fishing effort; accounting, on average, for only 8.2% of the variance in the catch rates. Prior research on the relationship between temperature fronts, and the aggregations and movements of yellowfin tuna in the GOM (Power and May, 1991), and swordfish in the western North Atlantic (Podesta*, et al.*, 1993) similarly could not identify a significant correlation. However, the coarse spatial and temporal scale of their data inherently impeded finding such a relationship. As evident in this study, fronts are dynamic and move or oscillate several to tens of kilometers per day. Averaging this movement over a weekly or monthly period will not accurately represent the oceanographic conditions when fishing occurred. Conversely, movements of albacore *T. alalunga* and skipjack *Katsuwonus pelamis* were found to be associated with temperature fronts in the eastern Pacific (Laurs and Lynn, 1977; Laurs*, et al.*, 1977; Laurs*, et al.*, 1984). These results were successful largely due to a more fine-scaled analysis. The higher spatial and temporal resolution of the remotely sensed thermal data and the fisheries catch data allowed me to more accurately analyze the relationship between the relative apparent abundance of kingfish and surface thermal features. Despite the improved resolution, wind-induced frontal displacement and dissipation that led to unstable fronts during this study period are suggested to be the cause for an overall lack of correlation. However, fishing locations where baitfish were reported present on the warmer side of the nearest thermal front were positively correlated with catch rates suggesting a potential connection between thermal fronts and baitfish, and thus kingfish fishing success.

The exclusion of data influenced by non-persistent winds also demonstrated that water clarity and the chl+ front gradient vector most influenced the CPUE. Due to the limited occurrence of less variable winds, PCA and linear regression analysis were conducted on data for four of the 19 tournaments, accounting for 34% of the total fish caught. Although, the relationship between these variables and the catch represents a portion of the overall dataset, it supports the conclusion that as visual predators, the visibility within the water column plays a significant role in the kingfish's ability to prey on the bait that the anglers used, which increases the chances for angler success. Frontal SST gradient vectors appeared to account for a greater percent of the variance in the catch rates (34.6%) creating a greater influence on the relative apparent abundance of kingfish when wind was more persistent. However, this was not the case for the chl+ gradient vectors which accounted for less variance in the catch rates (-6.5%) in this subdataset compared to the entire dataset (-15.8%). This is consistent with the frontal gradient analysis (*see* Chapter 1 Section 3.3.5), which found no significant increase in gradients associated with sustained fronts. This may be attributed to the transportation of biomass with the moving front. Further data are needed to better define the influence of relatively strong, stable fronts on kingfish catch rates during periods of persistent wind conditions.

Kingfish catch were recorded within Tampa Bay on April 3 and 4, 2004, May 2 and 8, 2004, and October 30, 2004. The daily mean salinity readings corresponding to these tournament days, 29.3, 30.0, 30.5, 29.4, and 24.3, respectively, were lower than Godcharles and Murphy (1986) previously reported preferred salinity range, 32 to 36. This documents kingfish outside of this reported range suggesting that salinity does not play a dominant role in defining their environment. As baitfish presence were not observed at only five out of 18 (~28%) fishing locations additional factors, such as a food source, also likely contribute to the relative apparent abundance of kingfish. This is consistent with Blackburn (1965) who noted the transparency of the water is more likely the limiting factor for kingfish within estuaries where salinity may be lower but run-off is considerable.

4.1 Inherent and Apparent Variability

The relationships identified in the principal component and linear regression analyses provide some insight on the correlations between kingfish catch and environmental conditions, specifically water clarity and baitfish presence. However, the catch distribution was spatially dispersed and fishing success was inconsistent. This is demonstrated by the lack of a significant difference between the environmental conditions where fishing was successful (CPUE > 0) and where it was unsuccessful (CPUE = 0). The following potential causes are provided in an attempt to explain the large variability within the dataset.

Random movement, or 'milling' behavior, creates a possible stochastic influence on the apparent abundance of fish distributions. The net displacement of bonefish in Florida Bay due to random movement, also termed 'random walk', has been suggested to be approximately 8 km $day^{-1}$ compared to approximately 3 km $day^{-1}$ of fish movement due to kinesis, or reaction to ambient conditions (Humston*, et al.*, 2004). Observed in ABT in the Gulf of Maine (Humston*, et al.*, 2000), this behavior may help explain kingfish catch recorded in low water clarity and away from thermal and biologically productive fronts. Therefore, random dispersion may create a wide range of observed environmental conditions in which kingfish are caught. This is indicative of the weak and unstable fronts which did not provide the increased abundance of forage in a concentrated area that one would expect if the fronts were strong and stable (sustained).

The use of remote sensing data and dockside interviews at local tournaments provides a relatively simple and inexpensive method to obtain large-scale data synoptically. The satellite data were provided for free by the USF IMaRS. Unfortunately, there are limitations to these data collection methods. Cloud cover, the ability of the algorithms to correct for unwanted optical constituents present within the signal, and sensor calibration affect satellite data quality to varying degrees and thus create uncertainty that is carried into further applications of some of the data.

The design of this study was such that it did not take into account the water column depth at which the kingfish were caught, specifically their position with respect to the thermal structure of the water column including the mixed layer depth indication by the thermocline depth. The catch data provided only discrete pictures of their horizontal distribution and an approximate sense of abundance. Sharp (1978) and Roffer (1987) showed that catch success in tunas is strongly influenced by these characteristics. However, due to budget limitations water column measurements were not taken. Future

work should include three dimensional surveys of the environmental conditions in the fishery zone. Hopefully the concomitant coverage of the in situ data with the satellite data will allow for the development of indices based on the surface conditions as described by Roffer (1987) and e.g., Cury, *et al.* (1995) and Bakun (1996).

Catchability (q) is defined as the portion of a fish stock which is caught by a unit of fishing effort and depends on the availability, and vulnerability of the fish (Howard, 1963; Garrod, 1964; Ricker, 1975). Boat size, fishing gear, wind speed, sea state, and ocean conditions, such as thermocline depth, temperature, dissolved oxygen concentration, toxic algae, and frontal dynamics, also influence fishing ability. Since there is no professional or amateur distinction in the kingfish tournaments, there was no objective means to account for the different skill or experience levels among the hundreds of anglers that participate. Due to the lack of a control group of captains and vessels, it was not possible to normalize fishing power. Therefore, catchability is assumed equal among the anglers. This is also a current bias in the Marine Recreational Fisheries Statistics Survey, the main national survey method for recreational fisheries (OSB, 2006). The variability of the fisheries data may be attributed to the inherent ability of each individual angler to locate and catch kingfish and to report accurate fishing effort. In addition, intentional reporting errors by the anglers may have contributed to the variability of the data. While the quality control reduced these false reports as much as possible, the degree to which this influenced the data is unknown but considered insignificant. To alleviate this problem in future angler interview-based fisheries research, mandatory electronic log books and data loggers (CTD) are recommended. These technologies have been found to effectively track the location and levels of fishing effort (Rubec, *et al.*, 2005). Similar future research should involve the support of Tournament Directors and an angler education and outreach program, a critical and positive aspect of this research.

Anglers are known to influence the behavior of fish. Adding chum into the water creates an artificial increase in available forage that is independent of the natural concentrating effects by ocean fronts. This lures fish into a small radius, causing higher catch regardless of the environmental conditions (Davis and Stanley, 2002). The time limitations and significant prizes offered at tournaments have led "chumming" to be a common practice, especially when baitfish are scarce. Unfortunately, chumming was not recorded during the dockside interviews as we did not realize its importance during this study. Apparently some of the boats chummed at difference times and areas and the behavior was not consistent between boats and area. This practice may have increased fishing success and effort where baitfish were not reported present which may have muted the significance of fishing where live baitfish were present. The extent of its influence on the kingfish catch and locations is unknown.

Tournaments award prizes to the boat that catches the heaviest kingfish. Therefore, fishing behavior focuses on catching the largest fish, not on quantity, and this biases the study results by skewing fishing success towards a smaller number (*see* Fig. 2-2). Anglers may avoid areas where smaller (< 85 cm), schooling kingfish are observed to target the larger (> 85 cm) kingfish, which are known to exhibit different migratory behavior (Collette and Nauen, 1983; Fable, *et al.*, 1987) and are more commonly solitary. This may lead to different preferred environments based on their size. As large numbers of small kingfish caught at single fishing locations were reported, it is assumed that both

kingfish groups were analyzed jointly and the results indicate a preferred environmental condition for the mixed kingfish groups. This selective fishing behavior impedes further applications of this data for stock abundance or biomass calculations.

Locations where fishing was unsuccessful could result from the inability of the angler to hook the fish and the time of fishing pressure, which could reflect kingfish feeding patterns (Sharp, 1978; Holland, *et al.*, 1990; Buckley and Miller, 1994). However, a better estimate of apparent abundance may be derived by allowing the anglers to fish sunrise to sunset. This is suggested due the findings of previous studies where the movements of Scombrids mirrored the diel vertical migration of small nektonic prey, to depths where dissolved oxygen and temperature are not limiting, in order to exploit these resources (Sund, *et al.*, 1981; Brill, *et al.*, 1999). Additionally, the rapid ascension to the surface during sunrise shown by acoustically tracked yellowfin tuna and archival-tagged bluefin tuna is suggested to be associated with predatory behavior (Block, *et al.*, 1997). The majority of fishing success coincided with the morning to mid afternoon hours (i.e. 7 AM to 2 PM) regardless of lunar phase. Time limitations due to tournament regulations are responsible for the coherence of fishing pressure. In this study, the time of fishing was controlled by the tournaments and thus the data collected provide a measurement of only the relative apparent abundance.

4.2 Recommendations

From the results of this study, a model may be developed to diagnose the condition of the environment that can be used by resource managers to better understand variations in catch that are either the result of naturally occurring phenomena or man-induced overfishing. Models emphasizing water clarity, prey presence, and productive zones may help to link the contribution of these variables to the apparent abundance of this commercially valuable species as well as that of other migratory pelagic species that are less managed. The biological and physical variables identified in this study provide the foundation for future models of king mackerel and other coastal pelagic species, including their forage. This information is critical in understanding the interactions with the ecosystem which should facilitate improved fisheries management. Additionally, the multiple environmental variables influencing the kingfish catch rates show the importance of using environmental data in fisheries management and why the recent push toward an ecosystem-based management regime is warranted.

In order to better understand how the kingfish respond to the changes in the physical and biological components of the WFS, the application of pop-up satellite tags are recommended. The ability of this technique to continuously track the movement of other species, such as tuna, marlin, and marine mammals, proved beneficial towards understand their migratory patterns in addition to simultaneously collecting environmental data such as temperature, and depth (e.g. Jouventin and Weimerskirch, 1990; Block, *et al.*, 1998; Brill, *et al.*, 1999; Block, *et al.*, 2000; Boehlert, *et al.*, 2001; Marcinek, *et al.*, 2001; Graves, *et al.*, 2002; Kerstetter, *et al.*, 2003; Kerstetter, *et al.*, 2004; Wilson, *et al.*, 2005). The high spatial and temporal resolution data on their movements when integrated with remotely sensed satellite data and other in situ data should provide a substantially improved comprehension that this present study began to elucidate. Quantifying the effects of the environment on the baitfish is critically important to understanding the movements, concentration, and relative apparent

abundance of many other economically important and ecosystem important species, such as groupers (*Epinephelus* spp.) on the WFS (Pierce and Mahmoudi, 2001; Mahmoudi, *et al.*, 2002). Therefore, the tagging data should be supplemented with spatially and temporally coinciding fish light detection and ranging (lidar) (Churnside, *et al.*, 2003) and transect surveys that measure baitfish abundance and continuous sea surface temperature and chlorophyll *a* concentrations, which would provide the additional information necessary to analyze the movements of kingfish in relation to the surrounding environment without the influence of the anglers' behavior.

## Chapter 3
## Conclusions

Automated algorithms to detect frontal features in satellite-derived sea surface temperature (SST), chlorophyll concentrations (chl+), normalized water leaving radiance (nLw_443), and fluorescence line height (FLH) images were adapted to study linkages between recreational catch of king mackerel (*Scomberomorus cavalla*) and environmental parameters in coastal waters off west-central Florida. King mackerel (kingfish) catch data were collected through angler interviews during seasonal tournaments held in April to May and October to November of 2004 and 2005. These data were then used to assess the influence of distance to the fronts, strength of the fronts, particular water quality conditions, and abundance of baitfish to catch levels and catch effort. To date, there has been no previous literature reported of investigations that mapped the coastal fronts of the eastern Gulf of Mexico or analyzed the oceanographic conditions influencing the relative apparent abundance of *Scomberomorus* sp.

Thresholds within the Cayula and Cornillon (1992) front detection algorithm, which has mainly been applied to lake and shelf-break regions, were changed to effectively detect fronts on the gently sloping inner west Florida shelf for SST, nLw_443, and FLH data. In addition to using both a 32 x 32 and a 16 x 16 roving pixel box, the histogram ratio to identify frontal populations was changed from 0.76 to 0.72 to increase sensitivity, the coherence threshold of the frontal populations was increased from 0.90 to 0.95, and the frontal length requirement was increased from 10 to 20 pixels. With the threshold modifications developed in this research, it has proved to be useful in detecting realistically-shaped coastal surface thermal, water clarity, and fluorescence fronts and is suggested as an adequate method for future frontal work in similar coastal environments.

The Canny (1986) algorithm appeared to identify chlorophyll fronts better than the adjusted Cayula and Cornillon (1992) algorithm, particularly closer to shore. This study implemented a 7 x 7 pixel Gaussian mask and hysteresis thresholds of 0.05 and 0.08 gradient strength to identify significant edge pixels. Although this method was originally developed for arbitrary edge profiles, it shows promise for future applications of coastal satellite data when studying coastal chl+ fronts from satellite data. However, additional adjustments to the threshold criterion of this algorithm are necessary to improve front detection across the shelf, though sensitivity to noise may consequently increase.

The frontal algorithms were also applied to high-resolution bathymetry grid data. This is a new technique to identify bathymetric gradients and appears to be an effective method to analyze bottom topography. Strong topographic gradients were detected by both algorithms nearshore, north of 28° N, and along the 20 m and 40 m isobaths. Stronger oceanic fronts sustained for periods of about four days frequently coincided with areas of steep bathymetric gradients, particularly near the 20 m isobath. Bottom topography was shown to play a large, and often seasonal, role in the spatial stability of

fronts. However, bottom reflectance could also be reflected in the ocean color gradients detected closer inshore along the coast as it has been found to affect the accuracy of satellite-derived chl+ and nLw_443 estimations. Further investigation in quantifying the extent of the influence bottom reflectance had on the detected ocean color fronts is needed.

The hypothesis that higher CPUE would occur closer to an oceanic front was rejected statistically. Due to non-persistent ocean currents and wind velocities, fronts were generally not sustained or stable, with 80% loss of frontal pixels present from 48 to 72 hours prior to tournament dates. A weak correlation between fronts and the kingfish catch data due to highly variable fishing success and fishing effort in regards to distance of fishing activity to the nearest front. The dissipation and movement of the fronts between 3 and 10 km per day due to the effect of the destructive winds largely accounts for this low correlation. This led to the investigation of additional environmental conditions that contributed to successful fishing.

A strong correlation was found between fishing effort and catch success and water clarity and the presence of baitfish. As kingfish catch rates were highest for fishing locations in intermediate water clarity (0.7 to 1.0 mW $cm^{-2}$ $\mu m^{-1}$ $sr^{-1}$) and where baitfish were present these conditions, on the less chl+ side of a front, are expected to have the greatest influence on fishing success. This is supported by the principal component regression analysis. Due to their strong influence on the catch rates, it is possible that increased coastal development could negatively impact the water quality and thus the success of this coastal fishery. From the results of this study, a model may be developed to diagnose the condition of the environment that can be used by resource managers to better understand variations in catch that are either the result of naturally occurring phenomena or man-induced overfishing.

Kingfish catch significantly decreased in the fall of 2005 (208 kingfish) compared to fall 2004 (818) and spring 2005 (538); this was not apparent in the spring 2004 (404). The percentage of fishing locations where baitfish were observed also significantly decreased in the fall of 2005 (38%) compared to spring 2004 (54%) and 2005 (51%), and fall 2004 (54%). This shows the influence of abundant sources of available prey in aggregating kingfish, which help to increase fishing success. Significantly lower water clarity recorded in the fall of 2005 was also associated with lower catch rates. As they are visual predators, this supports that the clarity of the water influences the aggregations of kingfish and their ability to prey. Concurrent with the HAB episode in the fall of 2005, these observed decreases imply a relationship between kingfish catch rates and water quality.

The FLH satellite data are an effective tool to examine the spatial distribution of surface phytoplankton concentrations in coastal waters off west-central Florida. This product also provided the most accurate parameter to remotely identify the spatial extent of the HAB episode in the fall of 2005. When supplemented with in situ data collection, FLH is recommended for future HAB research to help resource managers easily detect and track the large-scale movements of these features and could potentially lead to identifying their cause and reducing the impact to coastal communities, both marine and terrestrial.

## References


Abrahams, M. and Kattenfeld, M. (1997) The role of turbidity as a constraint on predatory-prey interactions in aquatic environments. *Behav. Ecol. Sociobiol.* **40:** 169-174.

Adams, J. K. and Buchwald, V. T. (1969) The generation of continental shelf waves. *J. Fluid Mech*. **35:** 815-826.

Anderson, T. W. (1984) *An Introduction to Multivariate Statistical Analysis.* New York: John Wiley & Sons, Inc., 704pp.

Anon (1983) Fishery management plan, final environmental impact statement, regulatory impact review, final regulations for coastal migratory pelagic resources (mackerels) in the Gulf of Mexico and South Atlantic region.

Atema, J., Holland, K. and Ikehara, W. (1980) Olfactory responses of yellowfin tuna (*Thunnus albacares*) to prey odors: chemical search image. *J. Chem. Ecol.* **6:** 457-465.

Bakun, A. (1996) Coastal Upwelling Indices, West Coast of North America, 1946-71. *U.S. Dep. Commer., NOAA and NMFS Tech. Rep.* **NOAA-TM-NMFS-SWFSC-231:** 32pp.

Beaumarriage, D. A. (1973) Age, growth and reproductions of king mackerel, *Scomberomorus cavalla*. *Florida Marine Research Institute.* **1:** 45pp.

Belkin, I. M. and Cornillon, P. C. (2003) SST fronts of the Pacific coastal and marginal seas. *Pac. Oceanogr.* **1:** 90-113.

Belkin, I. M. and Cornillon, P. C. (2004) Surface thermal fronts of the Okhotsk Sea. *Pac. Oceanogr.* **2:** 6-19.

Bigelow, K. A., Boggs, C. H. and He, X. (1999) Environmental effects on swordfish and blue shark catch rates in the US North Pacific longline fisher. *Fish. Oceanogr*. **8:** 178-198.

Blackburn, M. (1965) Oceanography and the ecology of tunas. *Oceanogr. Mar. Biol. Ann. Rev.* **2:** 299-322.

Blanton, J. O. (1986) Coastal frontal zones as barriers to offshore fluxes of contaminants. *Rapp. P. v. Reun. Cons. int. Explor. Mer*. **186** 18-30.

Block, B. A. (2005) Physiological ecology in the 21st century: Advancements in biologging science. *Integr. Comp. Biol.* **45:** 305.

Block, B. A., Dewar, H., Blackwell, S. B., Williams, T. D., Prince, E. D., Farwell, C., Boustany, A., Teo, S. L., Seitz, A., Walli, A. and Fudge, D. (2000) Migratory movements, depth preferences, and thermal biology of Atlantic Bluefin Tuna. *Science*. **293:** 1310-1314.

Block, B. A., Dewar, H., Freund, E. V., Farwell, C. and Princes, E. D. (1998) A new satellite technology for tracking the movements of Atlantic bluefin tuna. *Proc. Natl. Acad. Sci. U.S.A.* **95:** 9384-9389.

Block, B. A., Keen, J. E., Castillo, B., Dewar, H., Freund, E. V., Marcinek, D. J., Brill, R. W. and Farwell, C. (1997) Environmental preferences of yellowfin tuna (*Thunnus albacares*) at the northern extent of its range. *Mar. Biol.* **130:** 119-132.

Boehlert, G. W., Costa, D. P., Crocker, D. E., Green, P., O'Brien, T., Levitus, S. and Le Boeuf, B. J. (2001) Autonomous Pinniped Environmental Samplers: Using Instrumented Animals as Oceanographic Data Collectors. *J. Atmos. Oceanic Technol*. **18:** 1882-1893.

Bontempi, P. S. and Yoder, J. A. (2004) Spatial variability in SeaWiFS imagery of the South Atlantic bight as evidenced by gradients (fronts) in chlorophyll a and water-leaving radiance. *Deep-Sea Res. Pt. II*. **51:** 1019-1032.

Bowman, M. J. and Esaias, W. E. (1978) *Oceanic Fronts in Coastal Processes*. New York: Springer-Verlag, 114pp.

Briggs, J. C. (1958) A list of Florida fishes and their distribution. *Bull. Fla. State Mus. Biol. Sci.* **2:** 221-318.

Brill, R. W. (1994) A review of temperature and oxygen tolerance studies of tunas pertinent to fisheries oceanography, movement models and stock assessments. *Fish. Oceanogr.* **3:** 204-216.

Brill, R. W., Bigelow, K. A., Musyl, M. K., Fritsches, K. A. and Warrant, E. J. (2005) Bigeye tuna (*Thunnus obesus*) behavior and physiology and their relevance to stock assessments and fishery biology. *Col. Vol. Sci. Pap. ICCAT*. **57:** 142-161.

Brill, R. W., Block, B. A., Boggs, C. H., Bigelow, K. A., Freund, E. V. and Marcinek, D. J. (1999) Horizontal movements and depth distribution of large adult yellowfin tuna (*Thunnus albacares*) near the Hawaiian Islands, recorded using ultrasonic telemetry: implications for the physiological ecology of pelagic fishes. *Mar. Biol.* **133:** 395-408.

Brill, R. W. and Bushnell, P. G. (2001) The cardiovascular system of tunas. In: *Tuna: Physiology, Ecology, and Evolution*. B. A. Block and E. D. Stevens (eds) San Diego: Academic Press, pp. 79-120.

Brill, R. W., Holts, D. B. G., Chang, R., Sullivan, S. G., Dewar, H. G. and Carey, F. G. G. (1993) Vertical and horizontal movements of striped marlin (*Tetrapturus audax*) near the Hawaiian Islands, determined by ultrasonic telemetry, with simultaneous measurement of oceanic currents. *Mar. Biol.* **117:** 567-574.

Brill, R. W., Lowe, T. E. and Cousins, K. L. (1998) How water temperature really limits the vertical movements of tunas and billfishes - it's the heart stupid! In: *International Conference on the Biology of Fish*. K. Gamperl, A. Farrell and D. MacKinlay (eds) Baltimore, MD: American Fisheries Society, pp. 57-62.

Brill, R. W. and Lutcavage, M. (2001) Understanding environmental influences on movements and depth distributions of tunas and billfishes can significantly improve population assessments. *Amer. Fish. Soc. Symp.* **25:** 179-198.

Broughton, R. I., Stewart, L. B. and Gold, J. R. (2002) Microsatellite variations suggest substantial gene flow between king mackerel (*Scomberomorus cavalla*) in the western Atlantic Ocean and Gulf of Mexico. *Fish. Res.* **54:** 305-316.

Buchwald, V. T. and Adams, J. K. (1968) The propagation of continental shelf waves. *Proc. Roy. Soc. Lond.* **305:** 235-250.

Buckley, T. W. and Miller, B. S. (1994) Feeding habits of yellowfin tuna associated with fish aggregation devices in American Samoa. *Bull. Mar. Sci.* **55:** 445-459.

Campana, S., Joyce, W. and Marks, L. (2002) Population dynamics of the porbeagle in the northwest Atlantic Ocean. *N. Am. J. Fish. Manage.* **22:** 106-121.

Cannizzaro, J. P., Carder, K. I., Chen, F. R., Heil, C. A. and Vargo, G. A. (2004) A novel technique for detection of the toxic dinoflagellate, *Karenia brevis*, in the Gulf of Mexico from remotely sensed ocean color data. *Cont. Shelf Res.* Accepted.

Cannizzaro, J. P. and Carder, K. L. (2006) Estimating chlorophyll *a* concentrations from remote-sensing reflectance in optically shallow waters. *Remote Sens. Environ.* **101:** 13-24.

Canny, J. (1986) A computational approach to edge detection. *IEEE Trans. Pattern Anal. Machine Intell.* **8:** 579-698.

Carder, K. L., Chen, F. R., Cannizzaro, J. P. and Campbell, B. G. (2004) Performance of the MODIS semi-analytical ocean color for chlorophyll-a. *Adv. Space Res.* 1152-1159.

Carder, K. L., Chen, F. R., Lee, Z. P., Hawes, S. K. and Kamykowski, D. (1999) Semianalytic Moderate-Resolution Imaging Spectrometer algorithms for chlorophyll a and absorption with bio-optical domains based on nitrate-depletion temperatures. *J. Geophys. Res.* **104:** 5403-5422.

Carder, K. L., Hawes, S. K., Baker, K. A., Smith, R. C., Steward, R. G. and Mitchell, B. G. (1991) Reflectance model for quantifying chlorophyll a in the presence of productivity degradation products. *J. Geophys. Res*. **96:** 20599-20611.

Carr, W. A. and Adams, C. A. (1973) Food habits of juvenile marine fishes occupying seagrass beds in the estuarine zone near Crystal River, Florida. *Trans. Amer. Fish. Soc.* **102:** 511-540.

Cayula, J.-F. and Cornillon, P. (1995) Multi-image edge detection for SST images. *J. Atmos. Oceanic Technol*. **12:** 821–829.

Cayula, J.-F., Cornillon, P., Holyer, R. and Peckinpaugh, S. (1991) Comparative study of two recent edge-detection algorithms designed to process sea-surface temperature fields. *IEEE Trans. Geosci. Remote Sens.* **29:** 175-177.

Cayula, J.-F. and Cornillon, P. C. (1992) Edge detection algorithm for SST images. *J. Ocean. Techn.* **9:** 67-80.

Chelton, D. B., deSzoeke, R. A., Schlax, M. G., Naggar, K. E. and Siwetz, N. (1998) Geographical variability of the first baroclinic Rossby radius of deformation. *J. Phys. Oceanogr*. **28:** 433-460.

Churnside, J. H., Demer, D. A. and Mahmoudi, B. (2003) A comparison of lidar and echosounder measurements of fish schools in the Gulf of Mexico. *ICES J. Mar. Sci.* **60:** 147-154.

Collette, B. B. and Nauen, C. E. (1983) *FAO Species Catalogue, Vol. 2. Scombrids of the World: An Annotated and Illustrated Catalogue of Tunas, Mackerels, Bonitos, and Related Species Known to Date*. Rome: FAO Fisheries Symposium, 137pp.

Cornillon, P. and Watts, D. R. (1987) Satellite thermal infrared and inverted echo sounder determinations of the Gulf Stream northern edge. *J. Atmos. Oceanic Technol*. **4:** 712–723.

Cury, P., Roy, C., Mendelssohn, R., Bakun, A., Husby, D. M. and Parrish, R. H. (1995) Moderate is better: Exploring nonlinear climatic effects on the Californian northern anchovy (*Engraulis mordax*). *Can. Spec. Publ. Fish. Aquat. Sci.* **121:** 417-424.

Dagorn, L., Bach, P. and Josse, E. (2000) Movement patterns of large bigeye tuna (*Thunnus obesus*) in the open ocean, determined using ultrasonic telemetry. *Mar. Biol.* **136:** 361-371.

Davis, T. L. O. and Stanley, C. A. (2002) Vertical and horizontal movements of southern bluefin tuna (*Thunnus maccoyii*) in the Great Australian Bight observed with ultrasonic telemetry. *Fish. Bull.* **100:** 448–465.

Del Castillo, C. E., Coble, P. G., Conmy, R. N., Muller-Karger, F. E., Vanderbloemen, L. and Vargo, G. A. (2001) Multispectral in situ measurements of organic matter and chlorophyll fluorescence in seawater: Documenting the intrusion of the Mississippi River plume in the West Florida Shelf. *Limnol. Oceanogr.* **46:** 1836-1843.

Del Castillo, C. E., Gilbes, F., Coble, P. G. and Muller-Karger, F. E. (2000) On the dispersal of riverine color dissolved organic matter over the West Florida Shelf. *Limnol. Oceanogr*. **45:** 1425-1432.

DeVries, D. A. (2003) A review of the stock structure of king mackerel off the southeastern U.S.

DeVries, D. A. and Grimes, C. B. (1997) Spatial and temporal variation in age and growth of king mackerel, *Scomberomorus cavalla*, 1977-1992. *Fish. Bull.* **95:** 694-708.

DeVries, D. A., Grimes, C. B. and Prager, M. H. (2002) Using otolith shape analysis to distinguish eastern Gulf of Mexico and Atlantic Ocean stocks of king mackerel. *Fish. Res.* **57:** 51-62.

DeVries, D. A. and Magnum, C. (2002) Maximum likelihood estimates of the stock composition of the east Florida 2000-2001 winter fishery for king mackerel using otolith shape analysis. Panama City, FL: Report to Mackerel Stock Assessment Panel.

Diehl, S. F., Budd, J. W., Ullman, D. and Cayula, J. F. (2002) Geographic window sizes applied to remote sensing sea surface temperature front detection. *J. Atmos. Oceanic Technol*. **19:** 1105-1113.

DiMego, G. J., Bosart, L. F. and Endersen, G. W. (1976) An examination of the frequency and mean conditions surrounding frontal incursions into the Gulf of Mexico and Caribbean Sea. *Mon. Wea. Rev.* **104:** 709–718.

Divins, D. L. and Metzger, D. NGDC Coastal Relief Model, Shaded Relief Images Florida and Eastern Gulf of Mexico Grids, Vol. 3. Available online at: http://www.ngdc.noaa.gov/mgg/coastal/coastal.htm (accessed 01 January 2005).

Dizon, A. E., Neil, W. H. and Magnuson, J. J. (1977) Rapid temperature compensation of volitional swimming speeds and lethal temperatures in tropical tunas (Scombridae). *Env. Biol. Fishes*. **2:** 83-92.

Edwards, R. E., 2006, US Geological Survey, St. Petersburg, FL, pers. comm.

Emery, W. J., Thomas, A. C., Collins, M. J., Crawford, W. R. and Mackas, D. L. (1986) An objective method for computing advective surface velocities from sequential infrared satellite images. *J. Geophys. Res*. **91:** 12865-12878.

Fable, W. A. J., Trent, L., Bane, G. W. and Ellsorth, S. W. (1987) Movements of king mackerel, *Scomberomorus cavalla*, tagged in southeast Louisiana, 1983-1985. *Mar. Fish. Rev.* **49:** 98-101.

Fable, W. A. J., Vasconcelos, J., Burns, K., Osburn, H. R., Schultz, L. and Sanchez, S. (Unpublished) King mackerel, *Scomberomorus cavalla*, movements and migration in the Gulf of Mexico.

Fan, S., Oey, L. Y. and Hamilton, P. (2004) Assimilation of drifter and satellite data in a model of the Northeastern Gulf of Mexico. *Cont. Shelf Res.* **24:** 1001-1013.

Fernandez-Partagas, J. and Mooers, C. N. K. (1975) A subsynoptic study of winter cold fronts in Florida. *Mon. Wea. Rev*. **103:** 742–744.

Fiedler, P. C. and Bernard, H. J. (1987) Tuna aggregation and feeding near fronts observed in satellite imagery. *Cont. Shelf Res.* **7:** 871.

Franklin, S. E., Wulder, M. A. and Lavigne, M. B. (1996) Automated derivation of geographic window sizes for use in remote sensing digital image texture analysis. *Comp. Geosci.* **22:** 665-673.

Franks, P. J. S. (1992) Phytoplankton blooms at fronts: patterns, scales, and physical forcing mechanisms. *Rev. Aquat. Sci.* **6:** 121-137.

Franks, P. J. S. and Chen, C. (1996) Plankton production in tidal fronts: A model of Georges Bank in summer. *J. Mar. Sci.* **54:** 631-651.

Franks, P. J. S. and Walstad, L. J. (1997) Phytoplankton patches at fronts: A model of formation and response to wind events. *J. Mar. Res.* **55:** 1-29.

Fratantoni, P. S., Lee, T. N., Podesta, G. P. and Muller-Karger, F. (1998) The influence of Loop Current perturbations on the formation and evolution of Tortugas eddies in the southern Straits of Florida. *J. Geophys. Res*. **103:** 24759-24780.

Fréon, P. and Misund, O. A. (1999) *Dynamics of Pelagic Fish Distribution and Behaviour Effects on Fisheries and Stock Assessment*. Oxford: Blackwell Science, 348pp.

Fromentin, J. M. and Powers, J. E. (2005) Atlantic bluefin tuna: population dynamics, ecology, fisheries and management. *Fish and Fisheries*. **6:** 281-306.

FWRI (2005) Florida Red Tide Current Status. Available online at: http://research.myfwc.com/gallery (accessed 30 November 2005).

FWRI (2006) Fish Kill Database. Available online at: http://research.myfwc.com/fishkill/ (accessed July 2006).

FWRI (2006) Preliminary Results of FWRI Research Cruise. St. Petersburg, FL: Fish and Wildlife Research Institute.

Garcia, V. M. T., Signorini, S., Garcia, C. A. E. and McClain, C. R. (2006) Empirical and semi-analytical chlorophyll algorithms in the south-western Atlantic coastal region (25–40° S and 60–45° W). *Inter. J. Remote Sens.* **27:** 1539-1562.

Garrod, D. J. (1964) Effective fishing effort and catchability coefficient *q*. *Rapp. R.-v. Réun Cons. Int. Explor. Mer*. **155:** 66–70.

Garver, S. A. and Siegel, D. A. (1997) Inherent optical property inversion of ocean color spectra and its biogeochemical interpretation, 1: Time series from the Sargasso Sea. *J. Geophys. Res*. **102:** 607-618.

Gilbes, F., Muller-Karger, F. E. and Del Castillo, C. E. (2002) New evidence for the West Florida Shelf Plume. *Cont. Shelf Res.* **22:** 2479-2496.

Gilbes, F., Tomas, C., Walsh, J. J. and Muller-Karger, F. E. (1996) An episodic chlorophyll plume on the West Florida Shelf. *Cont. Shelf Res.* **19:** 1201-1224.

Godcharles, M. F. and Murphy, M. D. (1986) Species Profiles: life histories and environmental requirements of coastal fishers and invertebrates (south Florida) – king mackerel and Spanish mackerel. FWS. **82:** 18pp.

Gohin, F., Druon, J. N. and Lampert, L. (2002) A five channel chlorophyll concentration algorithm applied to SeaWiFS data processed by SeaDAS in coastal waters. *Int. J. Remote Sens.* **23:** 1639-1661.

Gold, J. R., Kristmundsdottir, A. Y. and Richardson, L. R. (1997) Mitochondrial DNA variation in king mackerel (*Scomberomorus cavalla*) from the western Atlantic Ocean and Gulf of Mexico. *Mar. Biol.* **129:** 221-232.

Gold, J. R., Pak, E. and DeVries, D. A. (2002) Population structure of king mackerel (*Scomberomorus cavalla*) around peninsular Florida, as revealed by microsatellite DNA. *Fish. Bull.* **100:** 491-509.

GOM and SAFMC (1985) *Final amendment 1, fishing management plan and environmental impact statement for coastal migratory pelagic resources (mackerels) in the Gulf of Mexico and South Atlantic region*. Tampa, FL:

Gooding, R. M. (1962) World Scientific Meeting on the Biology of Tunas and Related Species.

Gordon, H. R. (1997) Atmospheric correction of ocean color imagery in the Earth Observing System era. *J. Geophys. Res*. **102:** 81–170.

Gordon, H. R. and Wang, M. (1994) Retrieval of water-leaving radiance and aerosol optical thickness over the oceans with SeaWiFS: a preliminary algorithm. *Appl. Opt.* **33:** 443-452.

Graves, J. E., Luckhurst, B. E. and Prince, E. D. (2002) An evaluation of pop-up satellite tags for estimating postrelease survival of blue marlin (*Makaira nigricans*) from a recreational fishery. *Fish. Bull*. **100:** 134-142.

Gulland, J. A. (1969) *Manual of Methods for Fish Stock Assessment. Part 1: Fish Population Analysis* FAO Man. Fish. Sci., 154pp.

Hamilton, P., Berger, T. J., Singer, J. J., Waddell, E., Churchill, J. H., Leben, R. R., Lee, T. N. and Sturges, W. (2000) DeSoto Canyon eddy intrusion study: Final report. *Volume II: Technical report. US Dept. of the Interior, Minerals Management Service, Gulf of Mexico OCS Region, New Orleans, LA. OCS Study MMS 2000-080. 275 pp.*

Harris, R. P., Boyd, P., Harbour, D. S., Head, R. N., Pingree, R. D. and Pomroy, A. J. (1997) Physical, chemical, and biological features of a cyclonic eddy in the region of 61°10’N 19°50’W in the North Atlantic. *Deep-Sea Res. Pt. I*. **44:** 1815-1839.

He, R. and Weisberg, R. H. (2002) Tides on the West Florida Shelf. *J. Phys. Oceanogr*. **32:** 3455-3473.

Hogg, R. V. and Ledolter, J. (1987) *Engineering Statistics*. Macmillan Publishing Company, 420pp.

Holland, K., Brill, R. W. and Chang, R. K. C. (1990) Horizontal and vertical movements of yellowfin and bigeye tuna associated with fish aggregating devices. *Fish. Bull.* **88:** 493-507.

Holyer, R. J. and Peckinpaugh, S. H. (1989) Edge detection applied to satellite imagery of the oceans. *IEEE Trans. Geosci. Remote Sens.* **27:** 46-56.

Houde, E. D. (1977a) Abundance and potential yield of the scaled sardine, *Harengula jaguana*, and aspects of its early life history in the eastern Gulf of Mexico. *Fish. Bull.* **75:** 613-628.

Houde, E. D. (1977b) Abundance and potential yield of the round herring, *Etrumeus teres*, and aspects of its early life history in the eastern Gulf of Mexico. *Fish. Bull.* **75:** 61-89.

Houde, E. D. (1977c) Abundance and potential yield of the thread herring, *Opisthonema oglinum*, and aspects of its early life history in the eastern Gulf of Mexico. *Fish. Bull.* **75:** 493-512.

Houde, E. D., Berkeley, S. A., Klinovsky, J. J. and Dowd, C. E. (1976) Ichtyoplankton survey data report. Summary of egg and larvae data used to determine abundance of clupeid fishes in the eastern Gulf of Mexico. *Univ. Miami Sea Grant.* **32:** 193pp.

Howard, G. V. (1963) The matter of availability and the harvest of tunas. *FAO Fish. Rep.* **6:** 1041-1055.

Hu, C., Carder, K. L. and Muller-Karger, F. E. (2000) Atmospheric Correction of SeaWiFS Imagery over Turbid Coastal Waters: A Practical Method. **74:** 195-206.

Hu, C., Carder, K. L. and Muller-Karger, F. E. (2000) Atmospheric correction of SeaWiFS imagery: assessment of the use of alternative bands. *Appl. Opt.* **39:** 3573-3581.

Hu, C., Hackett, K. E., Callahans, M. K., Andréfouët, S., Wheaton, J. L., Porter, J. W. and Muller-Karger, F. E. (2003) The 2002 ocean color anomaly in the Florida Bight: A cause of local coral reef decline? *Geophys. Res. Lett.* **30:** 1151.

Hu, C., Muller-Karger, F., Biggs, D. C., Carder, K. I., Nababan, B., Nadeau, D. and Vanderbloemen, L. (2003) Comparison of ship and satellite bio-optical measurements on the continental margin of the NE Gulf of Mexico. *Int. J. Remote Sens.* **24:** 2597-2612.

Hu, C., Muller-Karger, F. and Swarzenski, P. W. (2006) Hurricanes, submarine groundwater discharge, and Florida's red tides. *Geophys. Res. Lett.* **33:** L11601.

Hu, C., Muller-Karger, F., Taylor, C., Kelble, C., Johns, E. and Heil, C. A. (2005) Red tide detection and tracing using MODIS fluorescence data: A regional example in SW Florida coastal waters. *Remote Sens. Environ.* **97:** 311-321.

Hu, C., Muller-Karger, F., Vargo, G. A., Neely, M. B. and Johns, E. (2004) Linkages between coastal runoff and the Florida Keys ecosystem: A study of a dark plume event. *Geophys. Res. Lett.* **31:** L15307.

Huh, O. K., Wiseman, W. J. and Rouse, L. J. (1981) Intrusion of loop current waters onto the West Florida continental shelf. *J. Geophys. Res*. **86:** 4186-4192.

Humston, R., Ault, J. S., Lutcavage, M. and Olson, D. B. (2000) Schooling and migration of large pelagic fishes relative to environmental cues. *Fish. Oceanogr.* **9:** 136-146.

Humston, R., Osburn, H. R. and Ault, J. S. (2004) Behavioral assumptions in models of fish movement and their influence on population dynamics. *Trans. Amer. Fish. Soc.* **133:** 1304-1328.

Johnson, A. G., Fable, W. A. J., Grimes, C. B., Trent, W. L. and Perez, J. V. (1994) Evidence for distinct stocks of king mackerel, *Scomberomorus cavalla*, in the Gulf of Mexico. *Fish. Bull.* **92:**

Johnson, N. L. and Kotz, S. (1969) *Discrete Distributions*. New York: John Wiley & Sons, Inc., 328pp.

Johnson, N. L. and Kotz, S. (1972) *Distributions in Statistics: Continuous Multivariate Distributions*. New York: John Wiley & Sons, Inc., 333pp.

Josse, E., Dagorn, L. and Bertrand, A. (2000) Typology and behaviour of tuna aggregations around fish aggregating devices from acoustic surveys in French Polynesia. *Aquat. Living Resour.* **13:** 183-192.

Jouventin, P. and Weimerskirch, H. (1990) Satellite tracking of Wandering albatrosses. *Nature*. **343:** 746-748.

Kerstetter, D. W., Luckhurst, B. E., Prince, E. D. and Graves, J. E. (2003) Use of pop-up satellite archival tags to demonstrate survival of blue marlin (*Makaira nigricans*) released from pelagic longline gear. *Fish. Bull*. **101:** 939–948.

Kerstetter, D. W., Polovina, J. J. and Graves, J. E. (2004) Evidence of shark predation and scavenging on fishes equipped with pop-up satellite archival tags. *Fish. Bull.* **102:** 750-756.

Killworth, P. D. (1978) Coastal upwelling and kelvin waves with small longshore topography. *J. Phys. Oceanogr*. **8:** 188-205.

Kirby, D. S., Fiksen, O. and Hart, P. J. B. (2000) A dynamic optimisation model for the behaviour of tunas at ocean fronts. *Fish. Oceanogr.* **9:** 328-342.

Klima, E. F. (1971) Distribution of some coastal pelagic fishes in the western Atlantic. *Comm. Fish. Rev.* **33:** 21-34.

Koblinsky, C. J. (1981) The M 2 tide on the West Florida Shelf. *Deep-Sea Res.* **28A:** 1517–1532.

Laurs, R. M., Fiedler, P. C. and Montgomery, D. R. (1984) Albacore tuna catch distributions relative to environmental features observed from satellites. *Deep-Sea Res.* **31:** 1085-1099.

Laurs, R. M. and Lynn, R. J. (1977) Seasonal migration of North Pacific albacore, *Thunnus alalunga*, into North American coastal waters: distribution, relative abundance, and association with Transition Zone waters. *Fish. Bull.* **75:** 795-822.

Laurs, R. M., Yuen, H. S. H. and Johnson, J. H. (1977) Small-scale movements of albacore, *Thunnus alalunga*, in relation to ocean features as indicated by ultrasonic tracking and oceanographic sampling. *Fish. Bull.* **75:** 347-355.

Le Fevre, J. (1986) Aspects of the biology of frontal systems. *Adv. Mar. Biol.* **23:** 163-299.

Lenes, J. M., Darrow, B. P., Cattrall, C., Heil, C. A., Callahan, M., Vargo, G. A., Byrne, R. H., Prospero, J. M., Bates, D. E. and Fanning, K. A. (2001) Iron fertilization and the trichodesmium response on the West Florida Shelf. *Limnol. Oceanogr.* **46:** 1261-1277.

Li, Z. and Weisberg, R. H. (1999) West Florida shelf response to upwelling favorable wind forcing: Kinematics. *J. Geophys. Res*. **104:** 13507-13528.

Liew, S. C., Chia, A. S. and Kwoh, L. K. (2001) Evaluating the validity of SeaWiFS chlorophyll algorithm for coastal waters. *22nd Asian Conference on Remote Sensing*, 5-9.

Liu, Y., 2005, University of South Florida, St. Petersburg, FL, pers. comm.

Lutcavage, M., Brill, R. W., Skomal, G. B., Chase, B. C., Goldstein, J. L. and Tutein, J. (2000) Tracking adult North Atlantic bluefin tuna (*Thunnus thynnus*) in the northwestern Atlantic using ultrasonic telemetry. **137:** 347-358.

Lutcavage, M. E. (1997) Distribution, relative abundance, and behavior of giant bluefin tuna in New England waters, 1995. *International Commission for the Conservation of Atlantic Tunas*, Madrid. **XL VI 2:** 332-347.

Lutcavage, M. E., Brill, R. W., Skomal, G. B., Chase, B. C. and Howey, P. W. (1999) Results of pop-up satellite tagging of spawning size class fish in the Gulf of Maine: do North Atlantic bluefin tuna spawn in the Mid-Atlantic? *Can. J. Fish. Aquat. Sci.* **56:** 173-177.

Lutcavage, M. E., Brill, R. W. T., Skomal, G. B. T., Chase, B. C. T., Goldstein, J. L. T. and Tutein, J. T. (2000) Tracking adult North Atlantic bluefin tuna (*Thunnus thynnus*) in the northwestern Atlantic using ultrasonic telemetry. *Mar. Biol.* **137:** 347-358.

Mahmoudi, B., 2006, Fish and Wildlife Research Institute, St. Petersburg, FL, pers. comm.

Mahmoudi, B., Pierce, D., Wessel, M. and Lehnert, R. (2002) Trends in the Florida baitfish fishery and an update on baitfish stock distribution and abundance along the central West Coast of Florida. *Florida Fish and Wildlife Conservation Commission, Florida Marine Research Institute.* 41pp.

Manooch, C. S. I. (1979) Recreational and commercial fisheries for king mackerel, *Scomberomorus cavalla*, in the South Atlantic Bight and Gulf of Mexico, USA. In: *Proceedings of the Mackerel Colloquium.* E. L. Nakamura and J. H. R. Bullis (eds) Gulf States Marine Fisheries Commission, pp. 33-41.

Maravelias, C. D. (1999) Habitat selection and clustering of a pelagic fish: effects of topography and bathymetry on species dynamics. *Can. J. Fish. Aquat. Sci.* **56:** 337-450.

Marcinek, D. J., Blackwell, S. B., Dewar, H., Freund, E. V., Farwell, C., Dau, D., Seitz, A. C. and Block, B. A. (2001) Depth and muscle temperature of Pacific bluefin tuna examined with acoustic and pop-up satellite archival tags. *Mar. Bio.* **138:** 869-885.

Marr, J. C. (1951) On the Use of the Terms Abundance, Availability and Apparent Abundance in Fishery Biology. *Copeia*. **1951:** 163-169.

Marra, J., Houghton, R. W. and Garside, C. (1990) Phytoplankton growth at the shelf-break front in the Middle Atlantic Bight. *J. Mar. Res.* **48:** 851-868.

Maul, G., Williams, F., Roffer, M. and Sousa, F. M. (1984) Remotely sensed oceanographic patterns and variability of bluefin tuna catch in the Gulf of Mexico. *Oceanol. Acta*. **7:** 469-479.

Mavor, T. and Bisagni, J. (2001) Seasonal variability of sea-surface temperature fronts on Georges Bank. *Deep-Sea Res. Pt. II*. **48:** 215-243.

May, B. (1983) Genetic variation in king mackerel (*Scomberomorus cavalla*) FLDNR. **Contract C-14-34:** 20pp.

McGill, R., Tukey, J. W. and Larsen, W. A. (1978) Variations of Box Plots. *Amer. Statistician*. **32:** 12-16.

Meyers, S. D., Siegel, E. M. and Weisberg, R. H. (2001) Observations of currents on the West Florida Shelf break. *Geophys. Res. Lett.* **28:** 2037-2040.

Miller, I. and Freund, J. E. (1965) *Probability and Statistics for Engineers*. Englewood Cliffs, N.J: Prentice-Hall, Inc,

Mitchum, G. T. and Clarke, A. J. (1986) Evaluation of frictional, wind-forced long-wave theory on the west Florida shelf. *J. Phys. Oceanogr*. **16:** 1029-1037.

Mitchum, G. T. and Clarke, A. J. (1986) The frictional nearshore response to forcing by synoptic scale winds. *J. Phys. Oceanogr*. **16:** 934-946.

Molinari, R. L. and Morrison, J. (1988) The separation of the Yucatan current from the Campeche Bank and the intrusion of the Loop Current into the Gulf of Mexico. *J. Geophys. Res*. **93:** 10645-10654.

Morel, A. and Prieur, L. (1977) Analysis of variations in ocean color. *Limnol. Oceanogr.* **22:** 709-722.

Murphy, G. I. and Shomura, R. S. (1958) *Proc. 9th Pac. Sci. Congress*. **16:** 108-113.

Nakamura, E. L. (1968) Visual Acuity of Two Tunas, *Katsuwonus pelamis* and *Euthynnus affinis*. *Copeia*. **1968:** 41-49.

Nakamura, E. L. (1969) Visual acuity of yellowfin tuna *Thunnus albacares*. In: *FAO Fish. Rep.* A. Ben-Tuvia and W. Dickson (eds) pp. 463-468.

Nakamura, E. L. (1972) Development and uses of facilities for studying tuna behavior. In: *Behavior of Marine Animals*. H. E. Winn and B. A. Olla (eds) New York: Plenum Press, pp. 245-277.

Nakamura, E. L. (1987) MEXUS-Gulf coastal pelagic fish research, 1977-84. *Mar. Fish. Rev.* **49:** 36-38.

Napp, J. M. and Hunt, G. L. (2001) Anomalous conditions in the south-eastern Bering Sea 1997: linkages among climate, weather, ocean, and Biology. *Fish. Oceanogr.* **10:** 61-68.

O'Reilly, J. E., Maritorena, S., Mitchell, B. G., Kahru, M., Siegel, D. A., Carder, K. L., Garver, S. A. and McClain, C. (1998) Ocean color chlorophyll algorithms for SeaWiFS. *J. Geophys. Res*. **103:** 937–924.

O'Reilly, J. E., Maritorena, S., Siegel, D. A., O'Brien, M. C., Toole, D., Mitchell, B. G., Kahru, M., Chavez, F. P., Strutton, P., Cota, G., Hooker, S. B., McClain, C. R., Carder, K. L., Muller-Karger, F., Harding, L., Magnuson, A., Phinney, D., Moore, G. F., Aiken, J., Arrigo, K. R., Letelier, R. and Culver, M. (2000) Ocean color chlorophyll a algorithms for SeaWiFS, OC2, and OC4: Version 4. In: *SeaWiFS Postlaunch Technical Report Series Vol. 11, SeaWiFS Postlaunch Calibration and Validation Analyses, Part 3*. S. B. Hooker and E. R. Firestone (eds) Greenbelt, MD: NASA, Goddard Space Flight Center, pp. 9-23.

OCG (2006) West Florida Shelf C10 Mooring. Available online at: http://ocgweb.marine.usf.edu/shelf/Current/C10/C10AA-info.shtml (accessed September 2006).

Odum, W. E. and Heald, E. (1972) Trophic analyses of an estuarine mangrove community. *Bull. Mar. Sci.* **22:** 671-737.

Oey, L. Y., Ezer, T. and Lee, H. C. (2005) Loop current, rings and related circulation in the Gulf of Mexico: A review of numerical models and future challenges. In: *Ocean Circulation in the Gulf of Mexico*. W. F. Sturges, A.L. (eds) Washington, DC: Geophysical Monograph Series, American Geophysical Union, pp. 31-56.

Olson, D. B., Hitchcock, G. L., Mariano, A. J., Ashjian, C. J., Peng, G., Nero, R. W. and Podesta, G. P. (1994) Life on the edge: marine life and fronts. *Oceanography*. **7:** 52-60.

Olson, D. B., Hitchcock, G. L., Mariano, A. J., Ashjian, C. J., Peng, G., Nero, R. W. and Podesto, G. P. (1994) Life on the edge: marine life and fronts. **7:** 52-60.

OSB (2006) *Review of Recreational Fisheries Survey Methods*. Washington, DC: The National Academies Press, 187pp.

Palumbi, S. R. (2004) Marine reserves and ocean neighborhoods: The spatial scale of marine populations and their management. *Ann. Rev. Environ. Resour.* **29:** 31-68.

Paramo, J. E. and Viana, J. E. (2002) Hydroacoustic assessment of the Atlantic thread herring (*Opisthomena oglinum*) and the Spanish sardine (*Sardinella aurita*), in the north zone of the Columbian Caribbean. *Bol. Invest. Mar. Cost.* **31:** 33-52.

Pierce, D. (2002) Biomass and community structure of fishes collected in the nearshore waters along the central west coast of Florida, 1994-2002. *Florida Marine Research Instituion, Fisheries-Independent Monitoring program.* 22pp.

Pierce, D. and Mahmoudi, B. (2001) Nearshore fish assemblages along the central west coast of Florida. *Bull. Mar. Sci.* **68:** 243-270.

Pingree, R. D. and Le Cann, B. (1991) Drifting buoy in the field of flow of two eddies on East Thulean Rise (Northeast Atlantic). *J. Geophys. Res*. **96:** 16759-16777.

Pingree, R. D. and Mardell, G. T. (1981) Slope turbulence, internal waves and phytoplankton growth at the Celtic shelf-break. *Phil. Trans. Roy. Soc. Lond.* **302:** 663-682.

Pingree, R. D., Mardell, G. T., Holligan, P. N., Griffiths, D. K. and Smithers, J. (1982) Celtic Sea and Armorican current structure and the vertical distributions of temperature and chlorophyll. *Cont. Shelf Res.* **1:** 99-116.

Podesta, G. P., Browder, J. A. and Hoey, J. J. (1993) Exploring the association between swordfish catch rates and thermal fronts on U.S. longline grounds in the western North Atlantic. *Cont. Shelf Res.* **13:** 253-277

Polovina, J. J., Balazs, G. H., Howell, E. A., Parker, D. M., Seki, M. P. and Dutton, P. H. (2004) Forage and migration habitat of loggerhead (*Caretta caretta*) and olive ridley (*Lepidochelys olivacea*) sea turtles in the central North Pacific Ocean. *Fish. Oceanogr.* **13:** 36-51.

Polovina, J. J., Howell, E., Kobayashi, D. R. and Seki, M. P. (2001) The transition zone chlorophyll front, a dynamic global feature defining migration and forage habitat for marine resources. *Prog. Oceanogr.* **49:** 469–483.

Polovina, J. J. and Howell, E. A. (2005) Ecosystem indicators derived from satellite remotely sensed oceanographic data for the North Pacific. *ICES J. Mar. Sci.* **62:** 319-327.

Power, J. H. and May, L. N. (1991) Satellite observed sea-surface temperatures and yellowfin tuna catch and effort in the Gulf of Mexico. *Fish. Bull.* **89:** 429-439.

Ricker, W. E. (1975) Computation and interpretation of biological statistics of fish populations. *Bull. Fish. Res. Board Can.* **191:** 382p.

Ritchie, J. C., Schiebe, F. R. and McHenry, J. R. (1976) Remote sensing of suspended sediments in surface waters. *PgERS*. **42:** 1539-1545.

Roelke, R. D. and Cifuentes, L. A. (1997) Use of stable isotopes to assess groups of king mackerel, *Scomberomorus cavalla*, in the Gulf of Mexico and southeastern Florida. *Fish. Bull.* **95:** 540-551.

Roffer, M. (1987) Influence of the environment on the distribution and relative apparent abundance of juvenile Atlantic bluefin tuna along the United States east coast. Ph.D. thesis, University of Miami, 154pp.

Rossby, C.-G. (1937) On the mutual adjustment of pressure and velocity distributions in certain simple current systems. *J. Mar. Res.* **1:** 15-28.

Rubec, P., Lewis, J., Reed, D., Ashbaugh, C., Lashley, C., Versaggi, S., Weisberg, R. H., Zheng, L., He, R. and Jenkins, C. (2005) Refinement of an electronic logbook to support fishing operations by predicting abundance in relation to environmental conditions off the west coast of Florida. *FWC/FWRI.* **85-40-85000/89991:** 73pp.

Saraceno, M., Provost, C. and Piola, A. R. (2005) On the relationship between satellite-retrieved surface temperature fronts and chlorophyll a in the western South Atlantic. *J. Geophys. Res*. **110:** C11016.

Schaefer, H. C. and Fable, W. A. J. (1994) King mackerel, *Scomberomorus cavalla*, mark-recapture studies off Florida's east coast. *Mar. Fish. Rev.* **56:** 13-22.

Schick, R. S., Goldstein, J. L. and Lutcavage, M. (2004) Bluefin tuna (*Thunnus thynnus*) distribution in relation to sea surface temperature front in the Gulf of Maine (1994-96). *Fish. Oceanogr.* **13:** 225-238.

Schmidt, N., Lipp, E. K., Rose, J. B. and Luther, M. E. (2001) ENSO influences on seasonal rainfall and river discharge in Florida. *J. Climate*. **14:** 615-628.

Sedberry, G. and Loefer, J. (2001) Satellite telemetry tracking of swordfish, *Xiphias gladius*, off the eastern United States. **139:** 355-360.

Sedberry, G. R., McGovern, J. C. and Pashuk, O. (2001) The Charleston Bump: an island of essential fish habitat in the Gulf Stream. In: *Island in the Stream: Oceanography and Fisheries of the Charleston Bump*. G. R. Sedberry (eds) Bethesda, MD: American Fisheries Society, pp. 3-24.

Seemann, S. W., Li, J., Menzel, W. P. and Gumley, L. E. (2003) Operational retrieval of atmospheric temperature, moisture, and ozone from MODIS infrared radiances. *J. Appl. Meteorol.* **42:** 1072-1091.

Sharp, G. D. (1978) Behavioral and physiological properties of tunas and their effects on vulnerability to fishing gear. In: *The Physiological Ecology of Tunas*. G. D. Sharp and A. E. Dizon (eds) New York, NY: Academic Press, pp. 397-449.

Sharp, G. D. (2000) The past, present and future of fisheries oceanography: refashioning a responsible fisheries science. In: *Fisheries Oceanography an Integrated Approach to Fisheries Ecology and Management*. P. J. Harrison and T. R. Parsons (eds) Oxford, UK: Blackwell Science, pp. 207-263.

Sharp, G. D. and Dizon, A. E. (1978) *The Physiological Ecology of Tunas.* San Francisco and New York: Academic Press, 485pp.

Stegmann, P. M. and Ullman, D. S. (2004) Variability in chlorophyll and sea surface temperature fronts in the Long Island Sound outflow region from satellite observations. *J. Geophys. Res*. **109:** C07S03.

Stokesbury, M. J. W., Teo, S. L. H., Seitz, A., O'Dor, R. K. and Block, B. A. (2004) Movement of Atlantic bluefin tuna (*Thunnus thynnus*) as determined by satellite tagging experiments initiated off New England. *Can. J. Fish. Aquat. Sci.* **61:** 1976-1987.

Sturges, W. and Leben, R. (2000) Frequency of ring separations from the Loop Current in the Gulf of Mexico: A revised estimate. *J. Phys. Oceanogr*. **30:** 1814-1819.

Sund, P. N., Blackburn, M. and Williams, F. (1981) Tunas and their environment in the Pacific Ocean: a review. *Oceanogr. Mar. Biol. Ann. Rev.* **19:** 443-512.

Sutherland, D. F. and Fable, W. A. J. (1980) Results of a king mackerel (*Scomberomorus cavalla*) and Atlantic Spanish mackerel (*Scomberomorus maculatus*) migration study, 1975-79. USDOC. **NMFS-SEFC-12:** 18pp.

Sutter, F. C. I., Williams, R. O. and Godcharles, M. F. (1991) Movement patterns and stock affinities of king mackerel in the southeastern United States. *Fish. Bull.* **89:** 315-324.

Tamura, T. and Wisby, W. J. (1963) The visual sense of pelagic fishes especially the visual axis and accommodation. *Bull. Mar. Sci. Gulf Caribb.* **13:** 433–448.

Tang, T. Y. and Weisberg, R. H. (1993) Seasonal variations in equatorial Atlantic Ocean zonal volume transport at 28°W. *J. Geophys. Res*. **98:** 10145-10153.

Tolk, B. L. (2000) The impact of bottom brightness on spectral reflectance of suspended sediments. *Int. J. Remote Sensing*. **21:** 2259-2268.

Trent, L., Palko, B. J., Williams, M. L. and Brusher, H. A. (1987) Abundance of king mackerel, *Scomberomorus cavalla*, in the southeastern United States based on CPUE data from charterboats, 1982-1985. *Mar. Fish. Rev.* **49:** 78-90.

Ullman, D., 2005, University of Rhode Island, Kingston, RI, pers. comm.

Ullman, D. S. and Cornillon, P. C. (1999) Satellite-derived sea surface temperature fronts on the continental shelf off the northeast U. S. coast. *J. Geophys. Res*. **104:** 23459-23478.

Ullman, D. S. and Cornillon, P. C. (2001) Continental shelf surface thermal fronts in winter off the northeast US coast. *Cont. Shelf Res.* **21:** 1139-1156.

Utne-Palm, A. C. (2002) Visual feeding of fish in a turbid environment: Physical and behavioural aspects. *Mar. Fresh. Behav. Physiol.* **35:** 111-128.

Van Woert, M. (1982) The subtropical front: Satellite observations during FRONTS 80. *J. Geophys. Res*. **87:** 9523-9536.

Vázquez, D. P., Atae-Allah, C. and Escamilla, P. L. L. (1999) Entropic approach to edge detection for SST images. *J. Atmos. Oceanic Technol*. **16:** 970-979.

Virmani, J. I., 2006, University of South Florida, St. Petersburg, FL, pers. comm.

Virmani, J. I. and Weisberg, R. H. (2003) Features of the observed annual ocean–Atmosphere flux variability on the West Florida Shelf. *J. Climate*. **16:** 734-745.

Virmani, J. I. and Weisberg, R. H. (2005) Relative humidity over the West Florida Continental Shelf. *Mon. Wea. Rev.* **133:** 1671-1686.

Vlasenko, V. I. (1992) Non-linear model for the generation of baroclinic tides over extensive inhomogeneities of the seabed relief. *J. Phys. Oceanogr*. **3:** 417-424.

Wang, C. and Weisberg, R. H. (1998) Observations of meridional scale frequency dependence in the coupled tropical ocean-atmosphere system. *J. Geophys. Res.* **103:** 2811-2816.

Weatherly, G., Wienders, N. and Harkema, R. (2003) Temperature inversions in the open Gulf of Mexico. *J. Geophys. Res*. **108:** 3177.

Weisberg, R. H., Black, B. D. and Li, Z. (2000) An upwelling case study on Florida's west coast. *J. Geophys. Res*. **105:** 11459-11470.

Weisberg, R. H., Black, B. D. and Yang, H. (1996) Seasonal modulation of the west Florida continental shelf circulation. *Geophys. Res. Lett.* **23:** 2247-2250.

Weisberg, R. H. and He, R. (2003) Local and deep-ocean forcing contributions to anomalous water properties on the West Florida Shelf. *J. Geophys. Res*. **108:** 3184.

Weisberg, R. H., He, R., Kirkpatrick, G., Muller-Karger, F. and Walsh, J. J. (2004) Coastal Ocean Circulation Influences on Remotely Sensed Optical Properties: A West Florida Shelf Case Study. *Oceanography*. **17:** 68-75.

Weisberg, R. H., He, R., Liu, Y. and Virmani, J. I. (2005) West florida shelf circulation on synoptic, seasonal, and interannual time scales. *Geophys. Monogr.* **161:** 325-347.

Weisberg, R. H., Li, Z. and Muller-Karger, F. E. (2001) West Florida shelf response to local wind forcing: April 1998. *J. Geophys. Res*. **106:** 31239-31262.

Weisberg, R. H. and Zheng, L. (2005) Circulation of Tampa Bay driven by buoyancy, tides, and winds, as simulated using a finite volume coastal ocean model.

Williams, R. O. and Godcharles, M. F. (1984) Completion report, king mackerel tagging and stock assessment. Florida Department of Natural Resources, St. Petersburg. 45pp.

Wilson, S. G., Lutcavage, M. E., Brill, R. W., Genovese, M. P., Cooper, A. B. and Everly, A. W. (2005) Movements of bluefin tuna (*Thunnus thynnus*) in the northwestern Atlantic Ocean recorded by pop-up satellite archival tags. *Mar. Biol.* **146:** 409-423.

Yuen, H. S. H. (1970) Behavior of skipjack tuna, *Katsuwonus pelamis*, as determined by tracking with ultrasonic devices. *J. Fish. Res. Board Can.* **27:** 2071-2079.

Zar, J. H. (1999) *Biostatistical Analysis*. Upper Saddle River, NJ: Prentice-Hall, Inc., 663pp.

Zuenko, Y., Shershenkov, S., Bulatov, N. and Lapshina, V. (1992) A possibility to define the location of epipelagic fish concentrations with assistance of satellite sensing. *Conference for Pacific Ocean Environments and Probing*, Okinawa, Japan. **2:** 1235-1239.

**Appendices**

Appendix A: General assessment of the image quality of satellite images examined during tournament periods. Shaded cells identify the days used to determine sustained fronts. Tournament dates are in bold. Days when no data were available are marked by NA.

| 2004 | SST | Chl+ | nLw_443 | FLH |
|---|---|---|---|---|
| **3-Apr-04** | Good | Good | Good | Poor |
| 2-Apr-04 | Good | Good | Poor | Bad |
| 1-Apr-04 | Fair | NA | NA | Fair |
| 31-Mar-04 | Fair | Fair | Good | NA |
| **4-Apr-04** | Good | Good | Good | Bad |
| 3-Apr-04 | Good | Good | Good | Poor |
| 2-Apr-04 | Good | Good | Fair | Bad |
| 1-Apr-04 | Fair | NA | NA | Fair |
| **1-May-04** | Good | Good - Fair | Good - Fair | Fair |
| 30-Apr_04 | Poor | Fair | Fair - Poor | Bad |
| 29-Apr-04 | Poor | Poor | Bad | Bad |
| 28-Apr_04 | Good | NA | NA | NA |
| **2-May-04** | Fair | NA | NA | NA |
| 1-May-04 | Good | NA | NA | NA |
| 30-Apr_04 | Poor | NA | NA | NA |
| 29-Apr-04 | Poor | NA | NA | NA |
| **8-May-04** | Fair | Good | Fair - Poor | Bad |
| 7-May-04 | Bad | Fair - Poor | Poor | Bad |
| 6-May-04 | Fair | Poor | Poor | Bad |
| 5-May-04 | Fair | NA | NA | NA |
| **23-Oct-04** | Fair | Bad | Poor | Poor |
| 22-Oct-04 | Good - Fair | Poor | Poor | Good - Fair |
| 21-Oct-04 | Good - Fair | Poor | Poor | Poor |
| 20-Oct-04 | Poor | Bad | Bad | Bad |
| **30-Oct-04** | Good - Fair | Fair | Poor | Poor |
| 29-Oct-04 | Good | NA | NA | Poor |
| 28-Oct-04 | Good | Fair - Poor | Fair - Poor | Bad |
| 27-Oct-04 | Good - Fair | Good - Fair | Fair | Poor |

Appendix A (Continued)

| | | | | |
|---|---|---|---|---|
| **6-Nov-04** | Good | Good | Good | Good |
| 5-Nov-04 | Bad | NA | NA | NA |
| 4-Nov-04 | Fair | Poor | Bad | Poor |
| 3-Nov-04 | Fair | Fair | Fair | NA |

| | | | | |
|---|---|---|---|---|
| **7-Nov-04** | Good - Fair | Good - Fair | Fair | Fair |
| 6-Nov-04 | Good | Good | Good | Good |
| 5-Nov-04 | Bad | NA | NA | NA |
| 4-Nov-04 | Fair | Poor | Bad | Poor |

| | | | | |
|---|---|---|---|---|
| **13-Nov-04** | Fair - Poor | Bad | Bad | NA |
| 12-Nov-04 | Good | NA | NA | NA |
| 11-Nov-04 | Good | NA | NA | NA |
| 10-Nov-04 | Good | NA | NA | NA |

**2005**

| | | | | |
|---|---|---|---|---|
| **3-Apr-05** | Good | Good | Good | Bad |
| 2-Apr-05 | Good | Good | Good | NA |
| 1-Apr-05 | Good | Poor | Bad | Bad |
| 31-Mar-05 | Bad | NA | NA | NA |

| | | | | |
|---|---|---|---|---|
| **9-Apr-05** | Good | Good | Good | Good |
| 8-Apr-05 | Good | Fair | Fair | Bad |
| 7-Apr-05 | Good | NA | NA | NA |
| 6-Apr-05 | Good | Fair | Fair | Poor |

| | | | | |
|---|---|---|---|---|
| **16-Apr-05** | Good - Fair | Poor | Poor | Poor |
| 15-Apr-05 | Good - Fair | Fair - Poor | Fair - Poor | Good - Fair |
| 14-Apr-05 | Good | Good | Good | Bad |
| 13-Apr-05 | Bad | Poor | Poor | NA |

| | | | | |
|---|---|---|---|---|
| **17-Apr-05** | Good | Bad | Bad | Bad |
| 16-Apr-05 | Good - Fair | Poor | Poor | Poor |
| 15-Apr-05 | Good - Fair | Fair | Fair - Poor | Good - Fair |
| 14-Apr-05 | Good | Good | Good | Bad |

| | | | | |
|---|---|---|---|---|
| **23-Apr-05** | Fair | Poor | Bad | Bad |
| 22-Apr-05 | Good | Fair - Poor | Fair | Bad |
| 21-Apr-05 | Good | Fair | Good - Fair | Bad |
| 20-Apr-05 | Bad | Bad | Bad | NA |

Appendix A (Continued)

| | | | | |
|---|---|---|---|---|
| **30-Apr-05** | Fair | Good - Fair | Fair | Bad |
| 29-Apr-05 | Good | NA | NA | NA |
| 28-Apr-05 | Good | Good - Fair | Fair - Poor | Bad |
| 27-Apr-05 | Bad | NA | NA | Bad |

| | | | | |
|---|---|---|---|---|
| **29-Oct-05** | Good | Good - Fair | Good | Good |
| 28-Oct-05 | Good | Good - Fair | Fair | Bad |
| 27-Oct-05 | Good | Good - Fair | Bad | Good |
| 26-Oct-05 | Good | Fair | Fair - Poor | Fair |

| | | | | |
|---|---|---|---|---|
| **5-Nov-05** | Good - Fair | Bad | Bad | Fair |
| 4-Nov-05 | Good | Good | Good | Good |
| 3-Nov-05 | Good | Good | Good | Good |
| 2-Nov-05 | Bad | Poor | Poor | NA |

| | | | | |
|---|---|---|---|---|
| **6-Nov-05** | Poor | Bad | Bad | Bad |
| 5-Nov-05 | Good | Bad | Bad | Fair |
| 4-Nov-05 | Good | Good | Good | Good |
| 3-Nov-05 | Good | Good - Fair | Good | Good |

| | | | | |
|---|---|---|---|---|
| **12-Nov-05** | Good | Good - Fair | Good - Fair | Good |
| 11-Nov-05 | Good | Good | Good | Good |
| 10-Nov-05 | Good | Poor - Bad | Poor - Bad | Poor - Bad |
| 9-Nov-05 | Good | Fair | Fair | Good |

Appendix B: Outline of multivariate statistical methods

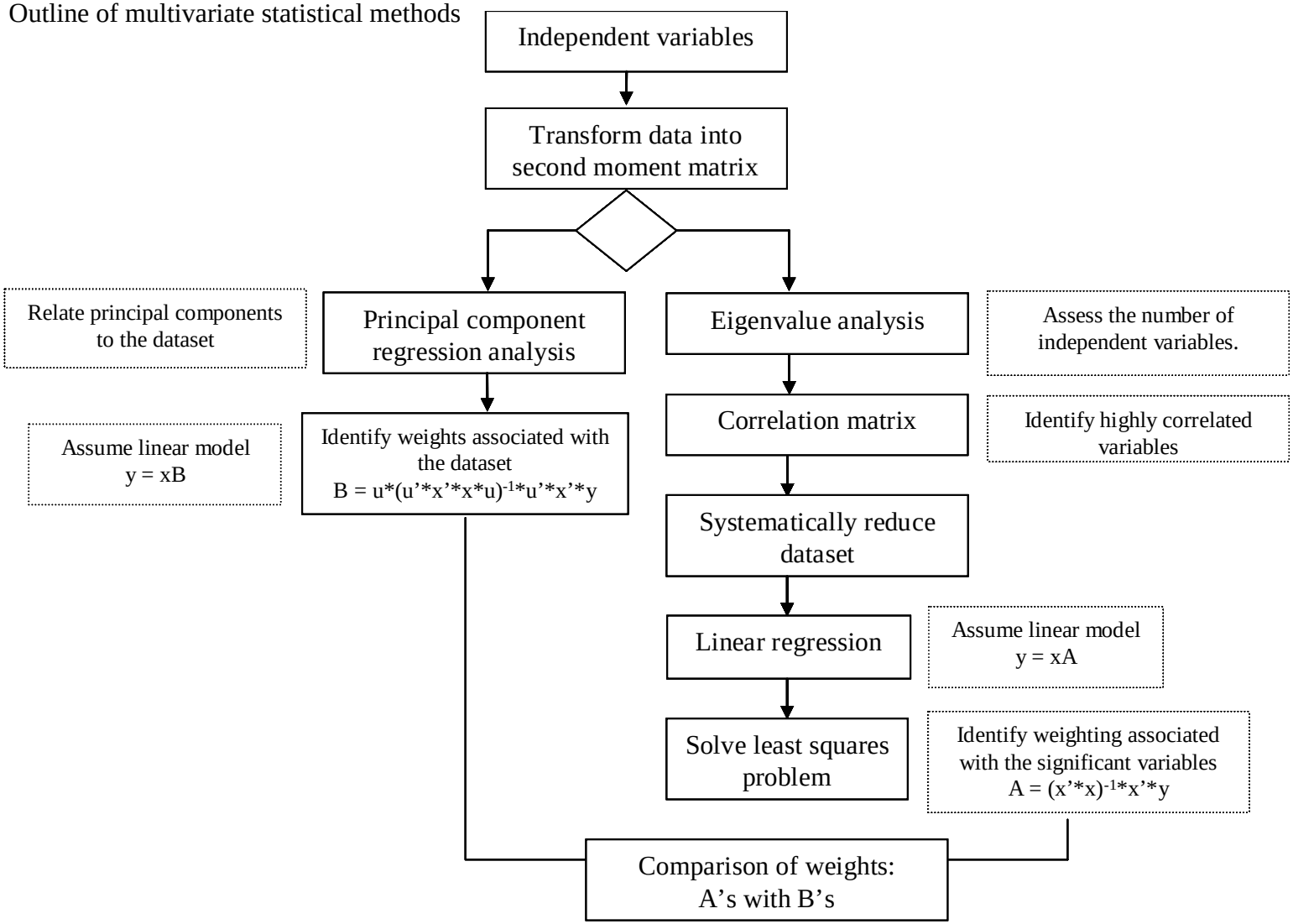

Appendix C: Anomalous SST values for all fall fishing locations (N=266).

| Year | Week | Mean (°C) | St. Dev. |
|---|---|---|---|
| 2004 | Oct. 21 - 27 | 0.1 | 0.3 |
| | Oct. 28 - Nov. 3 | 0.8 | 0.4 |
| | Nov. 4 - 10 | 0.7 | 0.2 |
| | Nov. 11 - 17 | 0.5 | 0.2 |
| 2005 | Oct. 22 - 28 | -1.0 | 1.1 |
| | Oct. 29 - Nov. 4 | -2.3 | 0.9 |
| | Nov. 5 - 11 | -1.2 | 0.4 |
| | Nov. 12 - 18 | -0.2 | 0.02 |

Appendix D: Student's *t*-test analysis comparing environmental conditions where fishing was and was not successful. Note the high standard deviation (SD) associated with the variables (except Latitude, Longitude, SST, and nLw_443). T = 1.960, $p = 0.05$, CPUE > 0: N =416; CPUE =0: N = 159.

| | | **CPUE >0** | | **CPUE = 0** | |
|---|---|---|---|---|---|
| Variable | *t* | Mean | SD | Mean | SD |
| Latitude (° N) | 0.54 | 27.72 | 0.31 | 27.75 | 0.23 |
| Longitude (° W) | 0.22 | 83.01 | 0.20 | 82.99 | 0.17 |
| SST front (km) | 0.24 | 6 | 7 | 7 | 7 |
| Chl+ front (km) | 0.25 | 6 | 5 | 6 | 5 |
| nLw_443 front (km) | 0.00 | 10 | 12 | 14 | 14 |
| SST (°C) | 0.75 | 22.9 | 1.7 | 22.9 | 1.6 |
| Chl+ (mg $m^{-3}$) | 0.49 | 2.3 | 2.3 | 2.4 | 2.2 |
| nLw_443 (mW $cm^{-2}$ $\mu m^{-1}$ $sr^{-1}$) | 0.33 | 0.8 | 0.4 | 0.8 | 0.4 |
| Bait presence | 0.01 | 1 | 1 | 1 | 1 |
| SST gradient ($km^{-1}$) | 0.62 | 0.1 | 0.5 | 0.1 | 0.5 |
| Chl+ gradient ($km^{-1}$) | 0.90 | 0.0 | 1.0 | 0.0 | 1.0 |
| nLw_443 gradient ($km^{-1}$) | 0.93 | 0.1 | 0.3 | 0.1 | 0.3 |
| Sustained SST front (km) | 0.95 | 22 | 20 | 23 | 19 |
| Sustained chl+ front (km) | 0.68 | 15 | 20 | 15 | 20 |
| Sustained nLw_443 front (km) | 0.03 | 20 | 20 | 25 | 20 |
| Bottom type | 0.59 | 3 | 1 | 3 | 1 |

Appendix E: Effects of wind on fishing behavior. Mean (μ) distance to land and CPUE and corresponding standard deviations (SD), and percentage of bottom type for each tournament day are provided. Highlighted rows represent days with strong and variable winds with observed decreased distance to land (km) and CPUE. For April 4, 2004, April 16 and 30, 2005, and November 12, 2005 this also resulted in a higher percentage of fishing recorded in the shipping channel.

| Tournament Day | N | Distance to land (km) | | CPUE | | Bottom type (%) | | |
|---|---|---|---|---|---|---|---|---|
| | | μ | SD | μ | SD | Bottom Relief | Channel | Other Bottom |
| 4/3/2004 | 30 | 22.00 | 13.50 | 0.41 | 0.44 | 26.7 | 3.3 | 70.0 |
| 4/4/2004 | 10 | 14.50 | 7.20 | 0.44 | 0.29 | 10.0 | 40.0 | 50.0 |
| 5/1/2004 | 39 | 23.20 | 19.50 | 0.45 | 0.47 | 10.3 | 10.3 | 79.4 |
| 5/8/2004 | 119 | 27.80 | 22.40 | 0.65 | 1.13 | 13.6 | 5.9 | 80.5 |
| 10/23/2004 | 13 | 26.40 | 26.30 | 0.51 | 0.61 | 7.7 | 15.4 | 76.9 |
| 10/30/2004 | 65 | 29.80 | 32.20 | 0.74 | 1.04 | 0.0 | 1.5 | 98.5 |
| 11/6/2004 | 16 | 30.20 | 16.90 | 0.59 | 0.78 | 6.3 | 12.5 | 81.2 |
| 11/7/2004 | 42 | 33.60 | 21.90 | 1.82 | 7.34 | 7.1 | 0.0 | 92.9 |
| 11/13/2004 | 99 | 22.90 | 28.70 | 0.73 | 1.01 | 16.2 | 6.1 | 77.7 |
| 4/3/2005 | 10 | 29.30 | 15.30 | 0.69 | 0.85 | 20.0 | 0.0 | 80.0 |
| 4/9/2005 | 39 | 21.20 | 14.70 | 1.14 | 1.98 | 15.4 | 12.8 | 71.8 |
| 4/16/2005 | 32 | 15.40 | 11.70 | 0.73 | 1.32 | 6.3 | 18.8 | 74.9 |
| 4/17/2005 | 26 | 7.10 | 8.00 | 0.36 | 0.40 | 15.4 | 7.7 | 76.9 |
| 4/23/2005 | 65 | 21.10 | 21.30 | 0.53 | 0.76 | 7.7 | 3.1 | 89.2 |
| 4/30/2005 | 44 | 12.40 | 9.00 | 1.21 | 4.51 | 15.9 | 13.6 | 70.5 |
| 10/29/2005 | 8 | 25.00 | 20.70 | 0.32 | 0.30 | 10.0 | 0.0 | 90.0 |
| 11/5/2005 | 20 | 54.90 | 34.00 | 0.66 | 0.52 | 20.0 | 0.0 | 80.0 |
| 11/6/2005 | 17 | 22.70 | 28.20 | 0.67 | 1.23 | 5.9 | 0.0 | 94.1 |
| 11/12/2005 | 69 | 13.60 | 18.60 | 0.33 | 0.57 | 7.3 | 17.4 | 75.3 |